University of Technology

Mechanical Engineering

Department

2017-2018

Chapter One

Basic Information & Introduction to Design of Flying Body

Dr. Ahmed Shandookh

AIRCRAFT BRANCH

1. Basic Information & Introduction to Flying Body Design:

1.1 Basic Definitions: There are many terms and definitions in aircraft engineering design field and it might be difficult for many non-specialists to distinguish between them, these terms as shown in the table 1.1 below.

Table 1.1: Basic definitions

Flying Body	Anybody or mass above earth surface or see level.
Aircraft	An aircraft is a machine that can fly by gaining support from the air
Airplane	An airplane is a powered, fixed-wing aircraft that is propelled forward by thrust from a jet engine or propeller.
Spacecraft	A spacecraft is a vehicle, or machine designed to fly in outer space.
Missile	A missile is a self-propelled precision-guided munition system
Rocket	Is a missile, spacecraft, aircraft or other vehicle that obtains thrust from a rocket engine
Gliders	A glider is a heavier-than-air aircraft that is supported in flight by the dynamic reaction of the air against its lifting surfaces, and whose free flight does not depend on an engine
Kites	A kite is traditionally a tethered heavier-than-air craft with wing surfaces that react against the air to create lift and drag.
Wings	A wing is a type modified shape that produces lift, while moving through air or some other fluid.
Foil	A foil is a solid object with a shape such that when placed in a moving fluid at a suitable angle of attack
Fin	A fin is a thin component or appendage attached to a larger body or structure. Fins typically function as foils that produce lift or thrust,
Stabilizer	An aircraft stabilizer is an aerodynamic surface, typically including one or more movable control surfaces
Rudder	A rudder is a primary control surface used to steer a ship, boat, submarine, aircraft, or other conveyance that moves through a fluid medium (generally air or water).
Elevator	Elevators are flight control surfaces, usually at the rear of an aircraft, which control the aircraft's pitch, and therefore the angle of attack and the lift of the wing.
Flaps	Flaps are a type of high-lift device used to increase the lift of an aircraft wing at a given airspeed.
Spar	In a fixed-wing aircraft, the spar is often the main structural member of the wing, running spanwise at right angles (or thereabouts depending on wing sweep) to the fuselage.
Span	The wingspan (or just span) of a bird or an airplane is the distance from one wingtip to the other wingtip.

Stringer	In aircraft and launch vehicle construction, a longeron, or stringer or stiffener, is a thin strip [not verified in body] of material to which the skin of an aircraft or propellant tank may be fastened.
Fuselage	An aircraft's main body section. It holds crew, passengers, and cargo.
Wing Chord	In aeronautics, chord refers to the imaginary straight line joining the leading and trailing edges of an airfoil. The chord length is the distance between the trailing edge and the point on the leading edge where the chord intersects the leading edge.
Wing Camber	In aeronautics and aeronautical engineering, camber is the asymmetry between the top and the bottom surfaces of an airfoil. An airfoil that is not cambered is called a symmetrical airfoil.
Aspect ratio	In aeronautics, the aspect ratio of a wing is the ratio of its span to its mean chord. It is equal to the square of the wingspan divided by the wing area. Thus, a long, narrow wing has a high aspect ratio, whereas a short, wide wing has a low aspect ratio.
Swept wing	A swept wing is a wing that angles either backward or, occasionally, forward, from its root rather than in a straight sideways direction.
Aerodynamic center	The point at which the pitching moment coefficient for the airfoil does not vary with lift coefficient (i.e. angle of attack), so this choice makes analysis simpler.
Pitching moment	In aerodynamics, the pitching moment on an airfoil is the moment (or torque) produced by the aerodynamic force on the airfoil if that aerodynamic force is applied, not at the center of pressure, but at the aerodynamic center of the airfoil.
C_L	The lift coefficient (C_L, C_N or C_Z) is a dimensionless coefficient that relates the lift generated by a lifting body to the fluid density around the body, the fluid velocity and an associated reference area.
C_D	the drag coefficient (commonly denoted as (C_D, C_X or C_W) is a dimensionless quantity that is used to quantify the drag or resistance of an object in a fluid environment, such as air or water.
C_M	The coefficients used for moment are similar to coefficients of lift, drag, and thrust, and are likewise dimensionless; however, these must include a characteristic length, in addition to the area
NACA	National Advisory Committee for Aeronautics
NASA	National Aeronautics and Space Administration

1.2 Brief Historical Background of Flying Body Design:

The desire to become airborne is ancient and it is reflected in our imagination and dreams. In the West, Daedalus and Icarus of Greek mythology were the first aviators; in the East, there are even more ancient myths – with no crashes. In Indian mythology, Pakshiraj is a white stallion with wings; the Greeks had a flying horse called Pegasus; and the Swedes also have flying horses. Garuda of Indonesia – half man and half bird – is another example from the Ramayana epic. Middle Eastern and South Asiatic "flying carpets" are seen in many Western cartoons and films.

These contraptions are fully aerobatic with the ability to follow terrain; there are no seat belts and they can land inside rooms as well as on rooftops. Recreational possibilities and military applications abound. Unfortunately, history is somewhat more "down to earth" than mythology, with early pioneers leaping from towers and cliffs, only to leave the Earth in a different but predictable manner because they underestimated the laws of nature. Our dreams and imagination became reality only about 100 years ago on December 17، 1903 ، with the first heavier-than-air flight by the Wright brothers. Yet, man first landed on the Moon about three decades ago, less than 70 years after the first powered flight.

The first scientific attempts to design a mechanism for aerial navigation were by Leonardo da Vinci (1452–1519) – he was the true grandfather of modern aviation، even if none of his machines ever defied gravity (Figure 1.1). He sketched many contraptions in his attempt to make a mechanical bird. However, birds possess such

refined design features that the human path into the skies could not take that route؛ da Vinci's ideas contradicted the laws of nature [1].

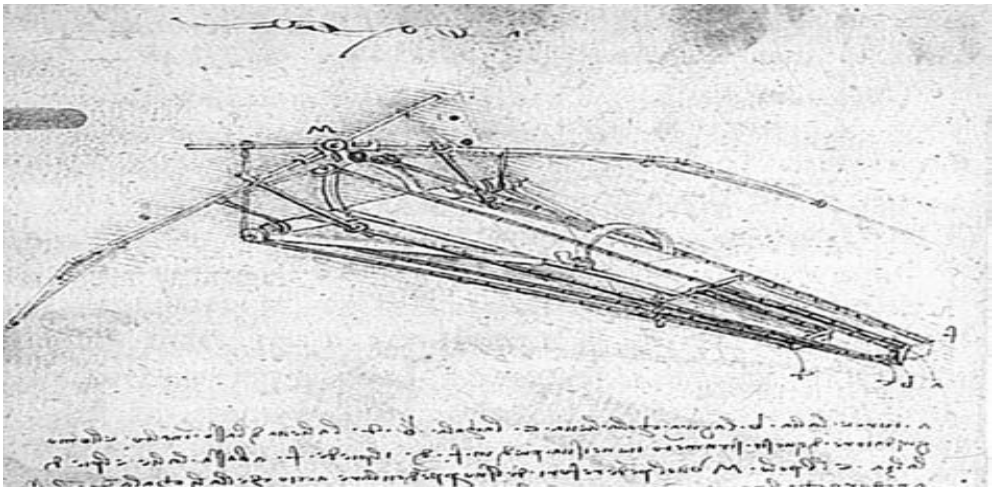

Figure 1.1: Da Vinci's flying machine

After da Vinci, and after an apparent lull for more than a century, the next prominent name is that of Sir Isaac Newton (1642–1727). Perhaps we lack the documentary evidence for I am convinced that human fascination with and endeavor for flight did not abate. Newton developed a theory of lift that although erroneous for low-speed flows, has some hypersonic application (although, of course، this was beyond his seventeenth-century understanding of fluid mechanics). Flight is essentially a practical matter, so real progress paralleled other industrial developments e.g., isolating gas for buoyancy. In 1783, de Rozier and d'Arlandes were the first to effectively defy gravity، using a Montgolfier (France) balloon (Figure 1.2). For the first time, it was possible to sustain and somewhat control altitude above the ground at will. However، these pioneers were subject to the prevailing wind direction and therefore were limited in their navigational options. To become airborne was an important landmark in human endeavor. The fact that the balloonists did not have wings does not diminish the importance of their achievement. The Montgolfier brothers (Joseph and Etienne) should be considered among the fathers of aviation. In 1784, Blanchard (France) added a hand-powered propeller to a balloon and was the first to make an aerial crossing of the English Channel on July 15, 1765. Jules Verne's fictional trip around the world in eighty days in a balloon became a reality when Steve Fossett circumnavigated the globe in fewer than fifteen days in 2002 – approximately three centuries after the first balloon circumnavigation. In 1855, Joseph Plane was the first to use the word Aeroplan in a paper he wrote proposing a gas-filled dirigible glider with a propeller. Tethered kites flew in the Far East for a long time – in China, 600 B.C. However، in 1804, Englishman Sir George Cayley constructed and flew a kite-like glider (Figure 1.3) with movable control surfaces – the first record of a successful heavier than air controllable machine to stay freely airborne. In 1842, English engineer Samuel Henson secured a patent on an aircraft design that was driven by a steam engine. With his brother Gustav, Otto Lilienthal was successfully flying gliders (Figure 1.4) in Berlin more than a decade (ca. 1890) before the Wright brothers' first model (Figure 1.5), and so until the next generation of airplanes (Figure 1.6).

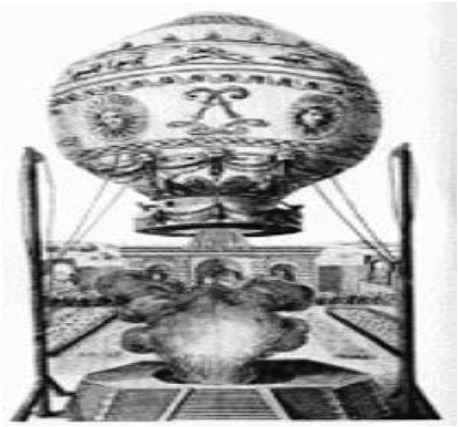

Figure 1.2: Montgolfier balloon

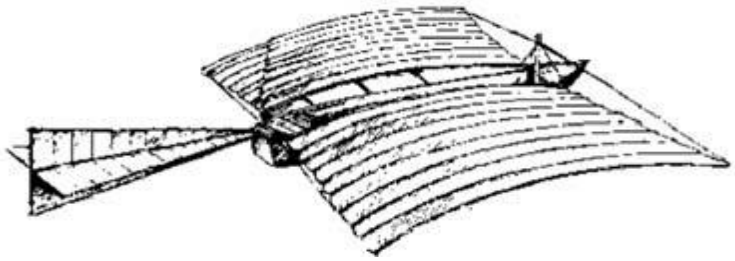

Figure 1.3: Cayley's kite glider

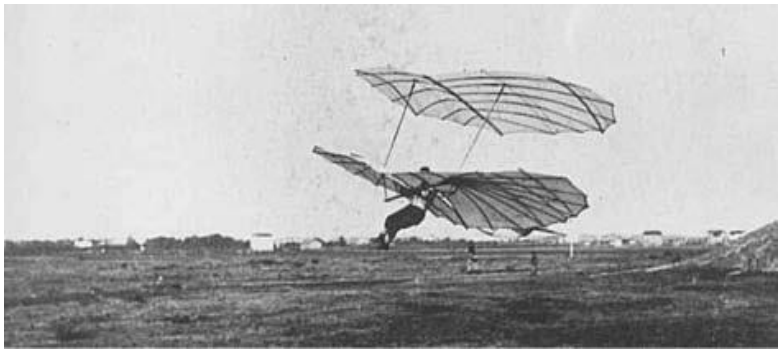

Figure 1.4: One of Lilienthal's gliders

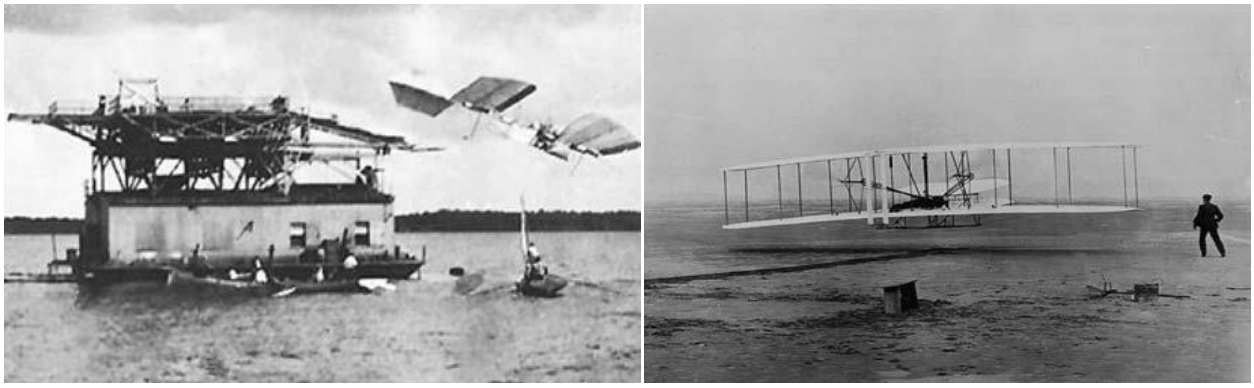

Figure 1.5: Langley's catapult launch & The Wright flyer

Figure 1.6: Future Trends Airplanes Boeing 787 Dreamliner & Airbus 380

1.3 Management concept of aircraft design

Existing aircraft indicate how the market is served and should indicate what is needed for the future. Various aircraft have been designed, and new designs should perform better than any existing designs. Designers are obligated to search for proven advanced technologies that emerge. There could be more than one option so the design team must conduct trade-off studies to arrive at a "satisfying" design that will satisfy the customer. Economy and safety are possibly the strongest drivers in commercial transport. Aircraft design drivers for combat are performance capability and survivability (i.e., safety).

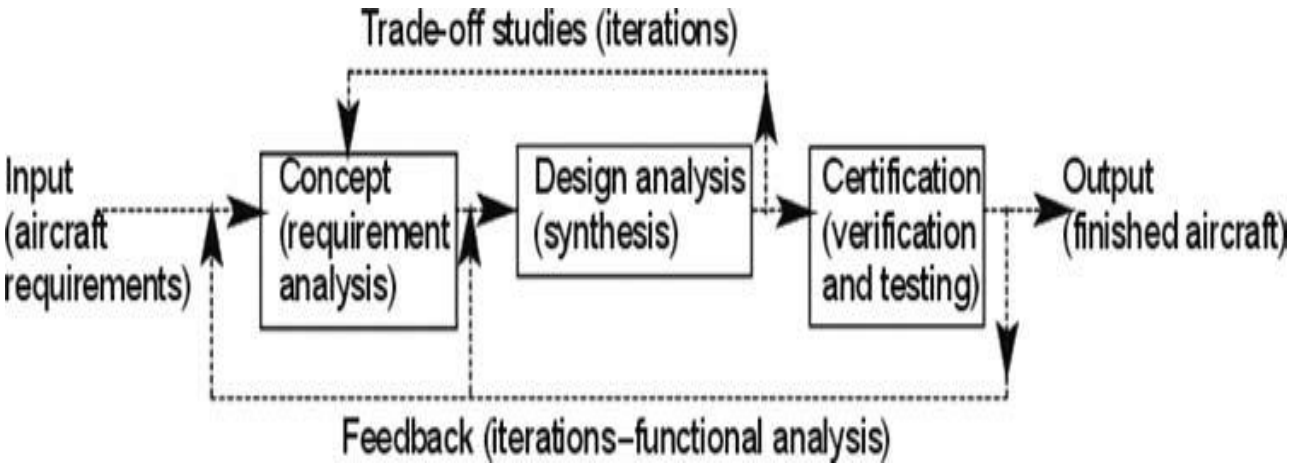

Figure 1.7: Aircraft design process

1.4 Typical Design Process:

Extensive wind-tunnel, structure, and systems testing is required early in the design cycle to ensure that safe flight tests result in airworthiness certification approval. The multidisciplinary systems approach to aircraft design is carried out within the context of IPPD (Intelligent Phase Process Design). Four phases comprise the generic methodology for a new aircraft to be conceived, designed, built, and certified (Figure 1.8).

Civil aircraft projects usually proceed to preproduction aircraft that will be flight-tested and sold, whereas military aircraft projects proceed with technical demonstrations of prototypes before the go-ahead is given. The prototypes are typically scaled-down aircraft meant to substantiate cutting-edge technologies and are not sold for operational use.

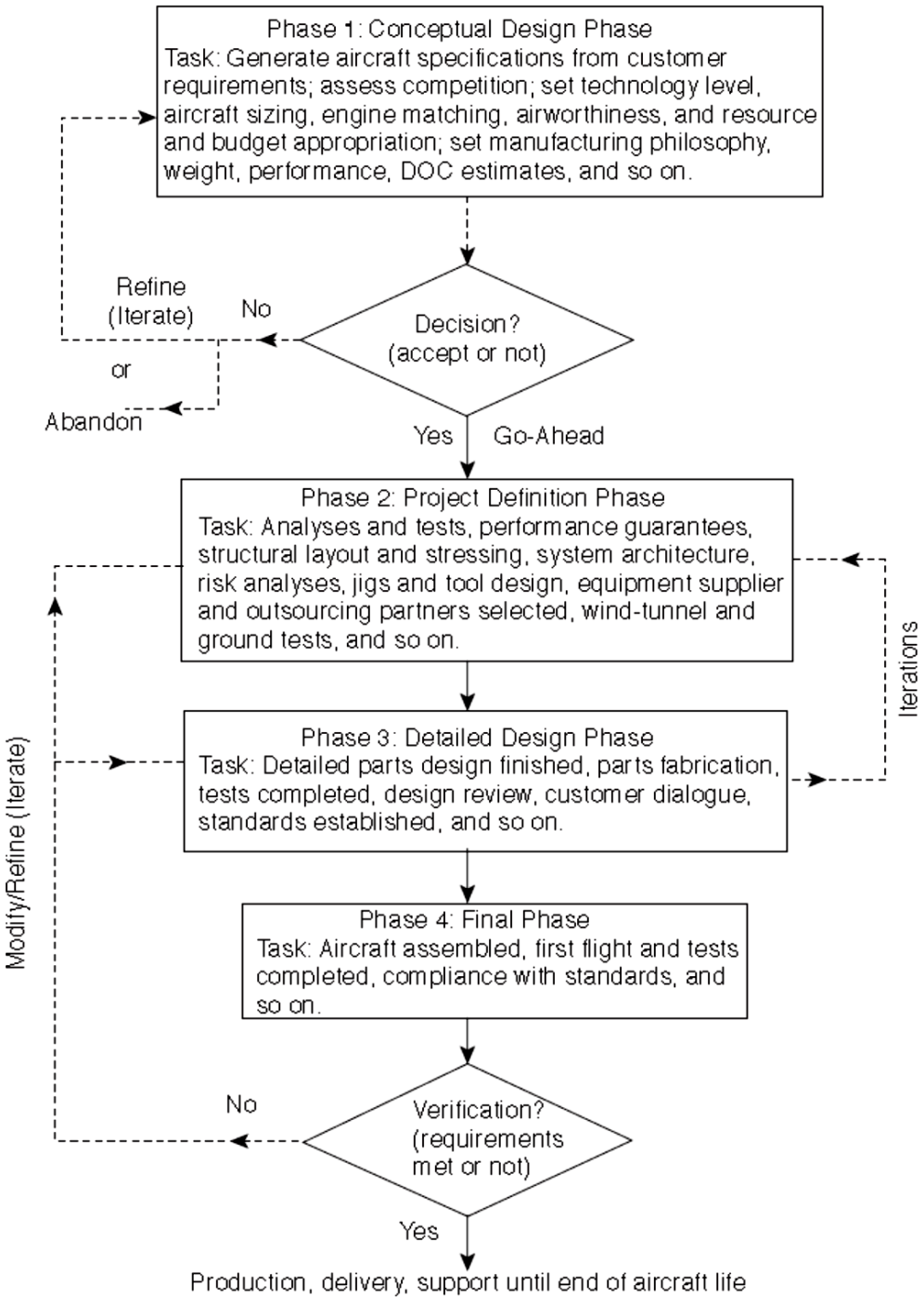

Figure 1.8: Four Phases of Aircraft Design and Development Process

So, to insure a typical design process we must:

1. Made four phases of aircraft design steps as classified above.
2. Prepare a typical resources deployment.
3. Calculate the typical cost frame.
4. Estimate the typical time frame.

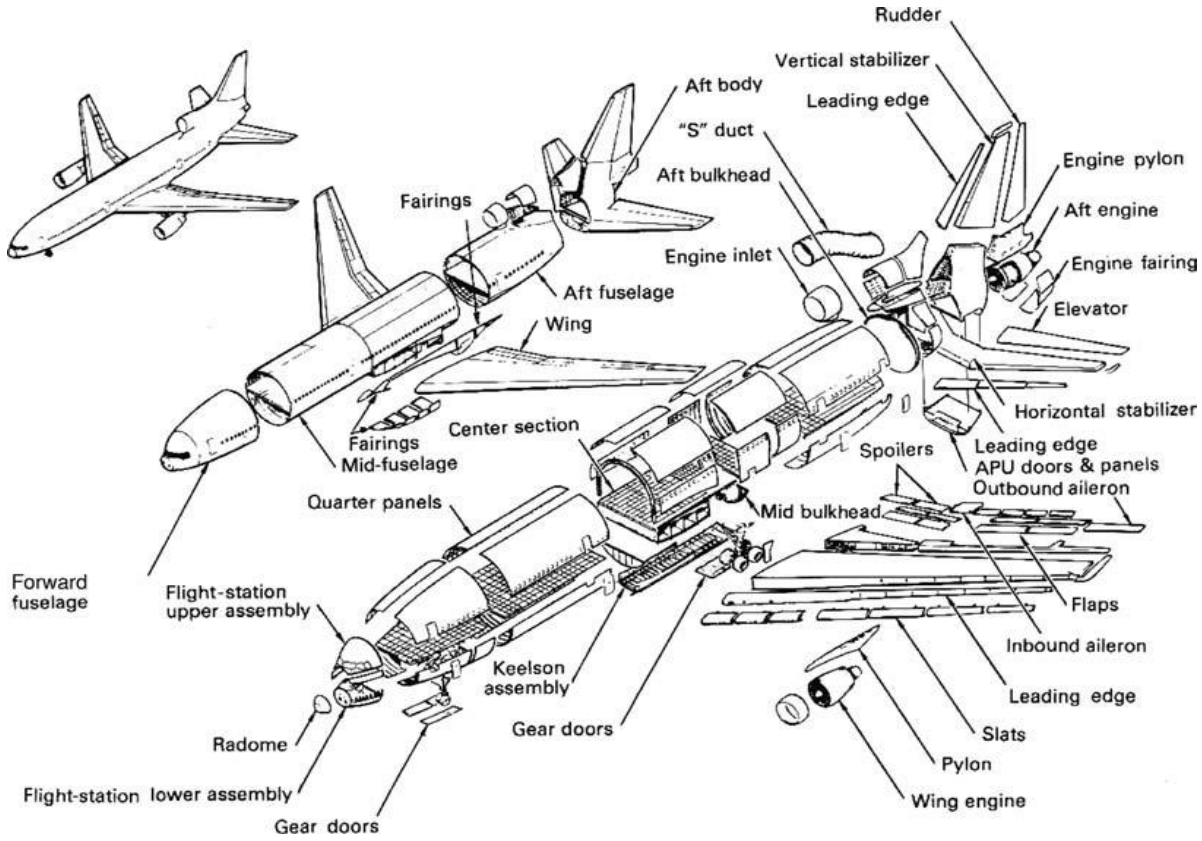

Figure 1.9: Lockheed 1011 diagram construction

1.5 Airfoil Section: An airfoil (American English) or aerofoil (British English) is the shape of a wing, blade (of a propeller, rotor, or turbine). An airfoil-shaped body moved through a fluid produces an aerodynamic force. The component of this force perpendicular to the direction of motion is called lift. The component parallel to the direction of motion is called drag. Subsonic flight airfoils have a characteristic shape with a rounded leading edge, followed by a sharp trailing edge, often with a symmetric curvature of upper and lower surfaces. Foils of similar function designed with water as the working fluid are called hydrofoils Figures 1.10 &1.11. The NACA airfoils are airfoil shapes for aircraft wings developed by (NACA). The shape of the NACA airfoils is described using a series of digits following the word "NACA". The parameters in the numerical code can be entered equations to precisely generate the cross-section of the airfoil and calculate its properties Figure 1.12.

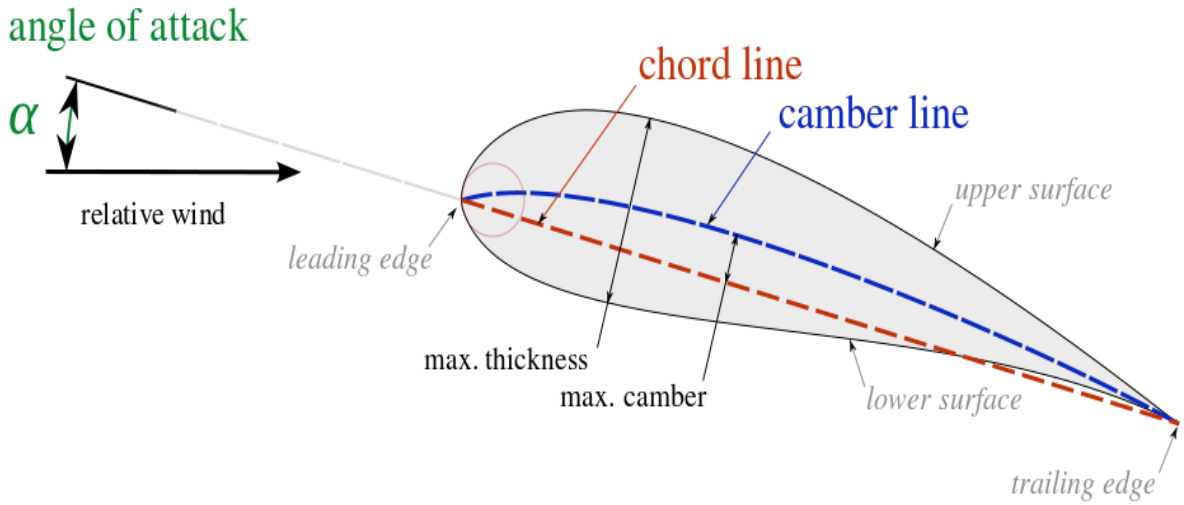

Figure 1.10: Airfoil nomenclature

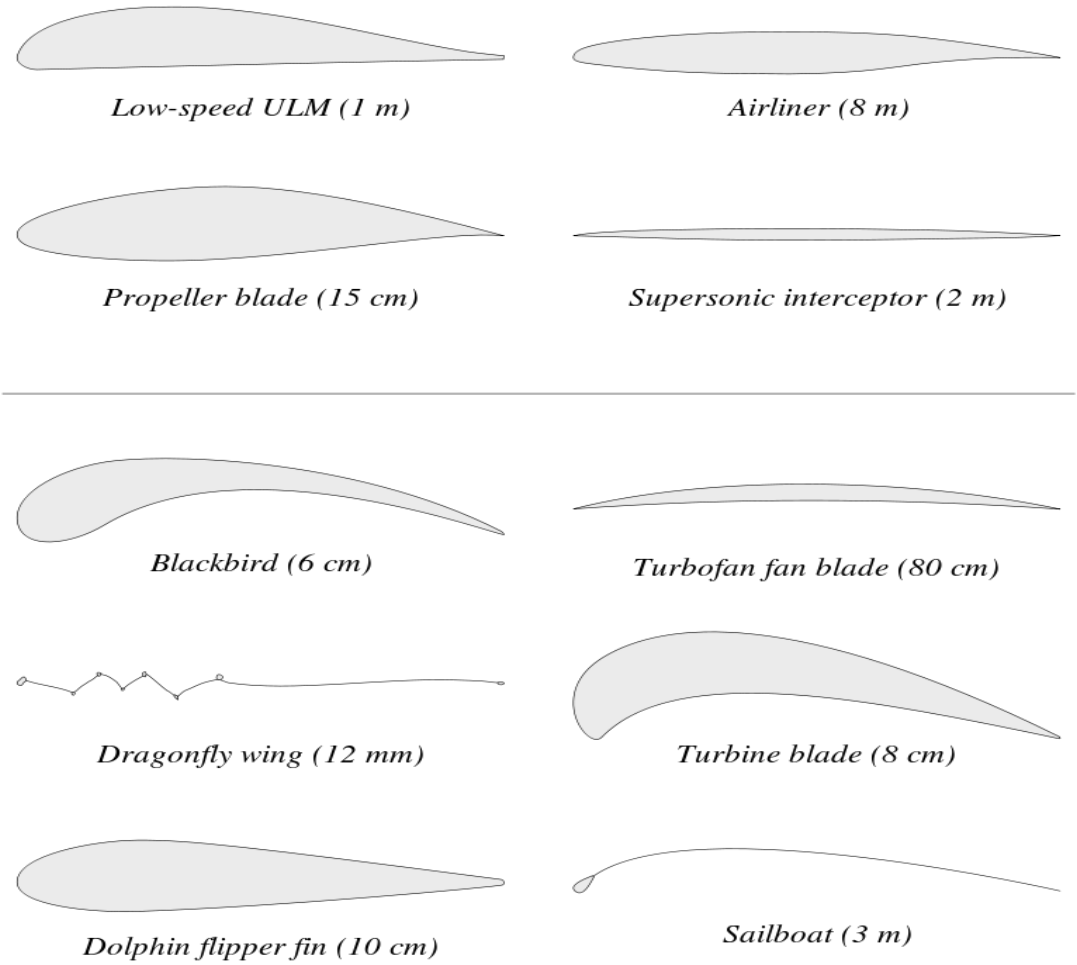

Figure 1.11: Examples of airfoils in nature and within various vehicles. Though not strictly an airfoil, the dolphin flipper obeys the same principles in a different fluid medium.

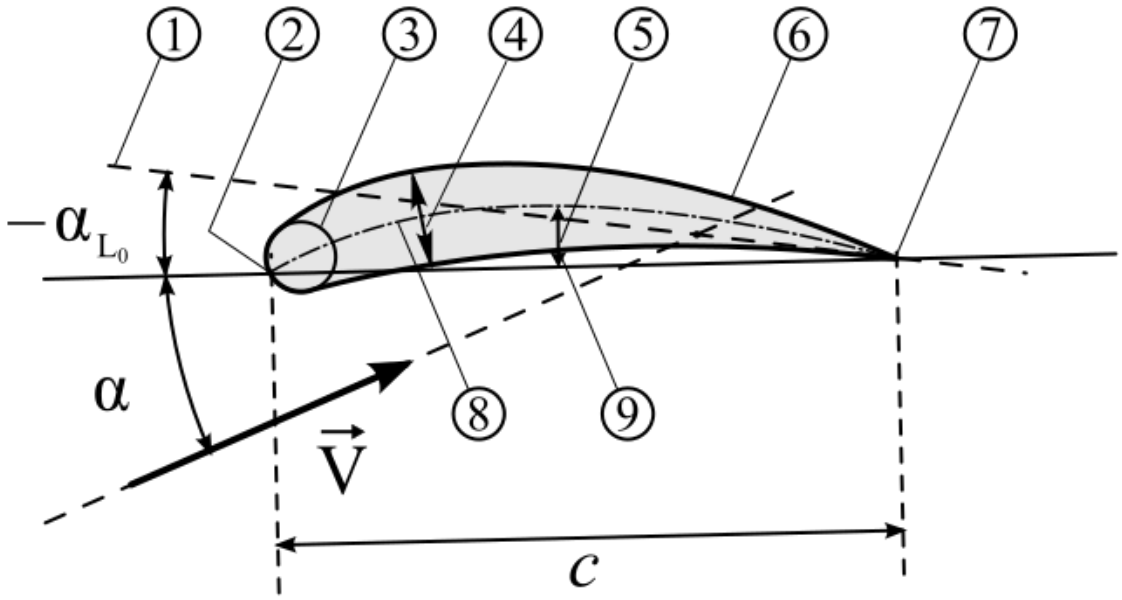

Figure 1.12: Airfoil geometry – 1: Zero lift line; 2: Leading edge; 3: Nose circle; 4: Max. thickness; 5: Camber; 6: Upper surface; 7: Trailing edge; 8: Camber mean-line; 9: Lower surface

1.5.1 NACA Airfoils: The focus of this section is how to select a wing airfoil from the available list of NACA airfoils, so this section is dedicated to the introduction of NACA airfoils. One of the most reliable resources and widely used data base is the airfoils that have been developed by NACA (predecessor of NASA) in 1930s and 1940s. Three following groups of NACA airfoils are more interesting:

a. *Four-digit NACA airfoils.*
b. *Five-digit NACA airfoils*.
c. *Six-series NACA airfoils*.

As the names imply, four-digit airfoils are named by four digits (such as 2415), five-digit airfoils are named by five digits (such as 23018), but 6-series airfoils names begin by number 6 (in fact, they have 5 main digits). Figure 1.13 illustrates a four-digit, a five-digit and a six-series airfoil.

a. Four-digit NACA airfoils

The four-digit NACA airfoil sections are the oldest and simplest NACA airfoils to generate. The camber of a four-digit airfoil has made up of two parabolas. One parabola generates the camber geometry from the leading edge to the maximum camber, and another parabola produces the camber shape from the maximum camber to the trailing edge. In a Four-digit NACA airfoil, the first digit indicates the maximum camber in percent

chord. The second digit indicates the position of maximum camber in tenths of chord length. The last two digits represent the maximum thickness-to-chord ratio. A zero in the first digit means that this airfoil is a symmetrical airfoil section. For example, the NACA **1408** airfoil section (see figure 1.13a) has a 8 percent $(t/c)_{max}$ (the last two digits), its maximum camber is 10 percent, and its maximum camber is located at 40 percent of the chord length. Although these airfoils are easy to produce, but they generate high drag compared with new airfoils

b. Five-digit NACA airfoils

The camber of a five-digit airfoil section has made up of one parabola and one straight line. The parabola generates the camber geometry from the leading edge to the maximum camber, and then a straight line connects the end the parabola to the trailing edge. In a five-digit NACA airfoil section; the first digit represents the 2/3 of ideal lift coefficient in tenths. It is an approximate representation of maximum camber in percent chord. The second digit indicates the position of maximum camber in two hundredths of chord length. The last two digits represent the maximum thickness-to-chord ratio. A zero in the first digit means that this airfoil is a symmetrical airfoil section. For example, the NACA **23012** airfoil section (see figure 1.13b) has a 12% maximum thickness-to-chord ratio; $(t/c)_{max}$. The ideal lift coefficient of this airfoil is 0.3 (the second digit), finally, its maximum camber is located at 12% of the chord length.

c. Six-digit NACA airfoils

The four- and five-digit airfoil sections where designed simply by using parabola and line. They were not supposed to satisfy major aerodynamic design requirements, such as laminar flow and no flow separation. When it became clear that the four- and five-digit airfoils have not been carefully designed, NACA researchers begin the investigation to develop new series of airfoils that have been driven by design requirements. On the other hands, newly designed faster aircraft require more efficient airfoil sections. Several series of airfoils were designed at that time, but the 6-series were found to be the best. The six series airfoils were designed to maintain laminar flow over a large

part of the chord, thus they maintain lower Cd_{min} compared with four- and five- digit airfoils. The 6-series NACA airfoils are designated by five main digits and begin with number 6. Some 6-series airfoils have a subscript number after the second digit. There is also a "-" between the second digit and the third digit. The meaning of each digit is as follows. The first digit is always 6; that is the series designation. The second digit represents the chordwise position of minimum pressure in tenths of chord for the basic symmetrical section at zero lift. The third digit indicates the ideal lift coefficient in tenths. The last two digits represent the maximum thickness-to-chord ratio. In case that the airfoil name has a subscript after the second digit, it indicates the lift coefficient range in tenths above and below the value of ideal lift coefficient in which favorable pressure gradient and low drag exist. A zero in the third digit means that this airfoil is a symmetrical airfoil section.

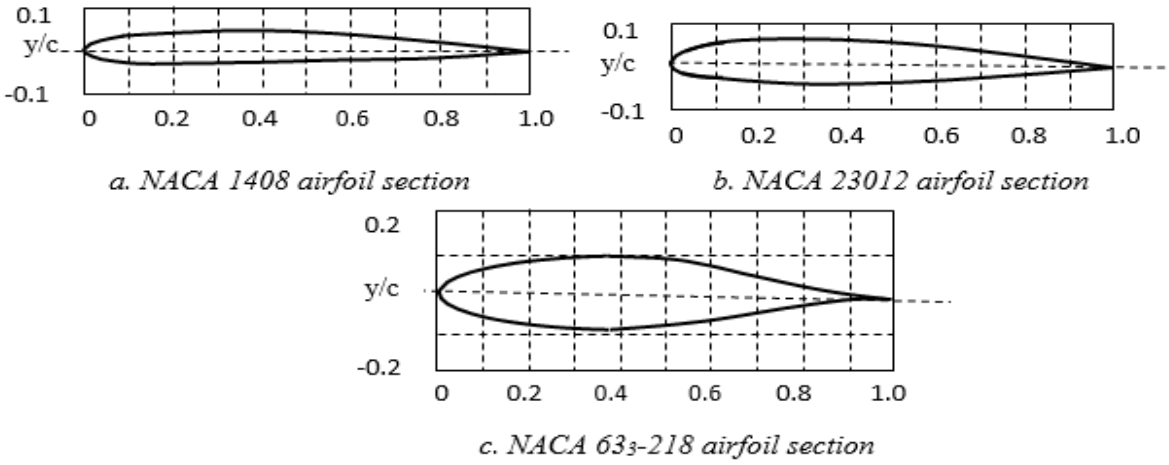

a. NACA 1408 airfoil section

b. NACA 23012 airfoil section

c. NACA 63₃-218 airfoil section

Figure 1.13. A four-digit, a five-digit and a 6-series airfoil sections

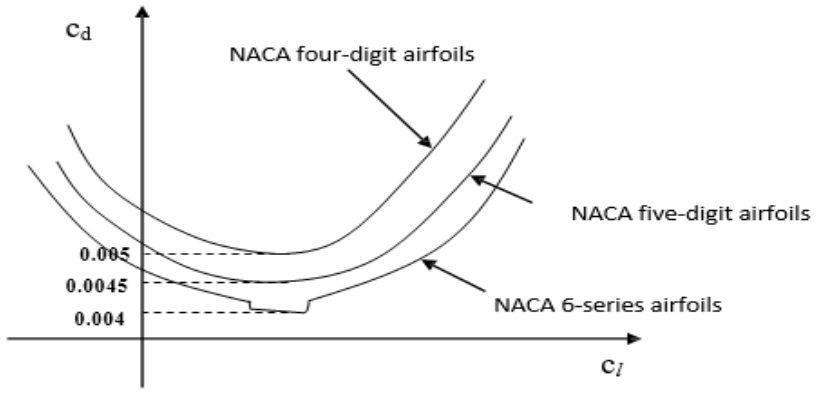

Figure 1.14. A general comparison between four-digit, five-digit and 6-series airfoil sections

Table 1.1: Characteristics of several NACA airfoil sections

No	Airfoil section	C_{lmax} at $Re=3\times10^6$	α_s (deg)	C_{mo}	$(C_l/C_d)_{max}$	C_{li}	C_{dmin}	$(t/c)_{max}$
1	0009	1.25	13	0	112	0	0.0052	9%
2	4412	1.5	13	-0.09	125	0.4	0.006	12%
3	2415	1.4	14	-0.05	122	0.3	0.0065	15%
4	23012	1.6	16	-0.013	120	0.3	0.006	12%
5	23015	1.5	15	-0.008	118	0.1	0.0063	15%
6	63_1-212	1.55	14	-0.004	100	0.2	0.0045	12%
7	63_2-015	1.4	14	0	101	0	0.005	15%
8	63_3-218	1.3	14	-0.03	103	0.2	0.005	18%
9	64-210	1.4	12	-0.042	97	0.2	0.004	10%
10	65_4-221	1.1	16	-0.025	120	0.2	0.0048	21%

For example, the NACA **633-218** airfoil section (see figure 1.13c) has 18% thickness-to-chord ratio. The position of the minimum pressure in this airfoil is located at 30 percent of the chord (the second digit). The ideal lift coefficient of the airfoil is 0.2 (the third digit). Finally, the lift coefficient range above and below the value of ideal lift coefficient is 0.3 (the subscript). It demonstrates that the bucket in Cd-C*l* diagram (see figure 1.14) begins from lift coefficient of 0 (since 0.3 - 0.3 = 0) and ends at 0.6 (since 0.3 + 0.3 = 0.6).

Table 1.2: The wing airfoil section of several prop-driven aircraft

No	Aircraft name	First flight	Max speed (knot)	Root airfoil	Tip airfoil	Average $(t/c)_{max}$
1	Cessna 550	1994	275	23014	23012	13%
2	Beech Bonanza	1945	127	23016.5	23015	15.75%
3	Cessna 150	1957	106	2412	2412	12%
4	Piper Cherokee	1960	132	65_2-415	65_2-415	15%
5	Dornier Do-27	1955	145	23018	23018	18%
6	Fokker F-27	1955	227	64_4-421	64_4-421	21%
7	Lockheed L100	1954	297	64A-318	64A-412	15%
8	Pilatus PC-7	1978	270	64_2-415	64_1-415	15%
9	Hawker Siddely	1960	225	23018	4412	15%
10	Beagle 206	1967	140	23015	4412	13.5%
11	Beech Super king	1970	294	23018-23016.5	23012	14.5%
12	Lockheed Orion	1958	411	0014	0012	13%
13	Mooney M20J	1976	175	63_2-215	641-412	13.5%
14	Lockheed Hercules	1951	315	64A318	64A412	15%
15	Thurston TA16	1980	152	64_2-A215	64_2-A215	15%
16	ATR 42	1981	269	43 series (18%)	43 series (13%)	15.5%
17	AIRTECH CN-235	1983	228	65_3-218	65_3-218	18%
18	Fokker 50	1987	282	64_4-421	64_4-415	18%

Figure 1.14 shows a general comparison between four-digit, five-digit and 6-series airfoil sections. Figure 1.15 demonstrates C*l*-α, Cm-α, and Cd-C*l* graphs for NACA 632-615 airfoil section. There are two groups of graphs, one for flap up and another one for flap down (60 degrees split flap). As noted, the flap deflection has doubled the airfoil drag (in fact Cd_{min}), increased pitching moment tremendously, but at the same time, has increased the lift coefficient by 1.2. Example 1.1 illustrates how to extract various airfoil characteristics (e.g. αs, C_{lmax}, and αo) from C*l*-α, Cm-α, and Cd-C*l* graphs.

Besides NACA airfoil sections, there are variety of other airfoil sections that have been designed in the past several decades for different purposes. Few examples are peaky, supercritical, modern, supersonic airfoils. Table 1.1 illustrates the characteristics of several NACA airfoil sections. Table 1.2 illustrates the wing airfoil sections for several prop-driven aircraft. Table 1.3 illustrates the wing airfoil sections for several jet aircraft. As noted, all are employing NACA airfoils, from GA aircraft Cessna 182 to fighter aircraft F-16 Falcon. Example 1.1 illustrates how to extract various airfoil characteristics (e.g. α_S, C_{lmax}, and α_O) from C*l*-α, C*l*-Cd, and Cm-α graphs.

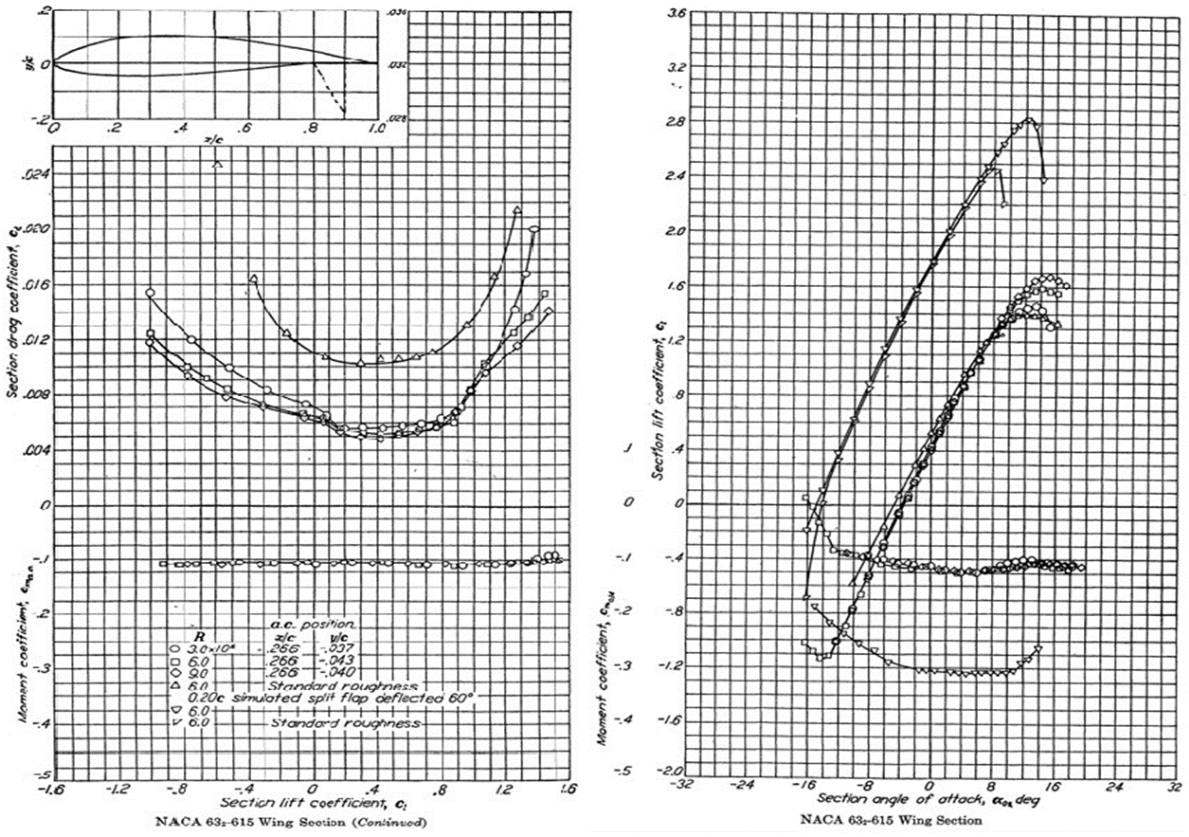

Figure 1.15: Cl-α, Cm-α, and Cd-Cl graphs of NACA 632-615 airfoil section

Table 1.3: The wing airfoil sections of several jet aircraft.

No	Aircraft name	First flight	Max speed (knot)	Root airfoil	Tip airfoil	Average $(t/c)_{max}$
1	F-15E strike Eagle	1982	Mach 2.5	64A (6.6%)	64A (3%)	4.8%
2	Beech Starship	1988	468	13.2%	11.3%	12.25%
3	Lockheed L-300	1963	493	0013	0010	11.5%
4	Cessna 500 Citation Bravo	1994	275	23014	23012	13%
5	Cessna 318	1954	441	2418	2412	15%
6	Gates Learjet 25	1969	333	64A-109	64_4-109	9%
7	Aero Commander	1963	360	64_1-212	64_1-212	12%
8	Lockheed Jetstar	1957	383	63A-112	63A-309	10.5%
9	Airbus 310	1982	595	15.2%	10.8%	13%
10	Rockwell/DASA X-31A	1990	1485	Transonic airfoil	Transonic airfoil	5.5%
11	Kawasaki T-4	1988	560	Supercritical airfoil (10.3%)	Supercritical airfoil (7.3%)	8.8%
12	Gulfstream IV-SP	1985	340	Sonic rooftop (10%)	Sonic rooftop (8.6%)	9.3%
13	Lockheed F-16	1975	Mach 2.1	64A-204	64A-204	4%
14	Fokker 50	1985	282	64_4-421	64_4-415	18%

Example 1.1

Identify C*l*i, Cdmin, Cm, (C*l*/C*d*)max, αo (deg), αs (deg), C*lmax*, ao (1/rad), (t/c)max of the NACA 63- 209 airfoil section (flap-up). You need to indicate the locations of all parameters on the airfoil graphs.

Solution:

By referring to figure 1.16, the required values for all parameters are as determined follows:

C*l*i	Cdmin	Cm	(C*l*/C*d*)max	αo (deg)	αs (deg)	C*lmax*	C*lα* (1/rad)	(t/c)max
0.2	0.0045	-0.03	118	-1.5	12	1.45	5.73	9%

The locations of all points of interest are illustrated in Figure 1.16.

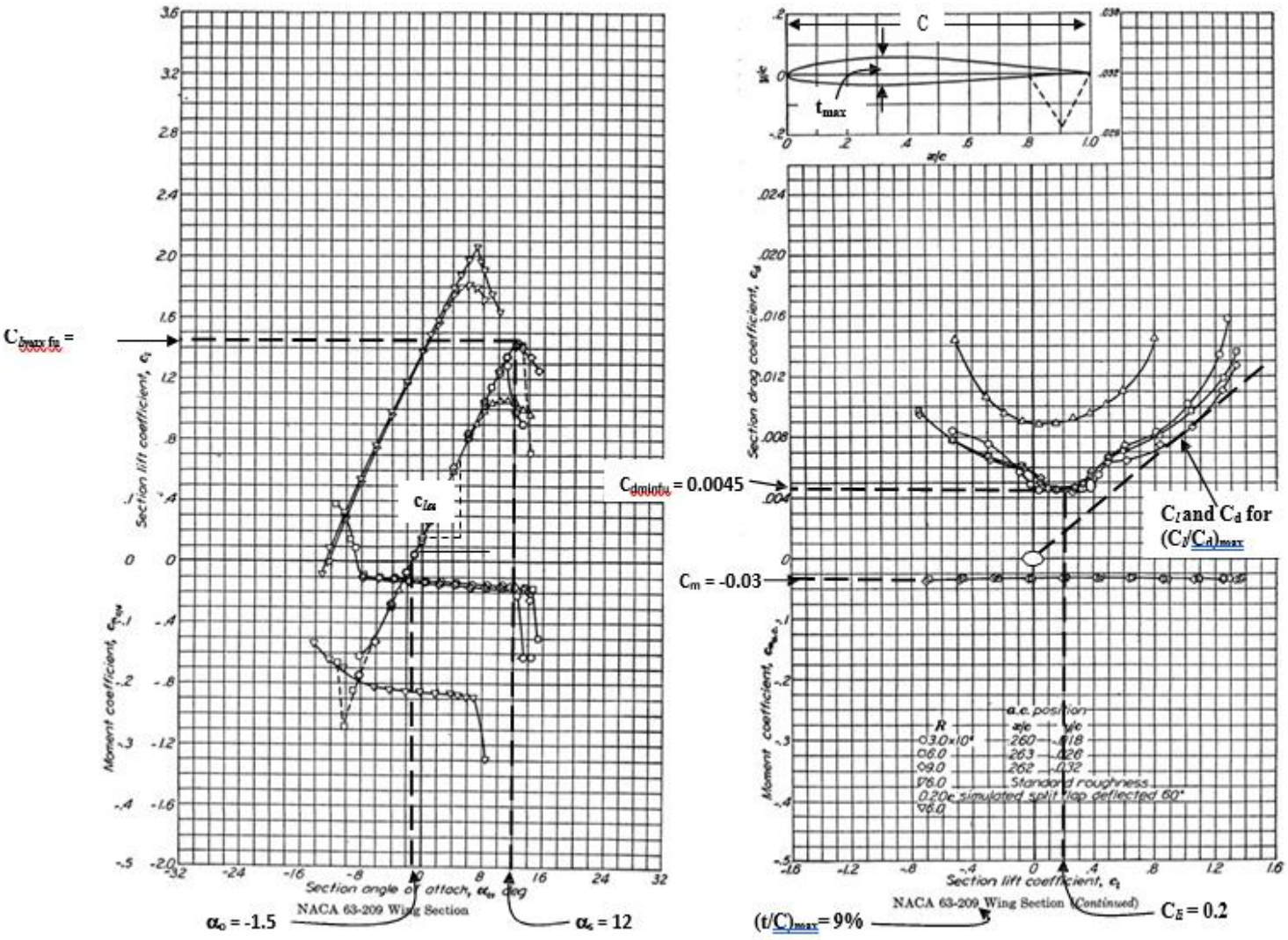

Figure 1.16 The locations of all points of interest of NACA 63-209 airfoil section (flap-up)

1.6 Practical Steps for Airfoil Section Selection: In the previous sections, the geometry of an airfoil section, airfoil design tools, NACA airfoil sections, significant airfoil parameters, and criteria for airfoil section are covered. In this section, the practical steps for wing airfoil section selection will be presented. It is assumed that an airfoil section data base (such as *NACA* or *Eppler*) is available and the wing designer is planning to select the best airfoil from the list. The steps are as follows:

1. Determine the average aircraft weight (W_{avg}) in cruising flight:

$$W_{avg} = \frac{1}{2}\left(W_i + W_f\right) \qquad 1.1$$

where W_i is the initial aircraft weight at the beginning of cruise and W_f is the final aircraft weight at the end of cruise.

2. Calculate the aircraft ideal cruise lift coefficient (C_{LC}). In a cruising flight, the aircraft weight is equal to the lift force ($L = W = \frac{1}{2}\rho v^2 S C_L = mg$), so: C_{LC}

$$C_{Lc} = \frac{2W_{avg}}{\rho V_c^2 S} \qquad 1.2$$

where V_c is the aircraft cruise speed, ρ is the air density at cruising altitude, and S is the wing planform area.

3. Calculate the wing cruise lift coefficient (C_{Lcw}). Basically, the wing is solely responsible for the generation of the lift. However, other aircraft components also contribute to the total lift; negatively, or positively; sometimes, as much as 20 percent. Thus the relation between aircraft cruise lift coefficient and wing cruise lift coefficient is a function of aircraft configuration. The contribution of fuselage, tail and other components will determine the wing contribution to aircraft lift coefficient. If you are at the preliminary design phase and the geometry of other components have not been determined yet, the following approximate relationship is recommended.

$$C_{Lcw} = \frac{C_{Lc}}{0.95} \qquad 1.3$$

In the later design phases; when other components are designed; this relationship must be clarified. A CFD software package is a reliable tool to determine this relationship.

4. Calculate the wing airfoil ideal lift coefficient (C_{Li}). The wing is a three-dimensional body, while an airfoil is a two-dimensional section. If the wing chord is constant, with no sweep angle, no dihedral, and the wing span is assumed to be infinity; theoretically; the wing lift coefficient would be the same as wing airfoil lift coefficient. However, at this moment, the wing has not been designed yet, we must resort to an approximate relationship. In reality, the span is limited, and in most cases, wing has sweep angle, and non-constant chord, so the wing lift coefficient will be slightly less than airfoil lift coefficient. For this purpose, the following approximate equation is recommended at this moment:

$$C_{Li} = \frac{C_{Lcw}}{0.9} \qquad 1.4$$

5. Calculate the aircraft maximum lift coefficient (C_{Lmax}):

$$C_{Lmax} = \frac{2W_{To}}{\rho_o V_s^2 S} \qquad 1.5$$

where V_S is the aircraft stall speed, ρ_o is the air density at sea level, and W_{TO} is the aircraft maximum take-off weight.

6. Calculate the wing maximum lift coefficient $(C_{L_{max}})_w$. With the same logic that was described in step 3, the following relationship is recommended.

$$(C_{L_{max}})_w = \frac{C_{Lmax}}{0.95} \qquad 1.6$$

7. Calculate the wing airfoil gross maximum lift coefficient $(C_{L_{max}})_{\text{gross}}$.

$$(C_{L_{max}})_{gross} = \frac{(C_{L_{max}})_w}{0.90} \qquad 1.7$$

where the wing airfoil "*gross*" maximum lift coefficient is the airfoil maximum lift coefficient in which the effect of high lift device (e.g. flap) is included.

8. Select/Design the high lift device (type, geometry, and maximum deflection). This step will be discussed in detail later.

9. Determine the high lift device (HLD) contribution to the wing maximum lift coefficient ($\Delta C_{L_{HID}}$). This step will also be discussed in detail later.

10. Calculate the wing airfoil "*net*" maximum lift coefficient ($C_{L_{max}}$)

$$C_{L_{max}} = (C_{L_{max}})_{gross} - \Delta C_{L_{HID}} \qquad 1.8$$

11. Identify airfoil section alternatives that deliver the desired C_{li} (step 4) and C_{lmax} (step 10). This is a very essential step. Figure 5.23 shows a collection of C_{li} and C_{lmax} for several NACA airfoil sections in just one graph. The horizontal axis represents the airfoil ideal lift coefficient while the vertical axis the airfoil maximum lift coefficient. Every black circle represents one NACA airfoil section. For C_{li} and C_{lmax} of other airfoil sections, if there is no airfoil section that delivers the desired C_{li} and C_{lmax}, select the airfoil section that is nearest to the design point (desired C_{li} and C_{lmax}).

12. If the wing is designed for a high subsonic passenger aircraft, select the thinnest airfoil (the lowest $(t/c)_{max}$). The reason is to reduce the critical Mach number (M_{cr}) and drag-divergent Mach number (M_{dd}). This allow the aircraft fly closer to Mach one before the drag rise is encountered. In general, a thinner airfoil will have a higher M_{cr} than a thicker airfoil. Figure 1.18 shows the typical variation of the wing zero-lift and wave drag coefficient versus Mach number for four wings with airfoil thickness ratio as a parameter. As noted, the M_{dd} of the wing with 9 percent thickness-to-chord ratio occurs at the value of about 0.88. By reducing the wing $(t/c)_{max}$ to 6 and 4 percent, the magnitude of the drag rise is progressively reduced, and the value of M_{dd} is increased, moving closer to Mach one.

13. Among several acceptable alternatives, select the optimum airfoil section by using a comparison table. A typical comparison table which includes a typical weight for each design requirement is a rich resource for the systematic procedure of the selection technique and table construction.

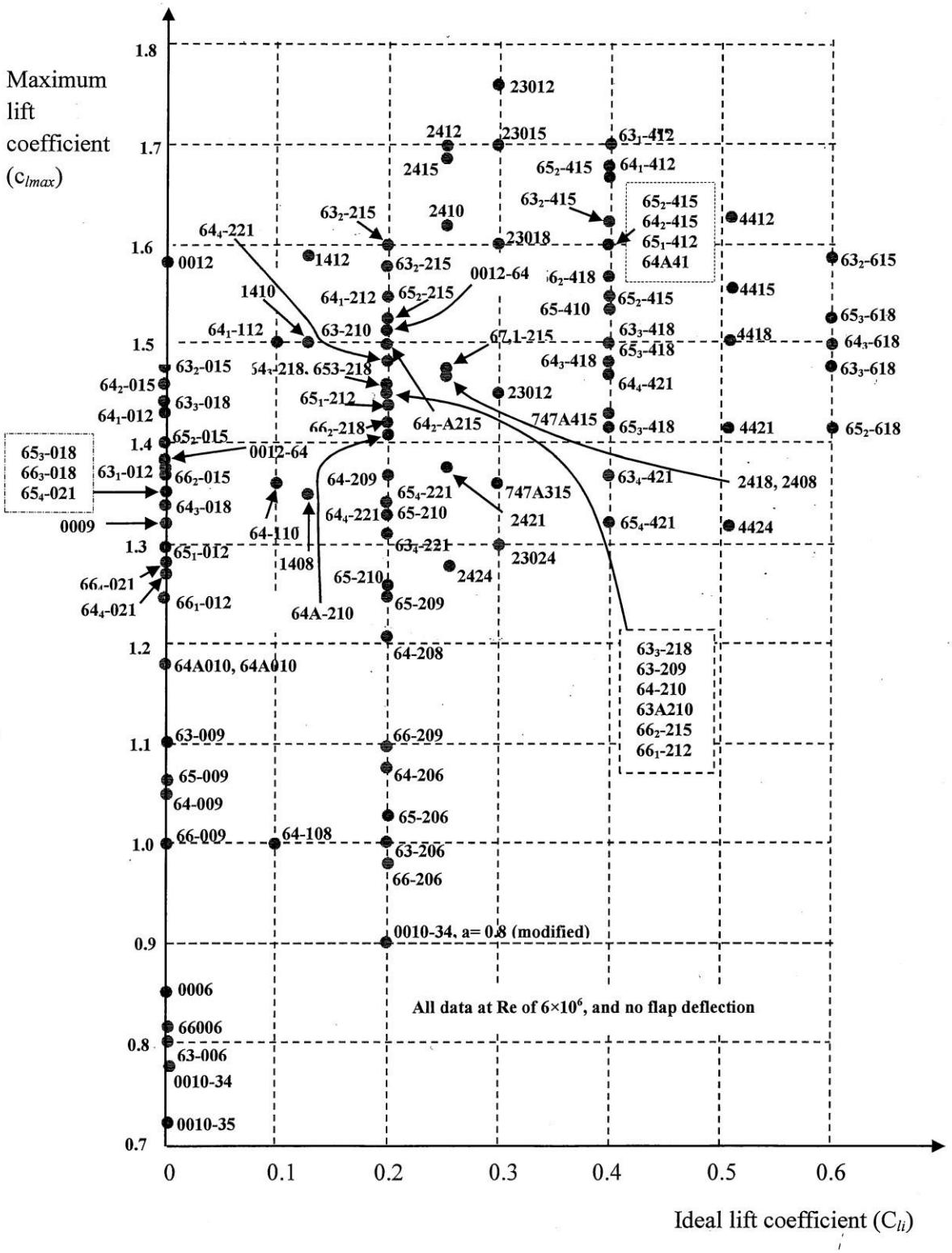

Figure 1.17: Maximum lift coefficient versus ideal lift coefficient for several NACA airfoil section

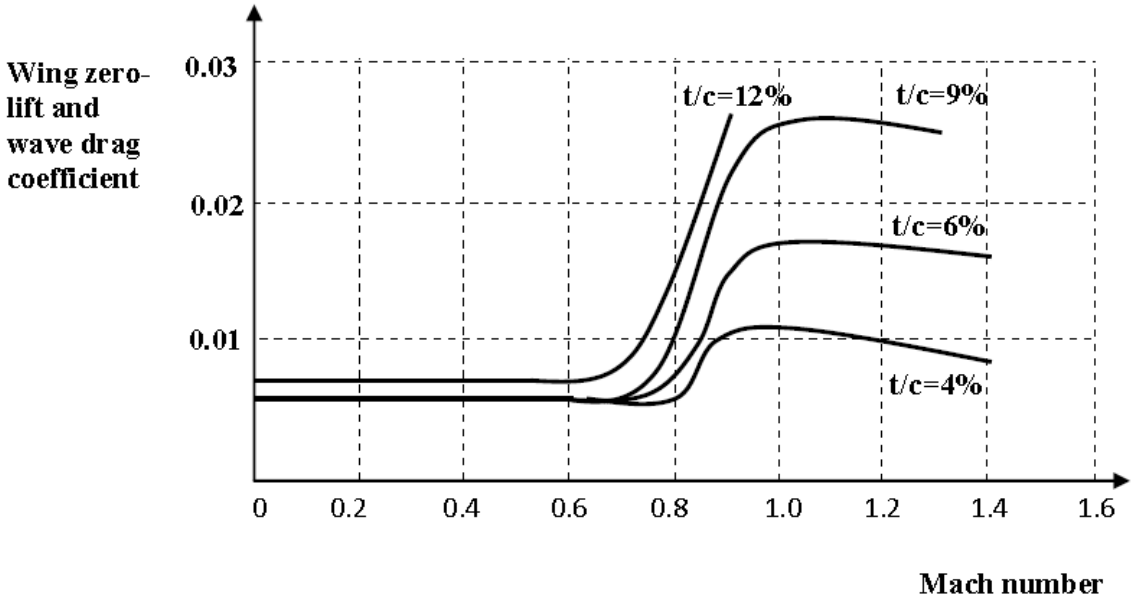

Figure 1.18: Variation of wing zero-lift and wave drag coefficient versus Mach number for various airfoil thickness ratio.

Example 1.2: Select a NACA airfoil section for the wing for a jet non-maneuverable aircraft with the following characteristics:
m_{TO} = 4000 kg, S = 30 m^2, Vc = 250 knot (at 3000 m), Vs = 65 knot (sea level)
The high lift device (split flap) will provide $\Delta C_{L_{HID}} = 0.8$ when deflected.

Solution:
Ideal lift coefficient:

$$C_{Lc} = \frac{2W_{avg}}{\rho V_c^2 S} = \frac{2 \times 4000 \times 9.81}{0.9(250 + 0.514)^2 \times 30} = 0.176$$

$$C_{Lcw} = \frac{C_{Lc}}{0.95} = \frac{0.176}{0.95} = 0.185$$

$$C_{Li} = \frac{C_{Lcw}}{0.9} = \frac{0.185}{0.9} = 0.205 \cong 0.2$$

Maximum lift coefficient:

$$C_{Lmax} = \frac{2W_{To}}{\rho_o V_S^2 S} = \frac{2\times4000\times9.81}{1.225(65+0.514)^2\times30} = 1.909$$

$$(C_{L_{max}})_w = \frac{C_{Lmax}}{0.95} = \frac{1.909}{0.95} = 2.01$$

$$(C_{L_{max}})_{gross} = \frac{(C_{L_{max}})_w}{0.90} = \frac{2.01}{0.90} = 2.233$$
$$\therefore C_{L_{max}} = (C_{L_{max}})_{gross} - \Delta C_{L_{HID}} = 2.233 - 0.8 = 1.433$$

Thus, we need to look for NACA airfoil sections that yield an ideal lift coefficient of 0.2 and a net maximum lift coefficient of 1.433. Referring to figure 1.16, we find the following airfoils whose characteristics match with our design requirements (all have C_{li} = 0.2, C_{lmax} =1.43):

633-218, 64-210, 661-212, 662-215, 653-218

Now we need to compare these airfoils to see which one is the best

Table 1.4: A comparison among five airfoil candidates for use in the wing

No	NACA	C_{dmin}	C_{mo}	α_s (deg) Flap up	α_o (deg) $\delta_f = 60^o$	$(C_l/C_d)_{max}$	Stall quality
1	63_3-218	0.005	-0.028	12	-12	100	Docile
2	64-210	0.004	-0.040	12	-13	75	Moderate
3	66_1-212	0.0032	-0.030	12	-13	86	Sharp
4	66_2-215	0.0035	-0.028	14	-13.5	86	Sharp
5	65_3-218	0.0045	-0.028	16	-13	111	Moderate

The best airfoil is the airfoil whose C_{mo} is the lowest, the C_{dmin} is the lowest, the α_s is the highest, the $(C_l/C_d)_{max}$ is the highest, and the stall quality is docile.

By comparing the numbers in the above table, we can conclude the followings:

1- The NACA airfoil section 66_1-212 yields the highest maximum speed, since it has the lowest C_{dmin} (0.0032).
2- The NACA airfoil section 65_3-218 yields the lowest stall speed, since it has the highest stall angle (16 degrees).
3- The NACA airfoil section 65_3-218 yields the highest endurance, since it has the highest $(Cl/Cd)_{max}$ (111).
4- The NACA 63_3-218 yields the safest flight, due to its docile stall quality.
5- The NACA airfoil sections 63_3-218, 662-215, and 653-218 deliver the lowest control problem in flight, due to the lowest C_{mo} (-0.028).

Since the aircraft is a non-maneuverable aircraft, the stall quality cannot be sharp; hence NACA airfoil sections 66_1-212 and 66_2-215 are not acceptable. If the safety is the highest requirement, the best airfoil is NACA 63_2-218. On the other hand, if the low cost is the most important requirement, NACA 64-210 with the lowest C_{dmin} is the best. However, if the aircraft performance (stall speed, endurance or maximum speed) are of greatest important design requirement, the NACA airfoil section 65_3-218, 65_3-218, or 66_1-212 are the best respectively. This may be performed by using a comparison table incorporating the weighted design requirements.

1.6 Other Types of Airfoils: After the six-series sections, aerofoil design became more specialized with airfoils designed for their application. In the mid-1960s, Whitcomb's "supercritical" aerofoil allowed flight with high critical Mach numbers (operating with compressibility effects, producing in wave drag) in the transonic region. The NACA seven and eight series were designed to improve some aerodynamic characteristics. In addition to the NACA aerofoil series, there are many other types of airfoils in use.

To remain competitive, the major industrial companies generate their own airfoils. One example is the peaky-section airfoils that were popular during the 1960s and 1970s for the high-subsonic flight regime. Aerofoil designers generate their own purpose-built airfoils with good transonic performance, good maximum lift capability, thick sections, low drag, and so on – some are in the public domain but most are held commercial in confidence for strategic reasons of the organizations. Subsequently, more transonic supercritical airfoils were developed, by both research organizations and academic institutions. One such baseline design in the United Kingdom is the RAE 2822 aerofoil section, whereas the CAST 7 evolved in Germany. It is suggested that readers examine various aerofoil designs.

1.7 National Aviation Authority: A national aviation authority (NAA) or civil aviation authority is a government statutory authority in each country that oversees the approval and regulation of civil aviation.

1.8 Airworthiness: Airworthiness is the measure of an aircraft's suitability for safe flight. Certification of airworthiness is initially conferred by a certificate of airworthiness from a national aviation authority NAA, and is maintained by performing the required maintenance actions. The application of airworthiness defines the condition of an aircraft and supplies the basis for judgment of the suitability for flight of that aircraft, in that it has been designed with engineering rigor, constructed, maintained and is expected to be operated to approved standards and limitations, by competent and approved individuals, who are acting as members of an approved organization and whose work is both certified as correct and accepted on behalf of the State.

University of Technology

Mechanical Engineering

Department

2017-2018

Chapter Four

Tail Unit Designing

Dr. Ahmed Shandookh

AIRCRAFT BRANCH

4.1. Introduction

As introduced in chapter 2, the next appropriate step after wing desig n would be the tail design. In this chapter, after describing the tail primary functions, and introducing fundamentals that govern the tai l performance, techniques and procedure to design the horizontal tail and vertical tail will be provided. At the end of the chapter a fu lly solved example that illustrates the implementation of the design technique will be presented.

Horizontal tail and vertical tail (i.e. tails) along with wing are re ferred to as lifting surfaces. This name differentiates tails and wing from control surfaces namely aileron, elevator, and rudder. Due to t his name, several design parameters associated with tails and wing; s uch as airfoil, planform area, and angle of attack; are similar. T hus, several tails parameters are discussed in brief. The major diffe rence between wing design and tail design originates from the primar y function of tail that is different from wing. Primary function of t he wing to generate maximum amount of lift, while tail is supposed t o use a fraction of its ability to generate lift. If at any instance of a fli ght mission, tail nears its maximum angle of attack (i.e. tail stall an gle); it indicates that there was a mistake in the tail design process. I n some texts and references, tail is referred to as empennage.

The ail in a conventional aircraft has often two components of horizontal tail and vertical
tail and carries two primary functions:

1. Trim (longitudinal and directional)
2. Stability (longitudinal and directional)

Since two conventional control surfaces (i.e. elevator and rudder) are indeed parts of the tails to
implement control, it is proper to add the following item as the third function of tails:

3. Control (longitudinal and directional)

These three functions are described in brief here; however, more details are presented in later sections. The first and primary function of horizontal tail is longitudinal trim; also referred to as equilibrium or balance. But the first and primary function of vertical tail is directional stability. The reason is that an aircraft is usually symmetric

about xz plane, while the pitching moment of the wing about aircraft center of gravity must be balanced via a component.

Longitudinal trim in a conventional aircraft is applied through the horizontal tail. Several pitching moments, namely, longitudinal moment of the wing's lift about aircraft center of gravity, wing aerodynamic pitching moment, and sometimes engine thrust's longitudinal moment need to be trimmed about y axis. The summation of these three moments about aircraft center of gravity is often negative; hence the horizontal tail often generates a negative lift to counteract the moment. For this reason, the horizontal tail setting angle is often negative. Since the aircraft center of gravity is moving along x axis; due to fuel burn during flight duration; the horizontal tail is responsible for longitudinal trim throughout flight time. To support the longitudinal trim ability of the aircraft, conventional aircraft employ elevator as part of its horizontal tail.

Since conventional aircraft are almost always manufactured symmetrically about xz plane, the trim is not a major function for vertical tail. However, in few instances, vertical tail has the primary function of directional trim or lateral trim. In a multi-engine aircraft, the vertical tail has great responsibility during one engine inoperative (OEI) situation to maintain directional trim. The vertical tail must generate a yawing moment to balance the aircraft for the yawing moment generated by active engines. Even in single engine prop-driven aircraft, the vertical must counteract the rolling moment generated by propeller rotation. This is to maintain aircraft lateral trim and prevent an unwanted roll. For this case, the vertical tail has often installed with few degrees relative to xz plane. The aircraft trim requirement provides the main design requirements in the tail design process.

The second function of the tails is to providing stability. The horizontal tail is responsible to maintain the longitudinal stability, while the vertical tail is responsible to maintain the directional stability. Aircraft stability is defined as the tendency of an aircraft to return to the original trim conditions if diverted by a disturbance. The major disturbance source is the atmospheric phenomena such as gust. The stability requirement must also be included in the tail design requirements' list.

The third major function of the tails is "control". The elevator as part of the horizontal tail is designed to provide longitudinal control, while

the rudder as part of the vertical tail is responsible for providing the directional control. Tails must be powerful enough to control the aircraft such that the aircraft is able to change the flight conditions from one trim condition (say cruise) to another new trim condition (say take-off and landing). For instance, during take-off, the tail must be able to lift the fuselage nose in a specified pitch rate.

In general, tail is designed based on the trim requirements, but later revised based on stability and control requirements. The following are the tail parameters which need to be determined during the design process:

1. Tail configuration
2. Horizontal tail location with respect to fuselage (aft tail or canard)

❖ Horizontal tail

3. Planform area (S_h)
4. Tail arm (l_h)
5. Airfoil section
6. Aspect ratio (AR_h)
7. Taper ratio (λ_h)
8. Tip chord ($C_{h\text{-}tip}$)
9. Root chord ($C_{h\text{-}root}$)
10. Mean Aerodynamic Chord (MAC_h or C_h)
11. Span (b_h)
12. Sweep angle (Λ_h)
13. Dihedral angle (Γ_h)
14. Tail installation
15. Incidence (i_h)

❖ Vertical tail

16. Planform area (S_V)
17. Tail arm (l_V)
18. Airfoil section
19. Aspect ratio (AR_V)
20. Taper ratio (λ_V)
21. Tip chord ($C_{V\text{-}tip}$)
22. Root chord ($C_{V\text{-}rot}$)
23. Mean Aerodynamic Chord (MAC_V or C_V)
24. Span (b_V)
25. Sweep angle (Λ_V)
26. Dihedral angle (Γ_V)
27. Incidence (i_V)

All 27 tail parameters listed above must be determined in the tail design process. Most parameters are finalized through technical calculations, while a few parameters are decided via an engineering selection approach. There are few other intermediate parameters such as downwash angle, side wash angle, and effective angle of attack which will be used to calculate some tail parameters. These are determined in the design process, but not employed in the manufacturing period.

As discussed in Chapter 2, the "Systems Engineering" approach has been adopted as the basic technique to design the tail. The tail design technique has been developed by this approach to satisfy all design requirements while maintaining low cost in an optimum fashion. Figure 4.1 illustrates the block diagram of the tail design process. As it was explained in Chapter 2, the aircraft design is an iterative process; therefore, this procedure (tail design) will be repeated several times until the optimum aircraft configuration has been achieved. The design of vertical and horizontal tails might be performed almost in parallel. However, there is one step in the vertical tail design (i.e. spin recovery) that the effect of horizontal tail into vertical tail is investigated. The details on each step will be introduced in the later sections. The purpose of this chapter is to provide design considerations, design technique, and design examples for the preliminary design of the aircraft tail.

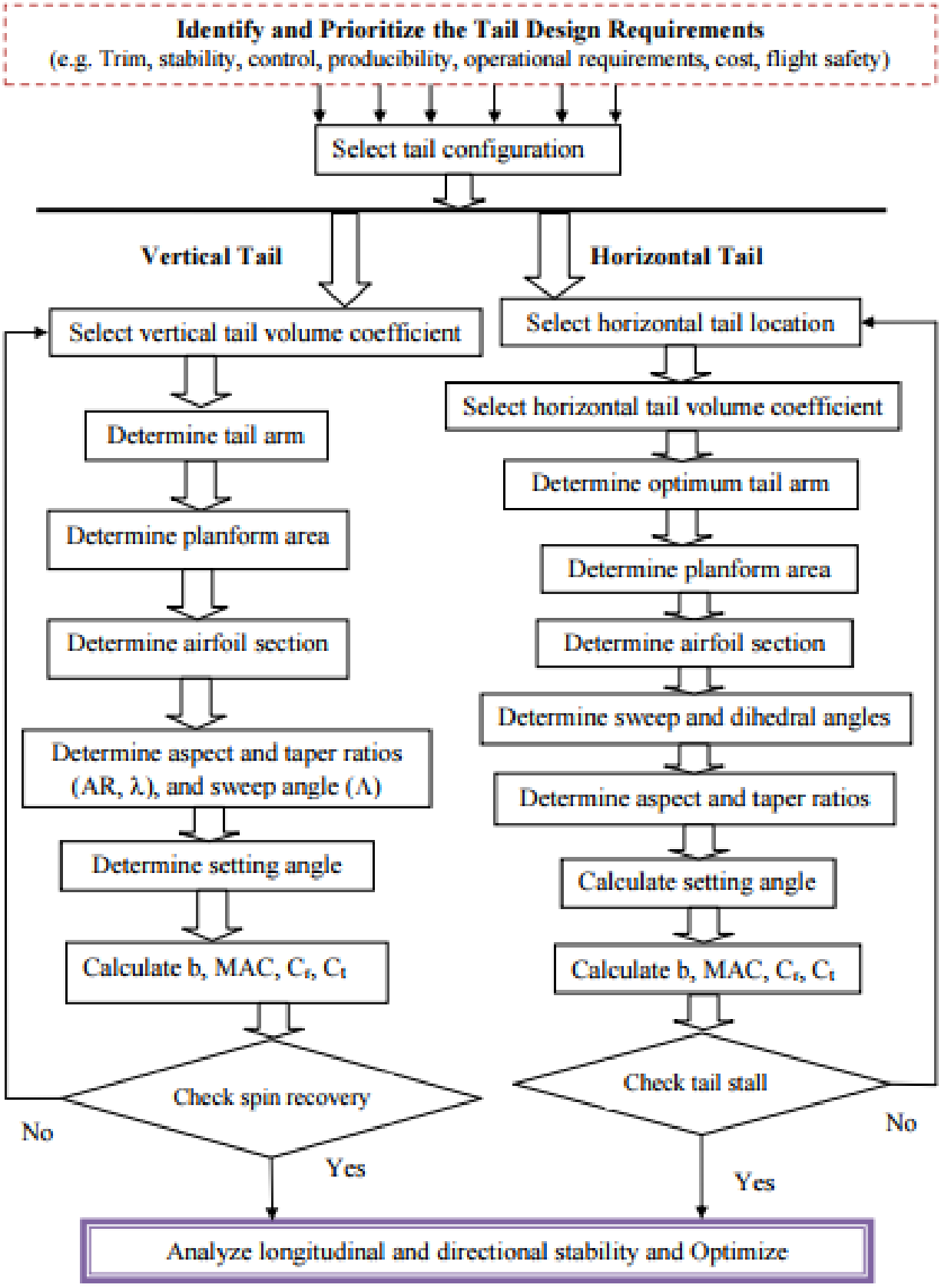

Figure 4.1. The tail design procedure

4.2. Tail configuration

4.2.1. Basic Tail Configuration

The purpose of this section is to present design requirements, and design information related to the selection of the tail configuration. The term “tail” in this section means the combination of horizontal and vertical tail. The first step in the tail design is the selection of the tail configuration. The choice of the tail configuration is the output of a selection process, not the result of a mathematical calculation. The decision for the selection of the tail configuration must be made based on the reasoning, logic and evaluation of various configurations against design requirements.

The list of design requirements that must be considered and satisfied in the selection of tail configurations are as follows:

1. Longitudinal trim
2. Directional trim
3. Lateral trim
4. Longitudinal stability
5. Directional stability
6. Lateral stability
7. Manufacturability and controllability
8. Handling qualities (e.g. passenger comfort)
9. Stealth (only in some specific military aircraft)
10. Operational requirements (e.g. pilot view)
11. Airworthiness (e.g. safety, tail stall, and deep stall)
12. Survivability (e.g. spin recovery)
13. Cost
14. Competitiveness (in the market)
15. Size limits (for example, an aircraft may be required to have a limited height; for instance, for the hangar space limits. This will influence the vertical tail configuration)

The technical details of these requirements must be established prior to the selection of the tail configuration. Often, no single tail configuration can satisfy all design requirements; hence, a

compromise must be made. After a few acceptable candidates are prepared, a table based on the systems engineering approach must be provided to determine the final selection; i.e. best choice. Sometimes a design requirement (such as lateral stability) is completely ignored (i.e. sacrificed), to satisfy other more important design requirements (such as maneuverability or stealth requirements). In general, the following tail configurations are available that can satisfy the design requirements in one way or another:

1. Aft tail and one aft vertical tail

2. Aft tail and twin aft vertical tail

3. Canard and aft vertical tail

4. Canard and twin wing vertical tail

5. Triplane (i.e. aft tail as aft plane, and canard as fore-plane plus wing as the third plane)

6. Tailless (delta wing with one vertical tail)

7. No formal tail (also known as “flying wing”, such as B-2 Spirit.

Figure 4.2 depicts these configurations. Based on the statistics, majority of aircraft designers (about 85 percent) are selecting the aft tail configuration. About 10 percent of current aircraft have canard. And about 5 percent of today’s aircraft have other configurations that could be called as unconventional tail configuration.

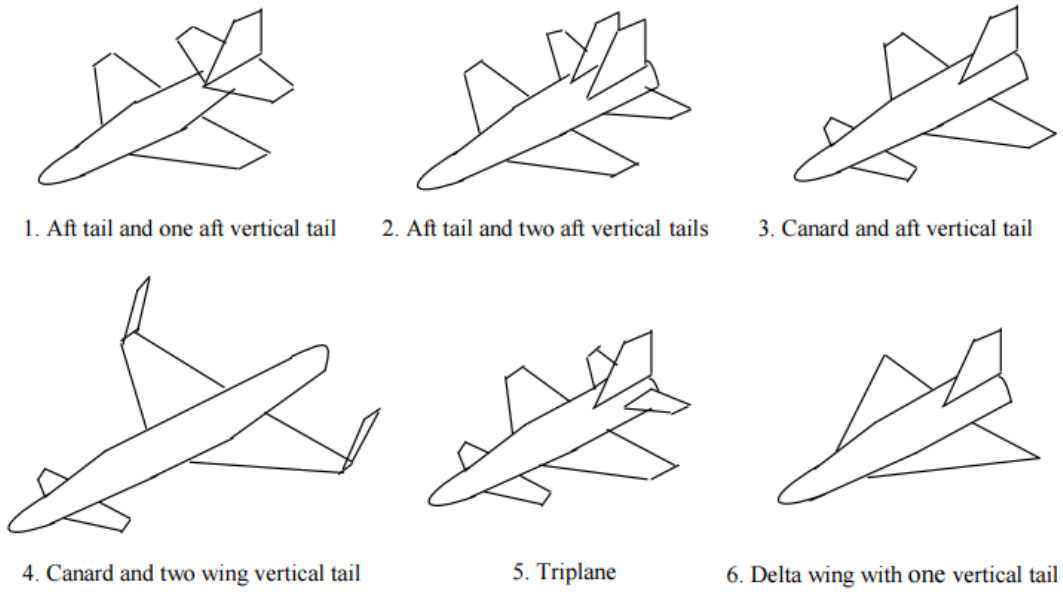

Figure 4.2. Basic tail configurations

The basic rule for the selection of the tail configuration is as follows: In general, the conventional aft tail configuration (Figure 4.2-1) is often able to satisfy all design requirements, unless one or more requirements imply for another configuration. Thus, it is recommended to begin with conventional aft tail configuration and then to evaluate its features against the design requirements. If one or more requirements are not satisfying, change to a new configuration nearest with the current configuration, until all requirements could be satisfied. If the aircraft is in the manufacturing phase and a change is needed to improve the longitudinal and directional stability, one can utilize a smaller auxiliary horizontal tail (sometimes referred to as stabilon) and ventral stake. These tricks are employed in the twin-turboprop regional transport aircraft Beech 1900D.

4.2.2. Aft Tail Configuration

Aft tail has several configurations that all can satisfy the design configurations. Each has unique advantages and disadvantages. The purpose of this section is to provide a comparison between these configurations to enable an aircraft designer to make decision and to select the best one. The aft tail configurations are as follows: 1. Conventional, 2. T-shape, 3. Cruciform, 4. H-shape, 5. Triple-tail, 6. V- tail, 7. Inverted V-tail, 8. Improved V-tail 9. Y-tail, 10. Twin vertical tail, 11. Boom-mounted, 12. Inverted boom-mounted, 13. Ring-shape, 14. Twin T, 15 .half T, 16. U-tail. Figure 4.3 and 4.5 provides several aft tail configurations.

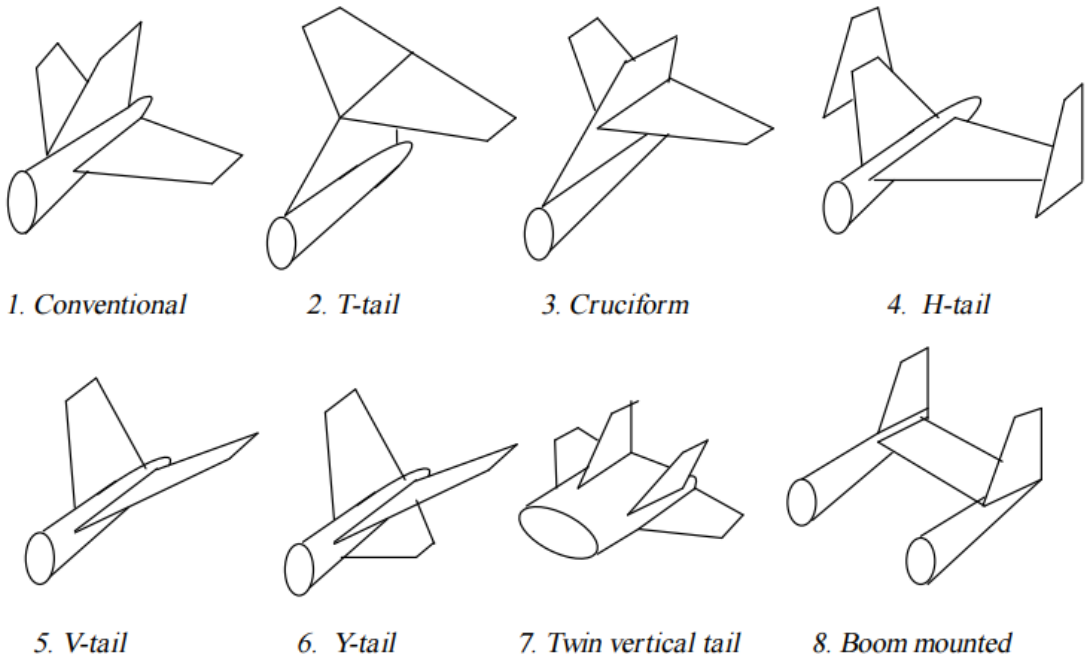

Figure 4.3. Several aft tail configurations

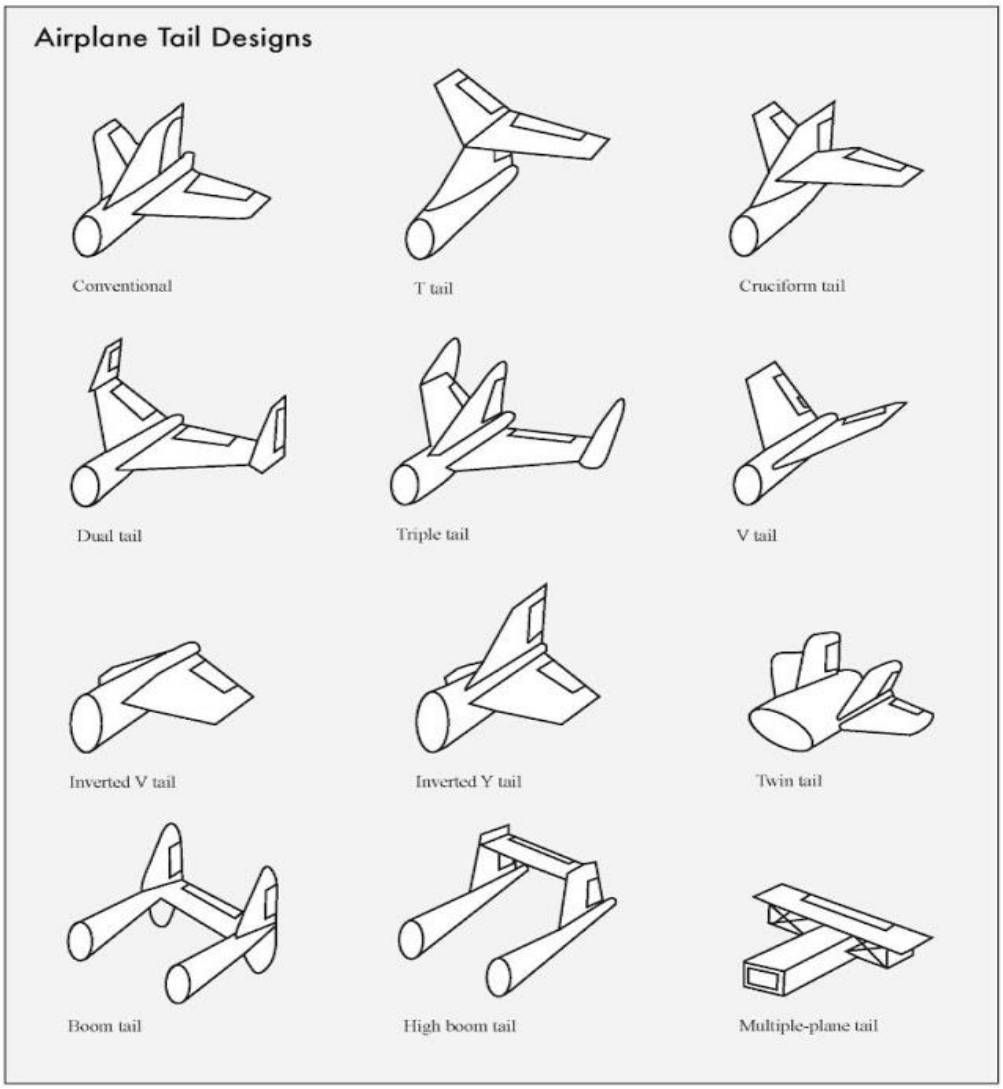

Figure 4.4. All aft tail configurations

1. Conventional

The conventional tail or inverted T-shape configuration (see figure 4.3-1) is the simplest configuration and the most convenient to perform all tail functions (i.e. trim, stability, and control). The analysis and evaluation of the performance of a conventional tail is straight forward. This configuration includes one horizontal tail (two left and right sections); located on the aft fuselage; and one vertical tail (one section); located on top of the aft fuselage. Both horizontal and vertical tails are located and mounted to the aft of fuselage. The horizontal tail is mainly employed to satisfy the longitudinal trim and stability requirements, while vertical tail is mainly used to satisfy the directional trim and stability requirements. If the designer has low experience, it is recommended to initially select the conventional tail configuration. Almost all flight dynamics textbook examines the features of a conventional tail, but not every flight dynamics textbook discusses the characteristics of other tail configurations. The

designer must be professional and skillful on the area of the trim analysis, stability analysis, and control analysis, if other configurations are selected. This is one of the reasons that about 60 percent of current aircraft in service have conventional tail. Furthermore, it has light weight, efficient, and performs at regular flight conditions. GA aircraft such Cessna 172, Cessna 560 Citation, Beech King Air C90B, Learjet 60, Embraer EMB-314 Super Tucano, Socata TBM 700, and Pilatus PC-9; large transport aircraft such as Fokker 60, Boeing 747, Boring 777, Airbus 340, and fighter aircraft such as F-16 Eagle, Harrier GR. Mk 7, and Panavia Tornado F. Mk3 all have conventional tail.

2 .T-tail

A T-tail is an aft tail configuration (see figure 4.3-2) that looks like the letter "T"; which implies the vertical tail is located on top of the horizontal tail. The T-tail configuration is another aft tail configuration that provides a few advantages, while it has a few disadvantages. The major advantage of a T-tail configuration is that it is out of the regions of wing wake, wing downwash, wing vortices, and engine exit flow (i.e. hot and turbulent high-speed gas). This allows the horizontal tail to provide a higher efficiency, and a safer structure. The lower influence from the wing results in a smaller horizontal tail area; and the lower effect from the engine leads in a less tail vibration and buffet. The less tail vibration increases the life of the tail with a lower fatigue problem. Furthermore, another advantage of the T-tail is the positive influence of horizontal tail on the vertical tail. It is referred to as the end-plate effect and results in a smaller vertical tail area .In contrast, the disadvantages that associated with a T-tail are: 1. heavier vertical tail structure, 2. deep stall. The bending moment created by the horizontal tail must be transferred to the fuselage through the vertical tail. This structural behavior requires the vertical tail main spar to be stronger; which cause the vertical tail to get heavier. Aircraft with T-tail are subject to a dangerous condition known as the deep stall ؛which is a stalled condition at an angle of attack far above the original stall angle. T-tail Aircraft often suffer a sever pitching moment instability at angles well above the initial stall angle of about 13 degrees, without wing leading edge high lift device, or about 18 degrees, with wing leading edge high lift device. If the pilot allows the aircraft to enter to this unstable region, it might rapidly pitch up to a higher angle of about 40 degrees. The causes of the instability are fuselage vortices, shed from the forward portion of the fuselage at high angles of attack, and the wing and engine wakes. Thus, the horizontal tail contribution on the longitudinal stability is largely reduced. Eventually, at a higher angle of attack, the horizontal tail exits the wing and nacelle wakes and the aircraft become longitudinally stable (see figure 4.5).

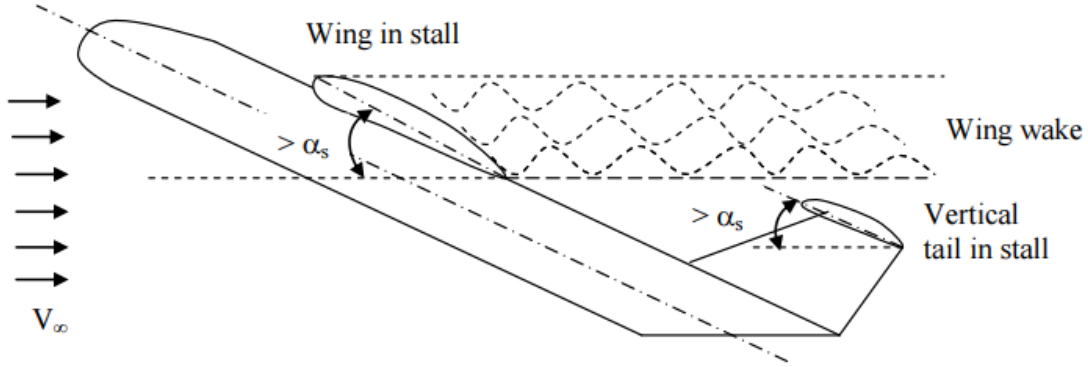

Figure 4.5. Deep stall in a T-tail configuration aircraft

This condition may be assumed as a stable condition, but it accompanies an enormous drag along with a resulting high rate of descent. At this moment, the elevator and aileron effectiveness have been severely reduced because both wing and horizontal tail are stalled at the very high angle of attack. This is known as a locked-in deep stall, a potentially fatal state. The design solutions to avoid a deep stall in a T-tail configuration are to:

1. Ensure a stable pitch down at the initial stall,

2. Extend the horizontal tail span substantially beyond the nacelles, and

3. Employ a mechanism to enable full down elevator angles if a deep stall occurs.

In addition, the aircraft must be well protected from the initial stall by devices such as stick shaker, lights, and stall horn. Despite above mentioned disadvantages of T-tail, it becomes more and popular among aircraft designers. About 25 percent of today's aircraft employ T-tail configuration. It is interesting to note that the GA aircraft Piper Cherokee has two versions; Cherokee III with conventional tail, and Cherokee IV with T-tail. The aircraft has a single piston engine at the nose and a low wing configuration. Several GA and transport aircraft such as Grob Starto 2C, Cessna 525 Citation-Jet, Beech Super King Air B200, Beech-jet T-1A Jayhawk, Learjet 60, Gulfstream IV, MD-90, Boeing 727, Fokker 100, AVRO RJ115, Bombardier BD 701 Global Express, Dassault Falcon 900, Sky Arrow 1450L, Embraer EMB-120, Airbus A400M, and Boeing (formerly McDonnell Douglas) C-17 Globemaster III employ T-tail configuration.

3. Cruciform

Some tail designers have combined the advantages of conventional tail and T-tail and came up with a new configuration known as cruciform (see figure 4.3-3). Thus, the disadvantages of both configurations are

considerably released. The cruciform; as the name implies; is a combination of horizontal tail and vertical tail such that it looks like a cross or "+" sign. This means that the horizontal tail is installed at almost the middle of the vertical tail. The location of the horizontal tail (i.e. its height relative to the fuselage) must be carefully determined such that the deep stall does not occur and at the same time, the vertical tail does not get heavy. Several aircraft such as Thurston TA16, Dassault Falcon 2000, ATR 42-400, Dassault Falcon 900B, Jetstream 41, Hawker 100, Mirage 2000D employ the cruciform tail configuration.

4. H-tail

The H-tail (see figure 4.3-4), as the name implies, looks like the letter "H". H-tail comprised of one horizontal tail in between two vertical tails. The features associated with an H-tail are as follows:

1. At high angles of attack, the vertical tail is not influenced by the turbulent flow coming from fuselage.
2. In a multiengine turboprop aircraft, vertical tails are located behind the prop-wash region. This causes the vertical tail to have higher performance in the inoperative engine situation.
3. The vertical tail end-plate effect improves the aerodynamic performance of the horizontal tail.
4. In military aircraft, the engine very hot exhaust gasses could be hidden from radars or infrared missiles. This technique has been employed the close support aircraft Fairchild A-10 Thunderbolt.
5. The H-tail allows the twin vertical tail span to be shorter. The aircraft "Lockheed constellation" had to employ an H-tail configuration to be able to park inside short height hangars.
6. The lateral control of the aircraft will be improved due to the shorter vertical tail span.
7. The H-tail allows the fuselage to be shorter, since the tail can be installed on a boom.
8. The H-tail is slightly heavier than conventional; and T-tail configuration. The reason is that the horizontal tail must be strong enough to support both vertical tails.
9. The structural design of the H-tail is more tedious than conventional tail.

As can be noticed, an H-tail configuration tends to offer several advantages and disadvantages; hence, the selection of an H-tail must be the result of a compromise process. Several GA and military aircraft such as Sadler A-22

Piranha, T-46, Short Skyvan, and Fairchild A-10 Thunderbolt utilize H-tail configuration.

5. V-tail

When the major goal of the tail design is to reduce the total tail area, the V-tail (see figure 4.3-5) is a proper candidate. As the name implies, the V-tail configuration has two sections, which forms a shape that looks like the letter "V". In another word, a V-tail is like a horizontal tail with high anhedral angle and without any vertical tail. Two sections of a V-tail act as both horizontal and vertical tails. Due to the angle of each section, the lift perpendicular to each section has two components; one in y-direction, and one in z-direction. If no controller is deflected, two components in the y-direction cancel each other, while two lift components in the z-direction are added together. The V-tail may perform the longitudinal and directional trim role satisfactorily, but it has deficiencies in maintaining the aircraft longitudinal and directional stability. In addition, the V-tail design is more susceptible to Dutch roll tendencies than a conventional tail, and total reduction in drag is minimal.

The V-tail design utilizes two slanted tail surfaces to perform the same functions as the surfaces of a conventional elevator and rudder configuration. The movable surfaces, which are usually called ruddervator, are connected through a special linkage that allows the control wheel to move both surfaces simultaneously. On the other hand, displacement of the rudder pedals moves the surfaces differentially, thereby providing directional control. When both rudder and elevator controls are moved by the pilot, a control mixing mechanism moves each surface the appropriate amount. The control system for the V-tail is more complex than that required for a conventional tail. Ruddervator induce the undesirable phenomenon of the adverse roll-yaw coupling. The solution could be an inverted V-tail configuration that has other disadvantages. Few aircraft such as Beechcraft Bonanza V35, Robin ATL Club, Aviation Farm J5 Marco, high-altitude, long-endurance unmanned aerial reconnaissance vehicle Global Hawk, and Lockheed F-117 Nighthawk, employ a V-tail. Unmanned aircraft General Atomic MQ-1 Predator has an inverted V-tail plus a vertical tail under the aft fuselage.

6. Y-tail

The Y-tail (see figure 4.3-6) is an extension to the V-tail, since it has an extra surface located under the aft fuselage. This extra surface reduces the tail contribution in the aircraft dihedral effect. The lower section plays the role of vertical tail, while the two upper sections play the role of the horizontal tail. Therefore, the lower surface has rudder, and the control

surface of the upper section plays the role of the elevator. Thus, the complexity of the Y-tail is much lower than the V-tail. One of the reasons this tail configuration is used is to keep the tail out of effect of the wing wake at high angles of attack. The lower section may limit the performance of the aircraft during take-off and landing, since the tail hitting the ground must be avoided. This configuration is not popular, and few old aircraft had this configuration. Unmanned aircraft General Atomic MQ-9 Reaper employ Y-tail configuration.

7. Twin vertical tail

A twin vertical tail configuration (see figure 4.3-7) has a regular horizontal tail, but two separate and often parallel vertical tails. The twin vertical tail largely improves the directional controllability of an aircraft. Two short span vertical tails have smaller mass moment of inertia about x-axis, compared with a long span vertical tail. Thus, a twin tail has the same directional control power, while it has a less negative effect of the roll control. In addition, both rudders are almost out of the fuselage wake region, since they are not located along fuselage center line. A disadvantage of this configuration is that they have slightly heavier weight compared with the conventional tail. Several modern fighter aircraft such as F-14 Phantom, McDonnell Douglas F-15 Eagle, and F/A-18 Hornet employ the twin tail configuration.

8. Boom-mounted

Sometime some specific design requirements do not allow the aircraft designer to select the conventional tail configuration. For instance, if a prop-driven engine must be installed at the rear of the fuselage, a conventional tail will tend to have a low efficiency. The reason is the interference between the propeller flow and the tail. One of the options is to use two booms and install the tail at the end of the booms (see figure 4.3-8). This option in turn, allows using a shorter fuselage, but overall aircraft weight would be slightly heavier. Two options are:

1. U-tail,

2. Inverted U-tail.

The reconnaissance aircraft Reims F337F Super Sky master and Rutan Voyager employs a boom mounted U-tail. The twin turboprop light utility aircraft Partenavia PD.90 Tapete Air Truck employs a boom mounted inverted U tail configuration which allows for an integrated loading ramp/air-stair.

9. Other configurations

There is variety of other unconventional tail configurations which are usually the forced options to a designer. For instance, sometimes some specific mission requirements such as loading, operational, structural, and engine requirements removes the conventional or T-tail configuration from the list of possible options. Thus, the designer must come up with a new configuration to make an aircraft trimmed and stable throughout flight. Few invented unconventional configurations are as follows:

1. Boom mounted twin vertical tails plus canard (e.g. Rutan Voyager),
2. Boom mounted twin vertical tails plus two separated horizontal tail (e.g. Space Ship
3. Twin T-tail (e.g. Global Flyer),
4. T-tail plus two fins and an auxiliary fixed horizontal tail (e.g. Beech 1900 D of Continental Express),
5. Ring tail (e.g. Cagny 2000), and
6. Triple vertical tail.

4.3. Canard or Aft Tail

One of the critical issues in the design of the horizontal tail is the selection of the location of horizontal tail. The options are: 1. Aft tail (or sometimes referred to as tail aft), and 2. Fore plane or Canard (sometimes referred to as tail-first). As discussed before, the primary function of the horizontal tail is longitudinal trim, and then, longitudinal stability. Both aft tail and canard are capable of satisfactorily fulfilling both mission requirements. However, there are several aspects of flight features that are influenced differently by either of these two options. It is interesting to note that the first aircraft in history (i.e. Wright Flyer) had canard configuration. Canard configuration is not as popular as aft tail, but several GA and military and few transport aircraft employ canard. Examples are Rutan VariEze, Rutan Voyager, Mirage 2000, Dassault Rafale, Eurofighter Typhoon, B-1B Lancer, Saab Viggen, Grumman X-29, Piaggio P-180 Avanti, XB-70 Valkyrie, and Beechcraft Starship.

To comprehend the fundamental differences between an aft tail and a canard, consider four aircraft configurations as shown in Figure 6.12 which two aircraft have aft tail while the other two have canard. In this figure, the wing nose-down pitching moment is not shown for simplicity. The difference between each two figures is the location of the cg compared with the wing-fuselage aerodynamic center. This simple difference causes a

variety of advantages and disadvantages for canard over the conventional aft tail. In all four configurations, the longitudinal trim must hold:

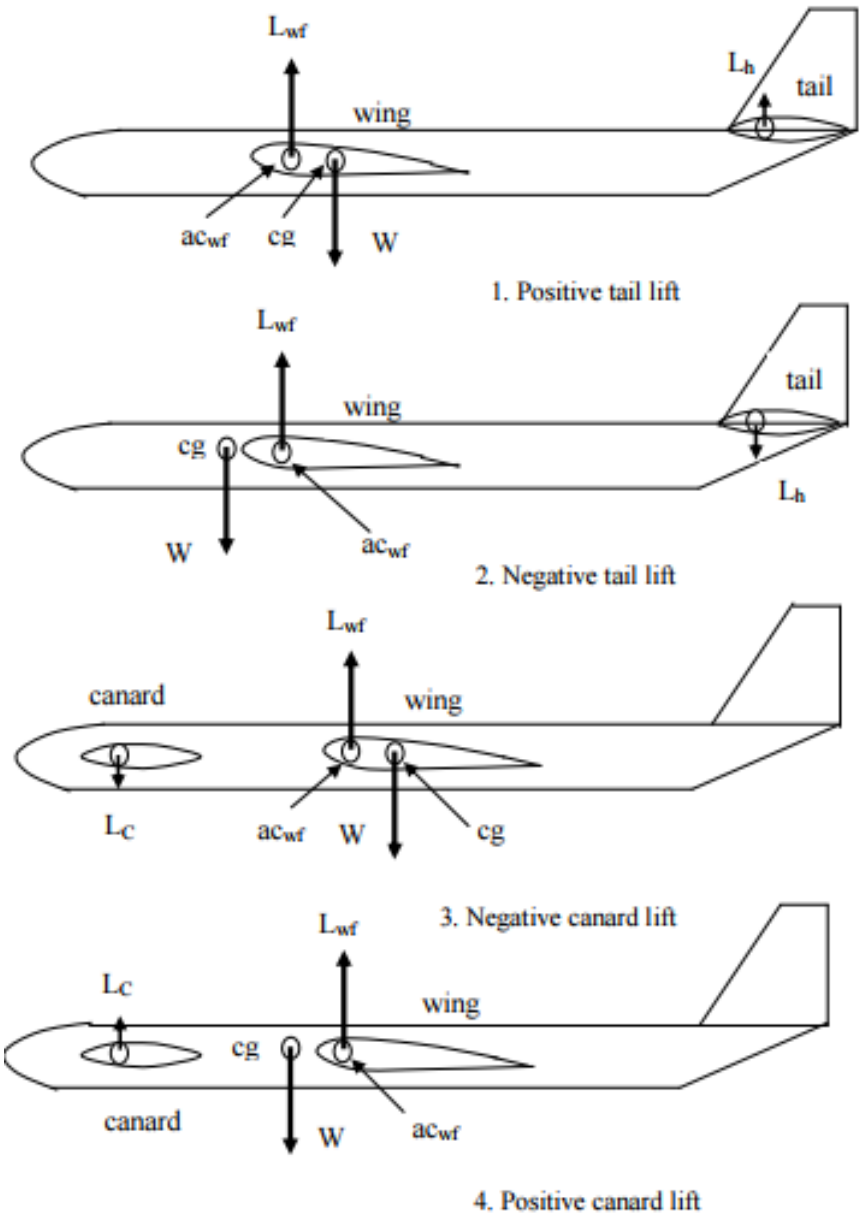

Figure 4.6 The lift of the tail (or canard) in four configurations

$$\sum M_{cg} = 0 \Rightarrow M_{o_{wf}} + L_h \cdot l_h + L_{wf}(h - h_o)\overline{C} = 0 \qquad \text{(aft tail configuration)} \qquad (2.1)$$

$$\sum M_{cg} = 0 \Rightarrow M_{o_{wf}} + L_C \cdot l_c + L_{wf}(h - h_o)\overline{C} = 0 \qquad \text{(canard configuration)} \qquad (2.2)$$

$$\sum F_z = 0 \Rightarrow W = L_{wf} + L_h \qquad \text{(aft tail configuration)} \qquad (2.3)$$

$$\sum F_z = 0 \Rightarrow W = L_{wf} + L_C \qquad \text{(canard configuration)} \qquad (2.4)$$

where LC denotes the canard lift. Equations 2.1 ~ 2.4 indicate that the aft tail lift or canard lift might be positive, or negative, depending upon the

location of aircraft cg relative to wing-fuselage aerodynamic center (see figure 4.6). Equations 2.2 and 2.4 are utilized to determine the value and the direction of the canard lift to satisfy trim requirements. It is obvious that the canard lift is sometimes negative (see figure 4.6-3). Keeping in mind the above basic difference between aft tail and canard, a comparison between features of canard as compared with aft tail is presented.

The canard avoids deep stall 100%. This gets interesting, when we note that about 23 percent of world aircraft crash relates to deep stall. Consider a pilot who intends to increase the wing angle of attack to either take-off, or climb, or land, or land. Since canard is located forward of the wing, the canard will stall first (i.e. before wing stalls). This causes the canard to drop and exits out of stall before the wing enters to stall. The canard drop is because when it stalls, its lift is reduced and causes the aircraft nose to drop. This is regarded as of the major advantages of canard and makes the canard configuration mush safer that aft tail configuration.

Since the canard stalls before the main wing, the wing can never reach its maximum lift capability. Hence, the main wing must be larger than on the conventional configuration, which increases its weight and zero-lift drag.

1. A canard has a higher efficiency when compared with aft tail. The reason is that it is in front of wing, so the wing wake does not influence the canard aerodynamic characteristics. Wing, however, is located aft of canard; hence, it is negatively affected by the canard wake. Thus, a wing in a canard configuration has a lower aerodynamic efficiency (i.e. lower lift) when compared with an aircraft with aft tail configuration.

2. It is not appropriate to employ canard when the engine is pusher and located at the fuselage nose. The reason is that the aircraft nose will be heavy, and the cg adjustment is difficult. Moreover, the structural design of fuselage nose is somewhat complicated, since it must hold both engine and canard.

3. An aircraft with a canard configuration tends to have a smaller static margin compared with an aircraft with a conventional aft tail configuration. In another word, the distance between aircraft neutral point and aircraft center of gravity is shorter. This makes the canard aircraft longitudinally statically less stable. This feature is regarded as a disadvantage for canard configuration.

4. The center of gravity range in an aircraft with a canard configuration tends to be wider; hence, it is more flexible in the load transportation area.

5. Due to the forward location of a canard, the aircraft cg moves slightly forward compared with an aircraft with a conventional aft tail configuration. This feature requires a slightly larger vertical tail for directional trim and stability.
6. A canard tends to generate a lower "trim drag" compared with an aft tail. In another word, a canard aircraft produces less lift-dependent drag to longitudinally trim the aircraft. However, this feature may lead in a larger wetted area (Swet).
7. One of the potential design challenges in a canard aircraft is to optimally locate the fuel tank. The general rule is to place the fuel tank near the aircraft center of gravity as close as possible, to avoid a large movement of cg during the flight operation. The aircraft cg in a canard configuration, if fuel tank is inside the wing, is often forward of the fuel tank. To improve the cg location, designers would rather to place the fuel tank into the fuselage, which in turn increases the possibility of aircraft fire. Another solution is to considerably increase the wing root chord (i.e. employing strake) and to place the fuel tank in wing root. But this technique increases the wing wetted area and reduces the cruise efficiency. The canard aircraft Beechcraft Starship has a wing strake and utilizes this technique.
8. A canard obscures the view of the pilot. This is another disadvantage of the canard configuration.
9. Often the canard generates a positive lift (see figure 4.6-4) while a conventional tail often produces a negative lift (see figure 4.6-2). The reason is that the aircraft cg in a canard configuration is often forward of the wing-fuselage ac. The aircraft cg in a conventional tail configuration is typically aft of the wing-fuselage ac. Recall that the cg moves during flight as the fuel burns. The cg range, in a modern aircraft with a conventional tail or a canard is usually determined such that the cg is most of the times forward of the wing aerodynamic center. However, in a fewer instances of cruising flight, the cg is aft of the wing aerodynamic center. Thus, in an aircraft with a conventional tail, during the cruising flight, the cg usually moves from the most forward location toward the most aft location. However, in an aircraft with a canard, during the cruising flight, the cg often moves from the most aft location toward the most forward location.

    Thus, a canard often generates part of the aircraft lift, while a tail most of the times cancels part of the lift generated by the wing. This

feature tends to reduce the aircraft weight and increases the aircraft cruising speed. In addition, during a take-off which the wing nose-down pitching moment is large, the canard lift is higher. Using the same logic, it can be shown that the canard lift is higher during supersonic speeds. Recall that in a supersonic speed, the wing aerodynamic center move aft toward about 50 percent of the mean aerodynamic chord. This is one of the reasons that some European supersonic fighters, such as Mirage 2000 (Figure 9.12), have employed the canard configuration.

10. Item 9 results in the following conclusion: An aircraft with a canard is slightly lighter than an aircraft with a conventional tail.
11. In general, the canard aerodynamic and stability analysis techniques are considerably more complicated than the technique to evaluate the aerodynamic feature and stability analysis of the conventional tail configuration aircraft. Literature surveys include a variety of published materials regarding conventional tail, while much less papers and technical reports are available for canard analysis. Thus, the design of a canard is more time intensive and more complicated than the conventional tail design.
12. A canard configuration seems to be more stylish and more attractive than a conventional tail.
13. A canard is more efficient for fulfilling the longitudinal trim requirements, while a conventional tail tends to be more efficient for fulfilling the longitudinal control requirements.

In general, canard designs fall into two main categories: the lifting-canard and the control-canard. As the name implies, in a lifting-canard the weight of the aircraft is shared between the main wing and the canard wing. The upward canard lift tends to increase the overall lift capability of the configuration. With a lifting-canard, the main wing must be located further aft of the cg range than with a conventional aft tail, and this increases the pitching moment caused by trailing-edge flaps. The first airplane to fly, the Wright Flyer, and X-29 had a lifting-canard.

It is interesting to know that about 98% of American aircraft are conventional, not canard. In the control-canard, most of the weight of the aircraft is carried by the main wing and the canard wing serves primarily as the longitudinal control device. A control-canard could be all moving or could have a large elevator. The control-canard has often higher aspect ratio and employs a thicker airfoil section than a lifting-canard. A control-canard mostly operates at zero angle of attack. Fighter aircraft with a

canard configuration, such as Eurofighter Typhoon, typically have a control-canard. One benefit obtainable from a control-canard is avoidance of pitch-up. An all-moving canard capable of a significant nose-down deflection will protect against pitch-up. Control canards have poor stealth characteristics, because they present large moving surfaces forward of the wing.

The pros and cons of the canard versus a conventional tail configuration are numerous and complex and it is hard to say which is superior without considering a specific design requirement. One must systems engineering technique to compromise and to decide the tail configuration. In the preliminary design phase, the suggestion is to begin with a conventional tail, unless the designer has a solid reasoning on to employ a canard configuration.

4.4. Optimum Tail Arm

One of the tail parameters that must be determined during the tail design process is the tail arm (l_t), which is the distance between tail aerodynamic center to the aircraft center of gravity. Tail arm serves as the arm for the tail pitching moment (i.e. tail lift multiplied by tail arm) about aircraft cg to maintain the longitudinal trim. To determine the tail arm, one must establish the criteria based on the design requirements. Two basic tail parameters which interact most are tail arm and tail area; the latter is responsible for generation of the tail lift. As the tail arm is increased, the tail area must be decreased, while as the tail arm is reduced, the tail area must be increased. Both short arm (as in fighters), or long arm (as in most transport aircraft) can satisfy longitudinal trim requirements, given the appropriate necessary tail area. But the question is that what tail arm is the optimum one. To answer this question, one must look at the other design requirements.

Two very significant aircraft general design requirements are aircraft low weight and low drag. Both may be combined and translated as the requirement for a low aircraft wetted area. As the horizontal tail arm is increased, the fuselage wetted area is increased, but horizontal tail wetted area is decreased. Also, as the horizontal tail arm is decreased, the fuselage wetted area is decreased, but horizontal tail wetted area is increased. Hence, we are looking to determine the optimum tail arm to minimize drag; which in turn means to minimize the total wetted area of the aft portion of the aircraft. The following is a general educational approach to determine

the optimum tail arm; hence, one must develop his/her own technique and derive more accurate equation based on the suggested approach. The approach is since the aircraft zero-lift drag is essentially a function of the aircraft wetted area.

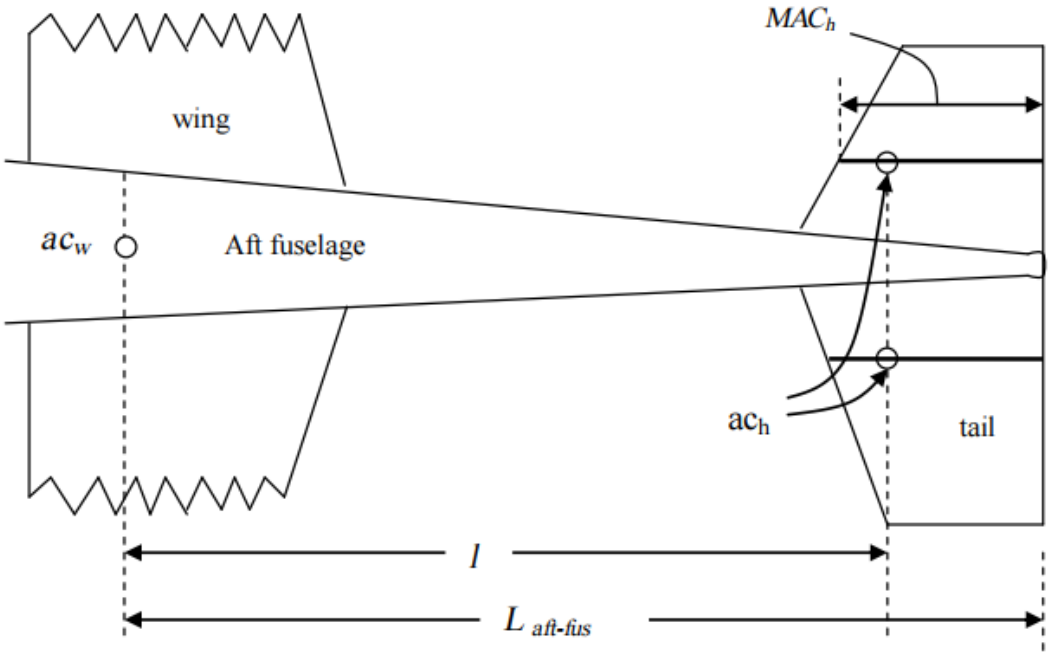

Figure 4.7. Top view of aft portion of the aircraft

Therefore, if the total wetted area is minimized, the aircraft zero-lift drag will be minimized. Moreover, the technique will influence the fuselage length, since the aft portion of the fuselage must structurally support the tail. Consider the top view of aft aircraft (see figure 4.7) that includes aft portion of the fuselage plus the horizontal tail. The wetted area of the aft portion of the aircraft is the summation of the wetted area of the aft portion of the fuselage ($Swet_{aftfus}$) plus the wetted area of the horizontal tail ($Swet_{ht}$).

$$Swet_{aft} = Swet_{aftfus} + Swet_{ht} \qquad 4.5$$

Here we assume that aft portion of the fuselage is conical. Hence, the wetted area of the aft portion of the fuselage is:

$$S_{wet_{aft_{fus}}} = \frac{1}{2}.\pi.D_f.L_{fus_{aft}} \qquad 4.6$$

where D_f is the maximum fuselage diameter and L_{fusaft} is the length of the aft portion of the fuselage. Now, it is assumed that L_{fusaft} is equal to half of the fuselage length (L_f). On the other hand, the wetted area of the horizontal tail is about twice the tail planform area:

$$S_{wet_t} \approx S_h$$

But, the tail volume coefficient is defined as:

$$\overline{V_H} = \frac{l.S_h}{CS} \rightarrow S_h = \frac{\bar{C}.S.\overline{V_H}}{l} \qquad 4.7$$

So,

$$S_{wet} \approx 2\frac{\bar{C}.S.\overline{V_H}}{l} \qquad 4.8$$

Then, by substituting into equation 4.5 yields:

$$S_{wet_{aft}} = \frac{1}{2}.\pi.D_f.L_{fus_{aft}} + 2\frac{\bar{C}.S.\overline{V_H}}{l} \qquad 4.9$$

The relationship between L_{fusaft} and l depends upon the location of the horizontal tail (figure 4.7). We simply assume they are equal ($L_{aftfus} = l$). This assumption is not accurate for every aircraft configuration, but it is a reasonable assumption based on available data. This assumption will be modified later. To minimize zero-lift drag of the aft part of the aircraft, we must differentiate the wetted area of the aft part of the aircraft with respect to tail arm (see figure 4.8) and then set it equal to zero. The differentiation yields:

$$\frac{\partial S_{wet_{aft}}}{\partial l} = \frac{1}{2}.\pi.D_f + 2\frac{\bar{C}.S.\overline{V_H}}{l^2} \qquad 4.10$$

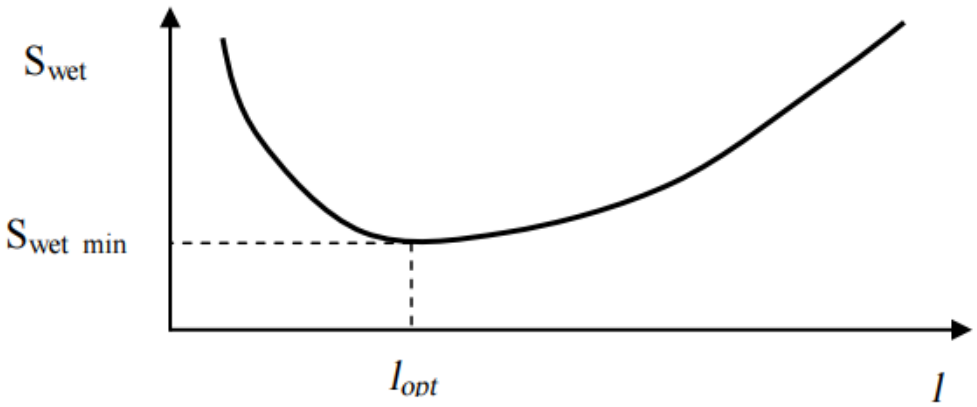

Figure 4.8. The variation of wetted area with respect to tail arm

The optimum tail arm is obtained by solving this equation as follows:

$$l_{opt} = \sqrt{\frac{4.\bar{C}.S.\overline{V_H}}{\pi.D_f}} \qquad 4.11$$

To compensate for our inaccurate assumption, we add a fudge factor as follows:

$$l_{opt} = K_c\sqrt{\frac{4.\bar{C}.S.\overline{V_H}}{\pi.D_f}} \qquad 4.11$$

Where Kc is a correction factor and varies between 1 and 1.4 depending on the aircraft configuration. The Kc = 1 is used when the aft portion of the fuselage has a conical shape. As the shape of the aft portion of the fuselage goes further away from a conical shape, the Kc factor is increased up to 1.4.

Generally, for a single-seat single engine prop-driven GA aircraft, the factor Kc is assumed to be 1.1, but for a transport aircraft, Kc will be 1.4. Note that in a large transport aircraft, most of the fuselage shape is cylindrical, and only its very aft portion has a conical shape. Therefore, if the horizontal tail is located at *lopt*, the wetted area of the aft part of the aircraft will be minimized, so the drag of the aft part of the aircraft will be minimized. When the horizontal tail arm is less than three time the wing MAC ($3\bar{C}$), the aircraft is said to be short-coupled. An aircraft with such tail configuration possesses the longitudinal trim penalty (e.g. fighters). Example 6.1 provides a sample calculation.

Example 4.1:

Consider a twin-seat GA aircraft whose wing reference area is 10 m^2 and wing mean aerodynamic chord is 1 m. The longitudinal stability requirements dictate the tail volume coefficient to be 0.6. If the maximum fuselage diameter is 117 cm, determine the optimum tail arm and then calculate the horizontal tail area. Assume that the aft portion of the fuselage is conical.

Solution:

The aircraft is a GA and has two seats, so the factor Kc is assumed to be 1.4. Using equation 4.11, we have:

$$l_{opt} = K_c\sqrt{\frac{4.\bar{C}.S.\overline{V_H}}{\pi.D_f}} = 1.4\sqrt{\frac{4\times0.6\times1\times10}{3.14\times1.17}} \rightarrow l_{opt} = 3.577\ m$$

The horizontal tail area is calculated by employing tail volume coefficient equation as follows:

$$\overline{V_H} = \frac{l.S_h}{CS} \rightarrow S_h = \frac{\bar{C}.S.\overline{V_H}}{l} = \frac{0.6\times1\times10}{3.577} = 1.677\ m^2$$

4.5. Horizontal Tail Parameters

After the tail configuration is determined, the horizontal tail and vertical tail can be designed almost independently. This section presents the technique to design the horizontal tail and the method to determine horizontal tail parameters. Since the horizontal tail is a lifting surface and, several characteristics of wing and tail are similar (as discussed in Chapter 2), some aspects of the horizontal tail such as taper ratio, sweep angle, dihedral angle and airfoil section, are discussed in brief. The horizontal tail design is also an iterative process and is strongly functions
of several wing parameters and few fuselage parameters. Hence, as soon as the major wing and fuselage parameters are changed, the tail must be redesigned, and its parameters need to be updated.

4.5.1. Horizontal Tail Design Fundamental Governing Equation

Horizontal tail design fundamental governing equation must be driven based on the primary function of the horizontal tail (i.e. longitudinal trim). Figure 4.9 depicts a general case of an aircraft along with the sources of forces along x and z axes, and moments about y axis which are influencing the aircraft longitudinal trim. The longitudinal trim requires that the summation of all moments about y axis must be zero:

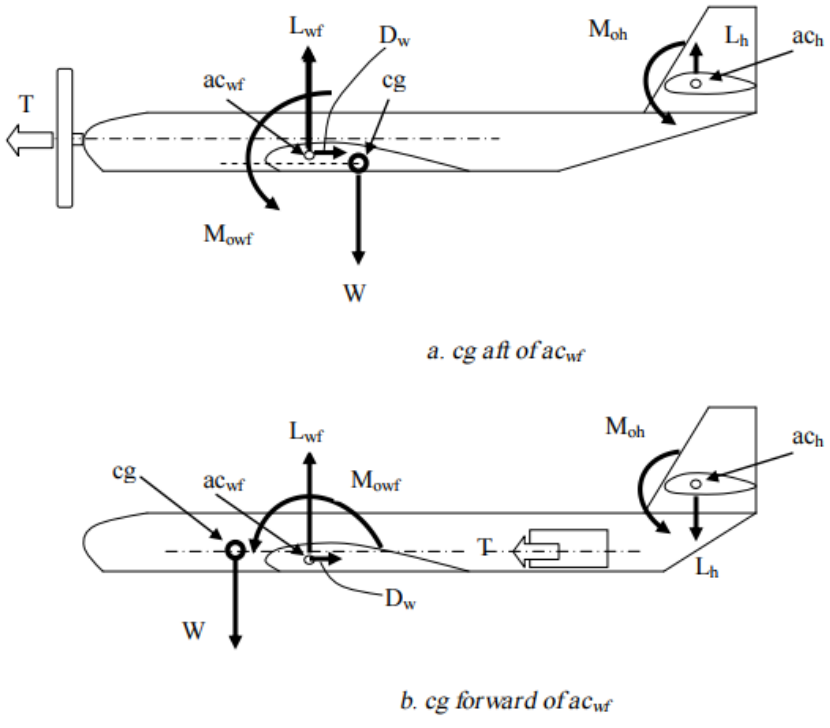

Figure 4.9. A conventional aircraft in longitudinal trim

$$\sum M_{cg} = 0 \rightarrow M_{owf} + M_{L_{wf}} + M_{L_h} + M_{o_h} + M_{T_{eng}} + M_{D_w} = 0 \qquad 4.12$$

Where M_{owf} denotes nose-down wing-fuselage aerodynamic pitching moment, M_{Lwf} denotes the pitching moment generated by the wing-fuselage lift, M_{Lh} denotes the pitching moment generated by the horizontal tail lift, M_{oh} denotes nose-down horizontal tail aerodynamic pitching moment, M_{Teng} denotes the pitching moment generated by the engine thrust, and M_{Dw} denotes the pitching moment generated by the wing drag. The sign of each pitching moment depends upon the location of the source force relative to the aircraft center of gravity. This equation must hold at all flight conditions, but the horizontal tail is designed for the cruising flight, since the aircraft spends much of its flight time in cruise. For other flight conditions, a control surface such as the elevator will contribute.

Based on the aerodynamics fundamentals, two aerodynamic pitching moments of wing and horizontal tail are always nose down (i.e. negative). The sign of wing drag moment depends on the wing configuration. For instance, a high-wing generates a nose up pitching moment, while a low-wing generates a nose down pitching moment. The sign of engine thrust moment depends on the thrust line and engine incidence. If the engine has a setting angle other than zero, both horizontal and vertical components will contribute to the longitudinal trim. The major unknown in this equation is the horizontal tail lift. Another requirement for longitudinal trim is that the summations of all forces along x and z-axes must be zero. Only the summation of forces along the z axis contributes to the tail design:

$$\sum F_Z = 0 \rightarrow L_{wf} + T \sin i_T + L_h = 0 \qquad 4.13$$

where T is the engine thrust and i_T is the engine thrust setting angle (i.e. the angle between the thrust line and the x-axis). This angle almost always is not zero. The reason is the engine thrust contribution to the aircraft longitudinal stability. The typical engine setting angle is about 2 to 4 degrees. The horizontal tail designer should expand two equations of 4.12 and 4.13 and solve simultaneously for two unknowns of wing lift and horizontal tail lift. The latter is employed in the horizontal tail designs. The derivation is left to the reader.

It is presumed that the horizontal tail designer is familiar with the flight dynamics principles and can derive the complete set of longitudinal trim equations based on the aircraft configuration. Since the goal of this textbook is educational, so a simple version of longitudinal trim equation is employed. If the pitching moments of engine thrust, wing drag, and horizontal tail pitching moment are ignored (as shown in figure 4.10), the

non-dimensional horizontal tail design principle equation is as derived earlier:

$$C_{m_{owf}} + C_L(h - h_o) - \eta_h . \bar{V}_H . C_{L_h} = 0 \qquad 4.14$$

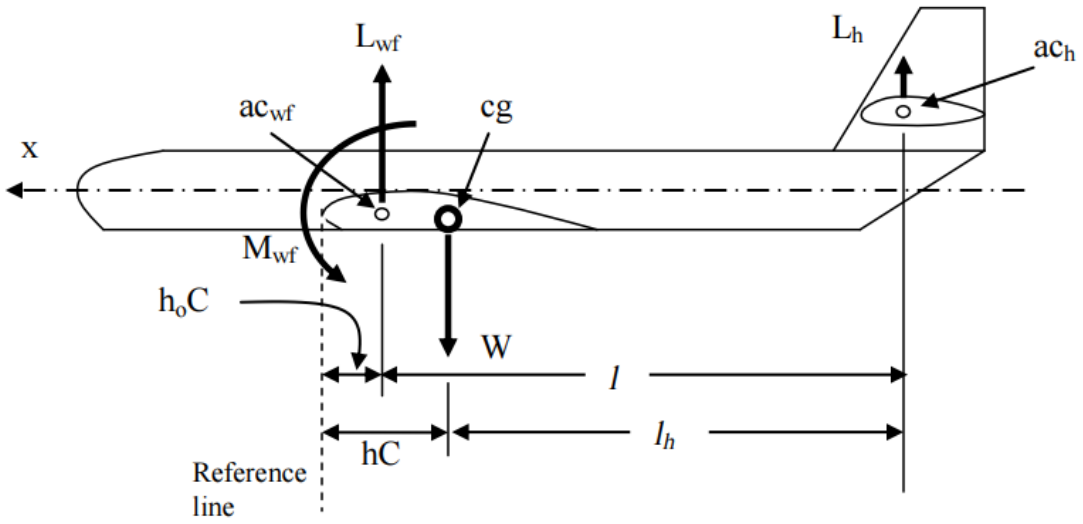

Figure 4.10. The distance between c_g, ac_t, and ac_{wf} to the reference line

The full derivation has been introduced is Section 6.2. This equation has three terms, the last of which is the horizontal tail contribution to the aircraft longitudinal trim. The cruising flight is considered for horizontal tail design application. The equation has only two unknowns (i.e. $\bar{V}_H$ and C_{L_h}). The first unknown (horizontal tail volume coefficient; $\bar{V}_H$) is determined primarily based on the longitudinal stability requirements. The longitudinal flying qualities requirements govern this parameter requirements. A higher value for $\bar{V}_H$ results in a longer fuselage, and/or smaller wing and/or a larger horizontal tail.

As the value of $\bar{V}_H$ is increased, the aircraft becomes longitudinally more stable. On the other hand, a more stable aircraft means a less controllable flight vehicle. Hence, a lower value for $\bar{V}_H$ causes the aircraft to become longitudinally more controllable and less stable. If the horizontal tail design is at the preliminary design phase; and the other aircraft components have not yet been designed; a typical value for $\bar{V}_H$ must be selected. Table 4.1 illustrates the typical values for horizontal and vertical tail volume coefficients. The values are driven from the current successful aircraft statistics. A number from this table based on the aircraft mission and configuration is recommended at the early design phase. When the other aircraft components are designed, and their data are available, a more accurate value for $\bar{V}_H$ may be determined.

The variable "ho" denotes the non-dimensional wing-fuselage aerodynamic center $\left(\frac{X_{ac_{wf}}}{\bar{C}}\right)$ position. A typical value for "ho" is about 0.2 to 0.25 for majority of aircraft configurations. Another significant parameter in equation 4.14 is "h". The parameter "h" denotes the non-dimensional aircraft center of gravity (cg) position $\left(\frac{X_{cg}}{\bar{C}}\right)$. The value for "h" must be known prior to the horizontal tail design.

Table 4.1 Typical values for horizontal and vertical tail volume coefficients

No	Aircraft	Horizontal tail volume Coefficient (V_H)	Vertical tail volume coefficient (V_V)
1	Glider and motor glider	0.6	0.03
2	Home-built	0.5	0.04
3	GA-single prop-driven engine	0.7	0.04
4	GA-twin prop-driven engine	0.8	0.07
5	GA with canard	0.6	0.05
6	Agricultural	0.5	0.04
7	Twin turboprop	0.9	0.08
8	Jet trainer	0.7	0.06
9	Fighter aircraft	0.4	0.07
10	Fighter (with canard)	0.1	0.06
11	Bomber/military transport	1	0.08
12	Jet Transport	1.1	0.09

Chapter 8 is dedicated to the techniques and methods to determine the aircraft cg position, provided the details of geometries of all aircraft components. However, if at the early stages of the horizontal tail design, the other aircraft components such as fuselage, engine, and landing gear have not yet been designed, the only option is to pick a value for "h". The best value is a mid-value between the most forward and the most aft position of the aircraft cg. This minimized the aircraft trim drag while in cruise. This is based on a logical assumption that the aircraft cg is at it one end of the extreme position (say most forward) at the beginning of the cruise, and moves to another end of the extreme position (say most aft) at the end of the cruise. In contrast, to reduce the longitudinal control effort during a cruising flight, the aircraft cg is recommended to be close to the wing-fuselage aerodynamic center. The aircraft non-dimensional center of gravity limit (Δh) is the difference between the most forward and the most aft position of the aircraft cg. The typical values for the aircraft non-dimensional center of gravity limit are:

$\Delta h = 0.1$ to 0.3 4.15

This means that a typical value for the most forward of the aircraft cg is about 10 percent of the wing mean aerodynamic chord. In addition, a typical value for the most aft of the aircraft cg is about 30% of the wing mean aerodynamic chord. Therefore, a proper assumption for the value of (h) at the early stage of the horizontal tail design would be about 0.2. As soon as a more realistic value for the aircraft cg position (h) is available, the horizontal tail design must be updated. The value for the aircraft lift coefficient (C_L) in equation 4.14 is determined based on the cruising velocity, cruise altitude, and the aircraft average weight. Finally, by solving the equation 4.14, the only unknown (C_{L_h}), is determined. At this moment, three horizontal tail parameters are decided (i.e. $\bar{V}_H$, C_{L_h} and l). On the other hand, since the tail volume coefficient is a function of horizontal tail area (S_h), the horizontal tail area is readily determined using equation 4.7. By the technique that has just been introduced, three horizontal tail parameters that have been determined are as follows:

1. horizontal tail planform area (S_h)
2. horizontal tail moment arm (l)
3. horizontal tail cruise lift coefficient (C_{L_h})

It is important to remember that the design is an iterated process, so as soon as any assumption (such as aircraft cg) is changed; the horizontal tail design must be revised.

4.5.2. Fixed, All Moving, or Adjustable

Since the aircraft has numerous flight conditions such as various speeds, cg locations, weights, and altitudes, the longitudinal trim requirements are satisfied only through change in horizontal tail lift. Since the horizontal tail has a fixed planform area and fixed airfoil section, the only way to change the tail lift is to vary its angle of attack (α_h). There are three tail setting configurations (as sketched in figure 4.11) to fulfill a change the angle of attack:

1. Fixed horizontal tail;
2. Adjustable tail;
3. All-moving tail.

A fixed tail is permanently attached to the fuselage by some joining techniques such as screw and nut or welding. A fixed tail angle of attack cannot be varied unless by pitching up or down the fuselage nose. On the other hand, the angle of attack of an all moving tail is easily changed by the pilot using the forward or aft motion of the stick inside the cockpit.

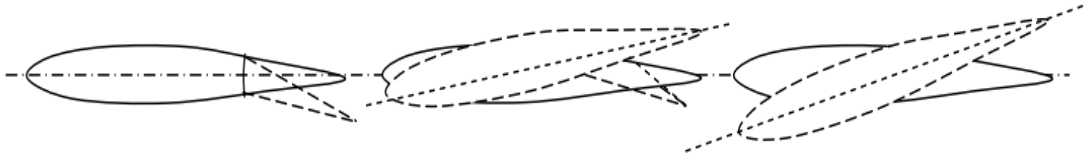

a. Fixed b. Adjustable c. All moving

Figure 4.11. Three horizontal tail setting configurations

There are several basic differences between these options. First, a fixed tail is much lighter, cheaper and structurally easier to design compared with an all moving tail. Moreover, a fixed tail is safer than all moving tail, due to the possibility of failure of a moving mechanism. On the other hand, an aircraft with all moving tail (such as in fighter aircraft Dassault Rafale) is more controllable and maneuverable than an aircraft with a fixed tail. One difference between these two tails is that a fixed tail is equipped with a longitudinal control surface (i.e. elevator); while an all moving tail does not have any separate deflectable section. In general, the trim drag of a fixed tail is higher than that of an all moving tail. An all moving tail is sometimes referred to as a variable incidence tail-plane.

A tail option which has some advantages of a fixed tail and some advantages of the moving tail is referred to as adjustable tail (such as in Fairchild C-26A Metro III). As the name implies, an adjustable tail allows the pilot to adjust its setting angle for a long time. The adjustment process usually happens before the flight; however, a pilot can adjust the tail setting angle during the flight operation. An adjustable tail employs an elevator, but a major between an adjustable tail and all moving tail is in the tail rotation mechanism. An all moving tail is readily and rapidly (in a fraction of a second) rotated about its hinge by the pilot. But, the angle of attack adjustment process for an adjustable tail takes time (few or even several seconds). The range of deflections of an adjustable tail (about +5 to -12 degrees) is considerably less than that of an all moving tail (about +15 to -15 degrees). For instance, the tail-plane deflection for transport aircraft Boeing 777 is 4° up and 11° down.

If the longitudinal maneuverability is not a desired design requirement, it is recommended to employ a fixed tail configuration. But the aircraft is required to be able to perform fats maneuver, the appropriate option is an all moving tail. On the other hand, if the flight cost is a significant issue in the design requirements list, it is better to employ an adjustable tail. In general, most GA and small transport aircraft (e.g. Cessna 172, Jetstream 41) have fixed tail, most

large transport aircraft (e.g. Boeing 767, Airbus 340) utilize the adjustable tail, and most fighter aircraft (e.g. F/A-18 Hornet, F-16 Falcon, and Harrier GR. Mk 7 employ all moving tail. Table 4.2 shows the setting configuration of horizontal tail for several aircraft. Figure 4.12 demonstrates the adjustable horizontal tail of Fairchild C-26A Metro III, and all moving horizontal tail of Panavia Tornado.

(1) (2)

1. Adjustable horizontal tail in Fairchild C-26A Metro III
2. All moving tail in Panavia Tornado

Figure 4.12. An adjustable tail and an all moving tail

4.5.3. Airfoil Section

Horizontal tail-plane is a lifting surface (like the wing) and requires a special airfoil section. The fundamentals about airfoil section (definition, parameters, selection criteria, and related calculation) has been presented in Section 2.4, hence they are not repeated here. In summary, tail-plane requires an airfoil section that can generate the required lift with minimum drag and minimum pitching moment. The specific horizontal tail airfoil requirements are described in this section.

Table 4.2. Horizontal tail characteristics for several aircraft

No	Aircraft	m_{TO} (kg)	Tail type	Airfoil	$(t/C)_{max}$ (%)	$\bar{V}_H$	S_h/S	AR_h	λ_h	Λ_h (deg)	Γ_h (deg)	i_h (deg)	
												+	-
1	Wright Flyer	420	Moving	Cambered plate	low	-0.36	0.16	5.7	1	0	0	-	-
2	Cessna 177	1,100	Fixed	NACA 0012/0009	10.5	0.6	0.2	4	1	0	0	-	-
3	Cessna Citation I	5,375	Fixed	NACA 0010/0008	9	0.75	0.26	5.2	0.5	-	9	-	-
4	Beech Starship	6,759	Fixed	-	-	-0.96	0.22	10.2	0.5	33	3	-	-
5	Fokker F-27	19,773	Fixed	NACA 63A-014	14	0.96	0.23	6	0.4	0	6	-	-
6	Boeing 737-100	50,300	Adjustable	12%-9%	10.5	1.14	0.32	4.16	0.38	30	7	-	-
7	Boeing 707-320	151,320	Adjustable	BAC 317	11.6	0.63	0.216	3.37	0.42	35	7	0.5	14
8	Boeing 747-100	333,390	Adjustable	-	9	1	0.267	3.6	0.26	37	8.5	1	12
9	DC-8-10	141,000	Adjustable	DSMA-89-90	8.75	0.59	0.203	4.04	0.33	35	10	2	10
10	Airbus 300B	165,000	Adjustable	-	-	1.07	0.27	4.13	0.5	32.5	6	3	12
11	Lockheed C-130 Hercules	70,305	Fixed	Inverted NACA	12	1	0.313	5.2	0.36	7.5	0	-	-
12	Lockheed L-1011	211,000	Adjustable	-	8	0.928	0.37	4	0.33	35	3	0	14
13	Lockheed C-5A	381,000	Adjustable	-	10	0.7	0.156	4.9	0.36	24.5	-4.5	4	12
14	Eurofighter 2000	21,000	Movable	-	-	-0.1	0.048	3.4	0.34	45	17	-	-
15	F-15 Eagle	36,741	Movable	-	-	0.24	0.183	2.3	0.36	48	0	-	-

a. Beech Starship *b. Saab JAS-39B Gripen*

Figure 4.13. Two aircraft with canard configuration

Basically, the tail-plane airfoil lift curve slope $(C_{L_{\alpha t}})$ must be as large as possible along with a considerably wide usable angle of attack. Since the aircraft center of gravity moves during the cruising flight, the airfoil section must be able to create sometimes a positive ($+L_h$) and sometimes a negative lift ($-L_h$). This requirement necessitates the tail-plane to behave similar in both positive and negative angles of attack. For this reason, a symmetric airfoil section is a suitable candidate for horizontal tail.

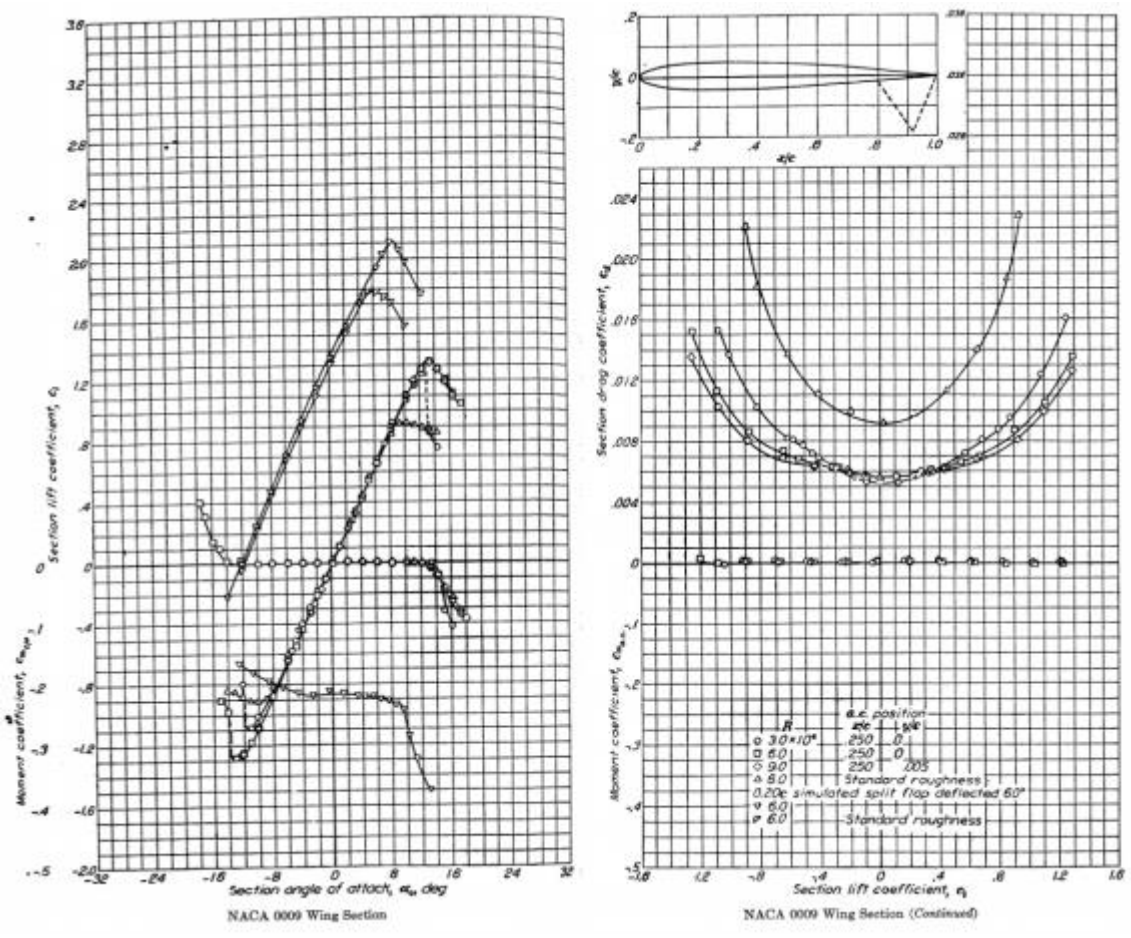

Figure 4.14. Characteristics graphs of NACA 0009 airfoil section

Recall from Chapter 1 that the indication of a symmetric airfoil is that the second digit in a 4-digit and the third digit in a 5-digit and 6-series NACA airfoil sections is zero. This denotes that the airfoil design lift coefficient and zero-lift angle of attack are both zero. NACA airfoil sections such as 0009, 0010, 0012, 63-006, 63-009, 63-012, 63-015, 63-018, 64-006, 64-012, 64A010, 65-009, 65-015, 66-012, 66-018, and 66-021 are all symmetric. In several GA aircraft, NACA airfoil sections 0009 or 0012 (with 9% or 12% maximum thickness-to-chord ratio) are employed for horizontal tail. Both of this NACA airfoil sections are symmetric. Moreover, it is desired that the horizontal tail never stalls, and the wing must stall before the tail. Hence, the stall feature of the tail airfoil section (sharp or docile) is not significant.

In addition, another tail requirement is that horizontal tail must be clean of compressibility effect. In order the tail to be out of the compressibility effect, the tail lift coefficient is determined to be less than the wing lift coefficient. To insure this requirement, the flow Mach number at the tail must be less than the flow Mach number at the wing. This objective will be realized by selecting a horizontal tail airfoil section to be thinner (say about 2 percent of MAC) than the wing airfoil section. For instance, if the wing airfoil section is NACA 23015 (i.e. $(t/C)_{max}$ = 0.15 or 15%), the horizontal tail airfoil section can be selected to be NACA 0009 (i.e. $(t/C)_{max}$ = 0.9 or 9%). Figure 4.14 shows the characteristics graphs of the NACA 0009 airfoil section. In an aircraft with an aft tail configuration, when the center of gravity, most of the time, is behind the wing-fuselage aerodynamic center, the horizontal tail must produce a negative lift to longitudinally trim the aircraft. If the aircraft center of gravity range is such that the tail must produce a negative lift coefficient most of the time, an inverted non-symmetric airfoil section may be utilized. This is the case for the cargo aircraft Lockheed C-130B tail airfoil section.

4.5.4. Tail Incidence

When a fixed tail configuration is adopted, the horizontal tail setting angle (i.e. tail incidence); it; must be determined. The tail setting angle (i_t) primary requirement is to nullify the pitching moment about cg at the cruising flight. This is the longitudinal trim requirement through which the tail is generating a lift to counteract all other aircraft pitching moments. Tail incidence is determined to satisfy trim design requirement when no control surface (i.e. elevator) is deflected.

Although this fixed setting angle satisfies only one flight condition, but it must be such that a mild change (through the application of elevator) is necessary to trim the aircraft on other flight situations.

Looking at the CL-α graph of the tail airfoil section (such as in figure 4.14), it is noticed that the tail angle of attack is simply a function of the tail lift coefficient. Therefore, as soon as the tail lift coefficient is known, the tail incidence is readily determined by using this graph as the corresponding angle. As already discussed in section 4.2, the tail lift coefficient is obtained from the non-dimensional longitudinal trim equation such as equation 4.14:

$$C_{m_{owf}} + C_L(h - h_o) - \eta_h . \bar{V}_H . C_{L_h} = 0 \qquad 4.14$$

In summary, the desired tail lift coefficient is calculated through equation 4.14, and then the tail incidence will be determined by using the CL-α graph of the tail airfoil section.

$$C_{L_{\alpha h}} = \frac{C_{L_h}}{\alpha_h} \rightarrow \alpha_h = \frac{C_{L_h}}{C_{L_{\alpha h}}} \qquad 4.16$$

This is an initial value for the setting angle and will be revised in the later design phases. The typical value would be about -1 degrees. In case, the tail configuration is adjustable, the highest incidence (usually positive angles) and lowest incidence (usually a negative angle) must be determined. For instance, the large transport aircraft Boeing 727 has an adjustable tail with +4 degrees for most positive incidence and -12.5 degrees for most negative incidence. Table 4.2 introduces the horizontal tail setting angles for several aircraft. So, the horizontal tail angle of attack in this aircraft is negative most of the time.

Another factor influencing the value of the tail setting angle is the requirement for longitudinal static stability. Several parameters will affect the aircraft longitudinal static stability, but it can be shown that the "longitudinal dihedral" will have a positive impact on the longitudinal static stability. The term "longitudinal dihedral" is invented by tail designers to transfer the technical meaning of the wing dihedral angle (Γ) form y-z plane to a similar angle in the aircraft x-z plane. As the aircraft lateral stability is benefited from the wing and tail dihedral angles, the aircraft longitudinal stability will be improved by a geometry referred to as the aircraft longitudinal dihedral angle. When the horizontal tail chord line and wing chord line can form a V-shape, it is said that the aircraft has the longitudinal dihedral.

There are a few other technical interpretations for longitudinal dihedral as follows:

1. When the wing (or fore-plane such as canard) setting angle is positive and the horizontal tail (or aft plane such as the wing in a canard configuration) angle is negative, the aircraft is said to have longitudinal dihedral.

$$i_w > i_h$$

2. When the wing (or fore-plane) lift coefficient is higher than that of the horizontal tail (or fore-plane), the aircraft is said to have longitudinal dihedral.

$$C_{Lw} > C_{Lh}$$

3. When the wing (or fore-plane) zero-lift angle of attack is higher than that of the horizontal tail (or aft plane), the aircraft is said to have longitudinal dihedral.

$$\alpha_{ow} > \alpha_{oh}$$

4. When the wing (or foreplane) effective angle of attack is higher than that of the horizontal tail (or aft plane), the aircraft is said to have longitudinal dihedral.

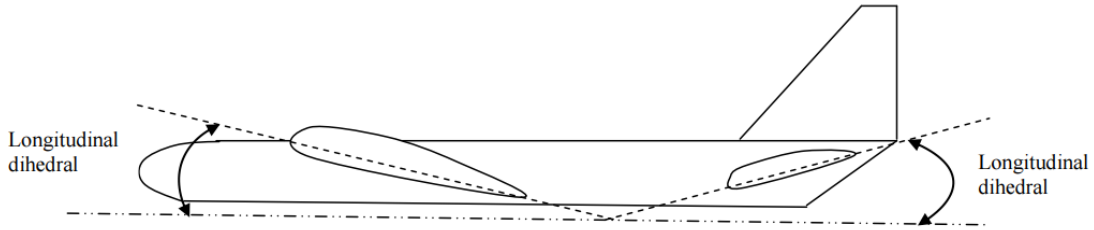

Figure 4.15. Longitudinal dihedral (angle is exaggerated)

These four above mentioned definitions are very similar, but it seems that the last one (see figure 4.15) is technically more accurate. Hence, in determining the horizontal tail setting angle, make sure that the aircraft has longitudinal dihedral. So, this requirement is as follows:

$\alpha_{eff_w} > \alpha_{eff_t}$ (Conventional configuration)

$\alpha_{eff_c} > \alpha_{eff_w}$ (Canard configuration) 4.17

The difference between tail setting angle and the effective tail angle of attack needs to be clarified. Due to the presence of the downwash at the horizontal tail location, the tail effective angle of attack is defined as follows:

$$\alpha_h = \alpha_f + i_h - \varepsilon \qquad 4.18$$

where (α_f) is the fuselage angle of attack and ε is the downwash at the tail (see figure 4.16).

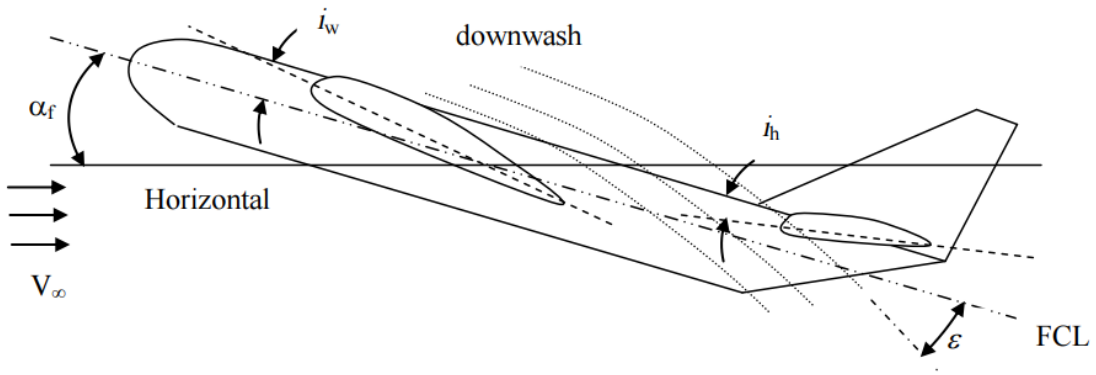

Figure 4.16. Horizontal tail effective angle of attack (downwash is exaggerated)

The fuselage angle of attack is defined as the angle between the fuselage center line and the aircraft flight path (V_∞). The downwash is the effect of the wing trailing vortices on the flow field after passing through the wing airfoil section. Each trailing vortex causes a downflow at and behind the wing and an up-flow outboard of the wing. The downwash is constant along the span of a wing with elliptical lift distribution. The downwash is a function of wing angle of attack (α_w) and is determined as follows:

$$\varepsilon = \varepsilon_o + \frac{\partial \varepsilon}{\partial \alpha}\alpha_w \qquad 4.19$$

where ε_o (downwash angle at zero angle of attack) and $\frac{\partial \varepsilon}{\partial \alpha}$ (downwash slope) are found as:

$$\varepsilon_o = \frac{2C_{L_w}}{\pi.AR} \qquad 4.20$$

$$\frac{\partial \varepsilon}{\partial \alpha} = \frac{2C_{L_{\alpha_w}}}{\pi.AR} \qquad 4.21$$

The wing lift curve slope ($C_{L_{\alpha_w}}$)is in 1/rad and ε is in rad. The parameter C_{Lw} is the wing lift coefficient. The typical value for ε_o is about 1 degree and $\frac{\partial \varepsilon}{\partial \alpha}$ is about 0.3 rad/rad. The ideal value for the horizontal tail setting angle (i_h) is zero; however, it is usually a few degrees close to zero (+ or -). The exact value for i_h is obtained in the calculation process as described in this section

An intermediate horizontal tail parameter that must be determined is its lift curve slope ($C_{L_{\alpha_h}}$). Since the horizontal tail is a lifting surface; like the

wing; the horizontal tail lift curve slope (3D) is determined as follows:

$$C_{L_{\alpha h}} = \frac{dC_{L_h}}{d\alpha_h} = \frac{C_{l_{\alpha h}}}{1+\frac{C_{l_{\alpha h}}}{\pi . AR_h}} \qquad 4.22$$

where $C_{l_{\alpha h}}$ denotes the horizontal tail airfoil section lift curve slope (2D).

4.5.5. Aspect Ratio

The definition, the benefits and the parameters affecting the aspect ratio was explained in Section 4.6 in Chapter 4, so they are not repeated here. The tail aspect ratio has influences on the aircraft lateral stability and control, aircraft performance, tail aerodynamic efficiency, and aircraft center of gravity. Most of the tail aspect ratio benefits are very similar to those of the wing benefits, but in a smaller scale. The tail designer is encouraged to consult with section 4.6 for more information. Like the wing, tail aspect ratio is defined as the ratio between tail span to the tail mean aerodynamic chord.

$$AR_h = \frac{b_h}{C_h} \qquad 4.23$$

The tail aspect ratio (AR_h) tends to have a direct effect on the tail lift curve slope. As the tail aspect ratio is increased, the tail lift curve slop is increased. There are several similarities between wing and horizontal tail in terms of aspect ratio, but in a smaller scale. The differences are as follows:

1. The elliptical lift distribution is not required for the tail.
2. A lower aspect ratio is desirable for tail, compared with that of the wing. The reason is that the deflection of the elevator creates a large bending moment at the tail root. Hence, the lower the aspect ratio results in a smaller bending moment.

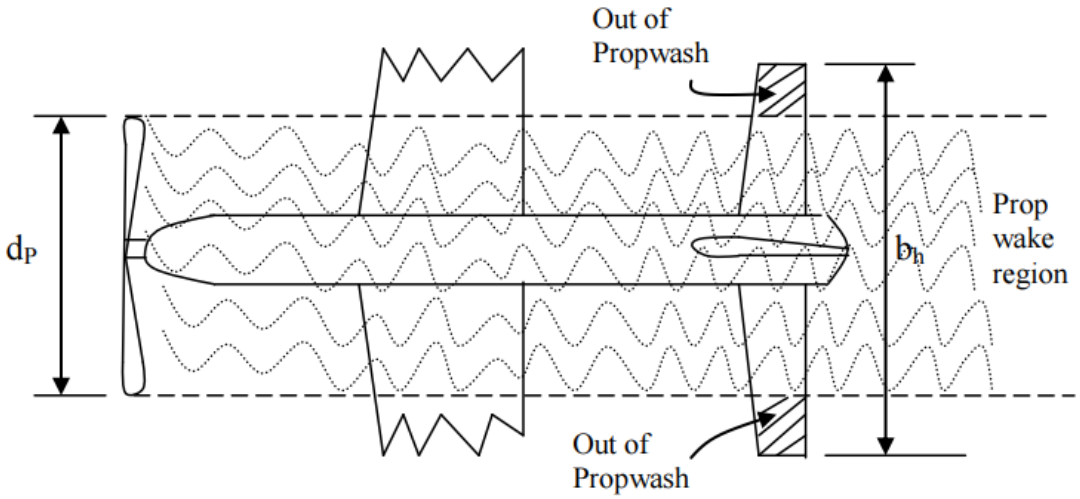

Figure 4.17. The tail span and propwash

3. In a single engine prop-driven aircraft, it is recommended to have an aspect ratio such that the tails span (b_h) is longer than the propeller diameter (d_P) (see figure 4.17). This provision insures that the tail flow field is fresh and clean of wake and out of propwash area. Therefore, the efficiency of the tail (η_h) will be increased.

Based on the above reasoning, an initial value for the tail aspect ratio may be determined as follows:

$$AR_h = \frac{2}{3} AR_w \qquad 4.24$$

A typical value for the horizontal tail aspect ratio is about 3 to 5. Table 4.2 illustrates the horizontal tail aspect ratio for several aircraft. The final value for tail aspect ratio will be determined based on the aircraft stability and control, cost, and performance analysis evaluations after the other aircraft components have been designed.

4.5.6. Taper Ratio

The definition, the benefits and the parameters affecting the taper ratio was explained in Section 4.7 in Chapter 4, so they are not repeated here. The tail taper ratio has influences on the aircraft lateral stability and control, aircraft performance, tail aerodynamic efficiency, and aircraft weight and center of gravity. Most of the tail taper ratio benefits are very similar to those of the wing benefits, but in a smaller scale. The tail designer is encouraged to consult with section 4.7 for more information. Like the wing, tail taper ratio (λ_h) is defined as the ratio between the tail tip chord to the tail root chord.

$$\lambda_h = \frac{C_{h(tip)}}{C_{h(root)}} \qquad 4.25$$

Thus, the value is between zero and one. The major difference with wing taper ratio is that the elliptical lift distribution is not a requirement for tail. Thus, the main motivation behind the value for the tail taper ratio is to lower the tail weight. For this reason, the tail taper ratio is typically smaller than the wing taper ratio. The tail taper ratio is typically between 0.7 and 1 for GA aircraft and between 0.4 and 0.7 for transport aircraft. For instance, transport aircraft Boeing B-727 and Boeing B-737 has a tail taper ratio of 0.4 and Airbus A-300 has a tail taper ratio of 0.5. Table 4.2 shows the horizontal tail taper ratio for several aircraft. The final value for tail taper ratio will be determined based on the aircraft stability and control, cost, and performance analysis evaluations after the other aircraft components have been designed.

4.5.7. Sweep Angle

The definition, the benefits and the parameters affecting the sweep angle was explained in Section 4.9 in Chapter 4, so they are not repeated here. Sweep angle is normally measured either relative to the leading edge or relative to the quarter chord line. Like the wing, tail leading edge sweep angle (Λ_{h_LE}) is defined as the angle between the tail leading edge and the y-axis in the x-y plane. The horizontal tail sweep angle has influences on the aircraft longitudinal and lateral stability and control, aircraft performance, tail aerodynamic efficiency, and aircraft center of gravity. Most of the tail sweep angle effects are very similar to those of the wing effects, but in a smaller scale. The tail designer is encouraged to consult with Section 4.9 for more information. The value of the horizontal tail sweep angle is often the same as wing sweep angle.

Table 4.2 shows the horizontal tail sweep angle for several aircraft. As an initial selection in preliminary design phase, select the value of the tail sweep angle to be the same as the wing sweep angle. The final value for tail sweep angle will be determined based on the aircraft stability and control, cost, and performance analysis evaluations after the other aircraft components have been designed.

4.5.8. Dihedral Angle

The definition, the benefits and the parameters affecting the dihedral angle was explained in Section 4.11 in Chapter 4, so they are not repeated here. Like the wing, tail dihedral angle (Λ_h) is defined as the angle between each tail half section and the y-axis in the y-z plane. The horizontal tail dihedral angle has contribution to the aircraft lateral stability and control, aircraft performance, and the tail aerodynamic efficiency. Most of the tail dihedral angle contributions are very similar to those of the wing effects, but in a smaller scale. The tail designer is encouraged to consult with Section 4.11 for more information.

The value of the horizontal tail dihedral angle is often the same as wing sweep angle. In some cases, the tail dihedral angle is totally different than the wing dihedral angle. There are several reasons for this difference including a need for the aircraft lateral stability adjustment (e.g. few transport aircraft such as tail dihedral of -3 degrees for Boeing 727); a need for lateral control adjustment (e.g. fighters such as McDonnell Douglas F-4 Phantom); and a need for a reduction in aircraft height and operational requirements (e.g. unmanned aircraft Predator). Table 4.2 shows the tail

dihedral angle for several aircraft. In some aircraft instances, the manufacturing limits and considerations force the designer not to employ any dihedral for the wing. So, the need for lateral stability requires a large dihedral for the tail. As an initial selection in preliminary design phase, select the value of the tail dihedral angle to be the same as the wing dihedral angle. The final value for tail dihedral angle will be determined based on the aircraft stability and control, and performance analysis evaluations after the other aircraft components have been designed.

4.5.9. Tail Vertical Location

In an aircraft with aft tail configuration, the height of the horizontal tail relative to the wing chord line must be decided. In a conventional aircraft, the horizontal tail has two options for the installation:

1. At the fuselage aft section,
2. At the vertical tail. Beside the structural

considerations and complexities, the horizontal tail efficiency and its contribution to aircraft longitudinal and lateral stability must be analyzed. Unlike wing vertical location, there are no locations for tail such as low tail, mid tail or high tail. However, the low tail implies a conventional tail, the high tail implies a T-tail and the mid tail implies a cruciform tail.

A complete aircraft computational fluid dynamic model allows the designer to find the best location to increase the effectiveness of the tail. There are few components that are sources of interference with the tail effectiveness. They include wing, fuselage, and engine.

The wing influences the horizontal tail via downwash, wake and tailing vortices. In general, wing downwash decreases the tail effective angle of attack. Moreover, the wing wake degrades the tail efficiency, reduces the tail efficiency (h_t), and decreases the tail dynamic pressure. Most important considerations about the location of the horizontal tail relative to the wing is the prevention of deep stall. The horizontal tail location must not be in the wing wake region when wing stall happens. As the figure 4.18 illustrates, there are three major regions for tail installation behind the wing:

1. out of wake region and downwash,
2. inside wake region but out of wing downwash,
3. out of wake region but affected by downwash.

In terms of deep stall avoidance criterion, the region 1 is the best and safest. The region 3 is safe from deep stall and pitch up, but tail is not efficient.

The region 2 is not safe and not recommended for the horizontal tail installation.

The decision about the vertical height of the horizontal tail must be made after a thorough analysis, since a variety of parameters including wing airfoil, tail airfoil, wing-fuselage aerodynamic pitching moment, and tail arm plus manufacturing considerations are contributing. The following experimental equations are recommended for the initial approximation of the horizontal tail vertical height:

$$h_t > l.tan(\alpha_s - i_w + 3) \qquad 4.26$$

$$h_t < l.tan(\alpha_s - i_w + 3) \qquad 4.27$$

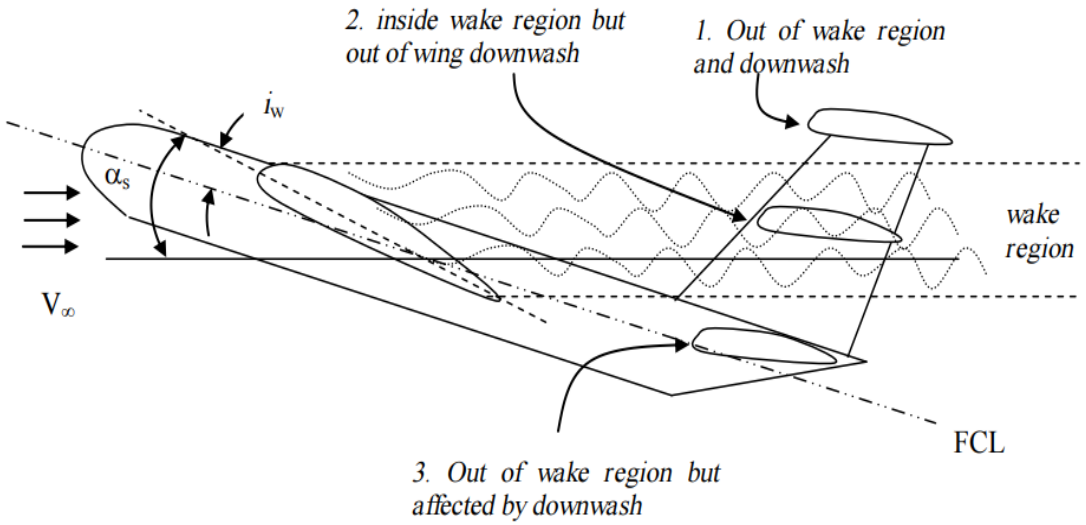

Figure 4.18. An aircraft with three tail installation locations when wing stalls

where h_t is the vertical height of the horizontal tail relative to the wing aerodynamic center, l is the horizontal tail moment arm, α_s is the wing stall angle (in degrees), and i_w denote the wing incidence (in degrees).

The fuselage interferes with the tail through fuselage wake and side-wash. The designer is referred to aerodynamic text for the details. In a multi-engine jet aircraft, the engine hot and fast speed gas has both positive and negative effects. The high-speed gas increases the tail dynamic pressure, while the hot gas creates a fatigue problem for tail structure. If the tail is made of composite materials, make sure that the tail is out of engine exhaust area. Hence, the horizontal tail location is the output of a compromise process to satisfy all design requirements.

4.5.10. Other Tail Geometries

Other horizontal tail geometries include tail span (b_h), tail tip chord ($C_{h(tip)}$), tail root chord ($C_{h(root)}$), and tail mean aerodynamic chord ($\bar{C}_h$ or MAC_h). These four tail parameters are sketched in Figure 4.19 that shows the top view of an aircraft aft section. These unknowns are determined by solving the following four equations simultaneously:

$$AR_h = \frac{b_h}{\bar{C}_h}$$

$$\lambda_h = \frac{C_{h_{tip}}}{C_{h_{root}}}$$

$$\bar{C}_h = \frac{2}{3} C_{h_{root}} \left(\frac{1 + \lambda_h + \lambda_h^2}{1 + \lambda_h} \right)$$

$$S_h = b_h \cdot \bar{C}_h$$

The first two equations have been introduced previously in this section, but the last two equations are reproduced from wing geometry governing equations (see Chapter 2). The required data to solve these equations are the tail planform area, tail aspect ratio, and tail taper ratio.

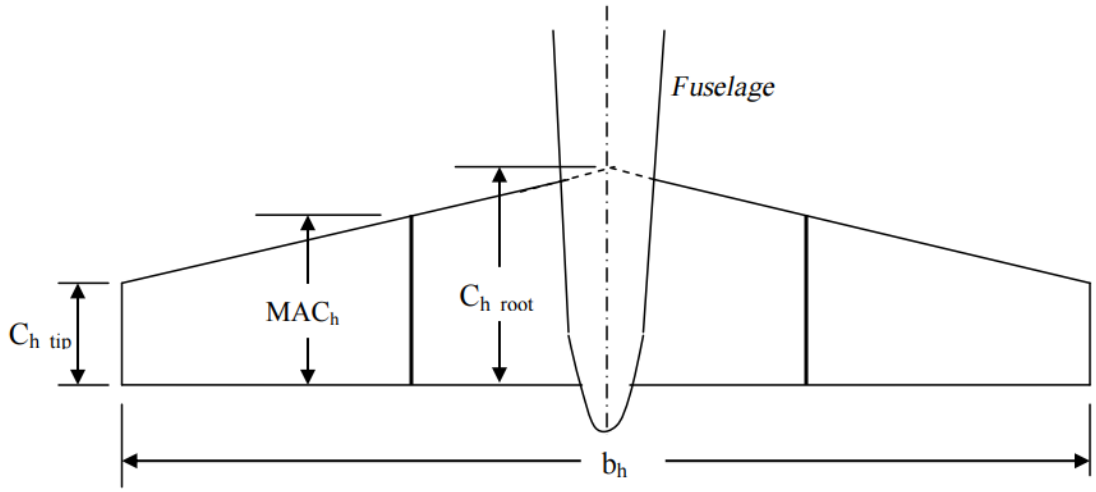

Figure 4.19. Horizontal tail geometry

4.5.11. Control Provision

One of the secondary functions of the horizontal tail is the aircraft longitudinal control. The horizontal tail must generate a variety of tail lift forces in various flight conditions to longitudinally trim the aircraft and create the new trim conditions. For this purpose, a fixed and an adjustable

horizontal tail have movable sections; which in a conventional aircraft; is called elevator. Therefore, in designing the horizontal tail, one must consider some provisions for future control applications. The provisions include insuring the sufficient space for elevator's area, span, and chord as well as elevator deflection angle to allow for an effective longitudinal control.

4.5.12. Final Check

When all horizontal tail parameters have been determined, two design requirements must be examined:

1. aircraft longitudinal trim,
2. aircraft static and dynamic longitudinal stability.

In the analysis of the longitudinal trim, the tail lift coefficient needs to be calculated. The generated horizontal tail lift coefficient should be equal to the required cruise tail lift coefficient. There are several aerodynamic software packages and tools to calculate the horizontal tail lift coefficient. In the early stage of design, it is recommended to employ the lifting line theory as described in Chapter 2. When whole aircraft is designed, modern CFD software is utilized to determine aerodynamic feature of the aircraft including horizontal tail. If the longitudinal trim requirements are not satisfied, horizontal tail parameters such as tail incidence must be adjusted.

4.6. Vertical Tail Design

4.6.1. Vertical Tail Design Requirements

The third lifting surface in a conventional aircraft is the vertical tail; which is sometimes referred to as vertical stabilizer or fin. The vertical tail tends to have two primary functions:

1. directional stability,
2. directional trim. Moreover,

The vertical tail is a major contributor in maintaining directional control; which is the primary function of the rudder. These three design requirements are described briefly in this section:

1. The primary function of the vertical tail is to maintain the aircraft directional stability. The static and dynamic directional stability requirements were discussed in Section 4.3. In summary, the stability derivatives Cn_{β} must be positive (to satisfy the static directional stability requirements), but the stability derivatives Cn_{r} must be negative (to satisfy the dynamic directional stability

requirements). Two major contributors to the value of these stability derivatives are vertical tail area (S_V) and vertical tail moment arm (l_V). If vertical tail area is large enough and vertical tail moment arm is long enough, the directional stability requirements could be easily satisfied.

2. The second function of the vertical tail is to maintain the aircraft directional trim. As discussed in Section 4.3, the summation of all forces along the y-axis and the summation of all moments about z-axis must be zero.

$$\sum F_y = 0$$

$$\sum N_{cg} = 0$$

An aircraft is normally manufactured symmetrical about x-z plane, so the directional trim is naturally maintained. Although this is an ideal case and is considered in the production of components such as right and left-wing sections, but in several cases, there is a slight asymmetricity in the aircraft x-y plane. One source for the asymmetricity could be a difference between manufacturing jigs and fixtures of right and left sections (wing and tail). Another reason for directional asymmetricity lies in the internal components inside fuselage such as fuel system, electrical wiring, and even load and cargo inside load compartment. However, in a single engine prop-driven aircraft, the aircraft directional trim is disturbed by the rotation of the engine propeller. In a multi-engine prop-driven aircraft, with odd number of engines, a similar problem exists. Hence, the vertical tail is responsible for maintaining the directional trim by providing an opposing yawing moment about z-axis. One of the critical parameters influencing the directional trim in such aircraft is the vertical tail incidence angle relative to the x-z plane.
Another directional trim case is in multi-engine aircraft, where one engine in inoperative. In such situation, the operative engines create a disturbing yawing moment and the only way to balance this asymmetric moment is the counteracting yawing moment generated by the vertical tail. A control surface (e.g. rudder) must be deflected to directionally trim the aircraft. Although the vertical tail is contributing to the aircraft lateral stability and control, but this item is not considered as a base for the design of the vertical tail. However, in the analysis of the vertical tail performance, the lateral

stability must be studied. This is to make sure that the vertical tail is improving the aircraft lateral stability and not having a negative impact. Recall that the aircraft lateral stability is primarily a function of the wing parameters. The static and dynamic directional trim requirements were discussed in Section 4.2.

3. The third aircraft design requirement in which the vertical tail is a major contributor is the directional control. Maneuvering operations such as turning flight and spin recovery are successfully performed by using a movable section of the vertical tail which is called rudder.

4.6.2. Vertical Tail Parameters

Basically, the vertical tail parameters must be initially determined such that the directional stability requirements are satisfied. In the second and third stage of the vertical tail design process, the directional trim requirements and directional control requirements will be examined.

In the design of the vertical tail, the following parameters must be determined:

1. Vertical tail location
2. Planform area (*Sv*)
3. Tail arm (lv_t)
4. Airfoil section
5. Aspect ratio (*ARv*)
6. Taper ratio (λv)
7. Tip chord ($C_{V(tip)}$)
8. Root chord ($C_{V(root)}$)
9. Mean Aerodynamic Chord (MACv or *Cv*)
10. Span (*bv*)
11. Sweep angle (*Λv*)
12. Dihedral angle (*Γv*)
13. Incidence (i_v)

Several of these vertical tail parameters are illustrated in figure 4.20. The vertical tail is a lifting surface, whose aerodynamic force of lift is generated in the direction of y-axis. In maintaining the directional stability, control and trim, an aerodynamic force along y-axis needs to be created by the vertical tail (i.e. vertical tail lift; L_V).

$$L_V = \frac{1}{2}\rho V^2 S_V C_{L_V} \qquad 4.30$$

where S_V is the vertical tail area, and the C_{Lv} is the vertical tail lift coefficient. The vertical tail lift is generating a yawing moment about z-axis:

$$N_{cg} = L_V \, l_V \qquad 4.31$$

This moment must be large enough to maintain directional trim and must have a positive contribution to the directional stability. As explained in Section 4.6.1, a preliminary evaluation of the directional stability is applied through a parameter called vertical tail volume coefficient ($\bar{V}_V$):

$$\bar{V}_V = \frac{l_V . S_V}{bS} \qquad 4.32$$

Where *lv* is the distance between vertical tail aerodynamic center (ac_v) and the wing-fuselage aerodynamic center (see figure 4.20), S_V is the vertical tail planform area, *b* is the wing span, and *S* denotes the wing reference area. The vertical tail aerodynamic center is located at the quarter chord of the vertical tail mean aerodynamic chord.

The vertical tail volume coefficient is a non-dimensional parameter which is directly functions of two significant vertical tail parameters: vertical tail area (S_V) and vertical tail moment arm (*lv*). Two parameters of *lv* and lv_t are very close, such that one can be determined from another one. The vertical tail volume coefficient is an indirect representative for the aircraft directional stability. The typical value for the vertical tail volume coefficient is between 0.02 and 0.12. Table 6.6 illustrates the vertical tail parameters including the vertical tail volume coefficient for several aircraft. Remember that the vertical tail planform area includes both the fixed section and the movable section (i.e. rudder).

Since the definitions and features of lifting surface basic parameters such as aspect ratio, taper ratio, and airfoil section have been presented in Chapter 2 and in horizontal tail design section (Section 4.5), they are introduced briefly here.

1. Vertical tail location

To maintain the directional stability, the only location for the vertical tail is aft of the aircraft center of gravity. Three possible candidates are:

1. aft of fuselage,
2. wingtips, and
3. boom(s).

If a single aft horizontal tail has been selected, the only place for the vertical tail is on the top of the aft fuselage. The vertical tail cannot be placed in front of the fuselage (i.e. forward of the aircraft cg), since it makes the aircraft directionally unstable. Other two options, namely

wingtips and boom, are appropriate for some special purposes that have been described earlier in Section 4.4.

2. Vertical tail moment arm (lv_t)

The vertical tail moment arm (see figure 4.20) must be long enough to satisfy directional stability, control, and trim requirements. In a spin-able aircraft, the vertical tail must also satisfy the spin recovery requirements. Increasing the vertical tail moment arm increases the values of the derivatives Cn_β and Cn_r and thus makes the aircraft directionally more stable. The major contributor to the static directional stability derivative (Cn_β) is the vertical tail:

In addition, an increase in the vertical tail moment arm improves the directional and lateral control. In the early stage of the vertical tail design; where other aircraft components have not been designed; the vertical tail moment arm is selected to be equal to the horizontal tail moment arm (l). This assumption means that the vertical tail is located at the same distance to the wing as the horizontal tail. The assumption will be modified in the later design stage when other aircraft components are designed, and the aircraft directional and lateral stability, control and trim are analyzed.

Another phenomenon that influences the vertical tail moment arm is spin. When an aircraft is spin-able, the aircraft is required to be able to recover from spin safely. Spin is a dangerous flight if the aircraft is not designed to recover safely from it. Some aircraft, however, are not spin-able by design. Most transport aircraft are not spin-able (i.e. spin resistant), while most fighters and maneuverable aircraft are spin-able.

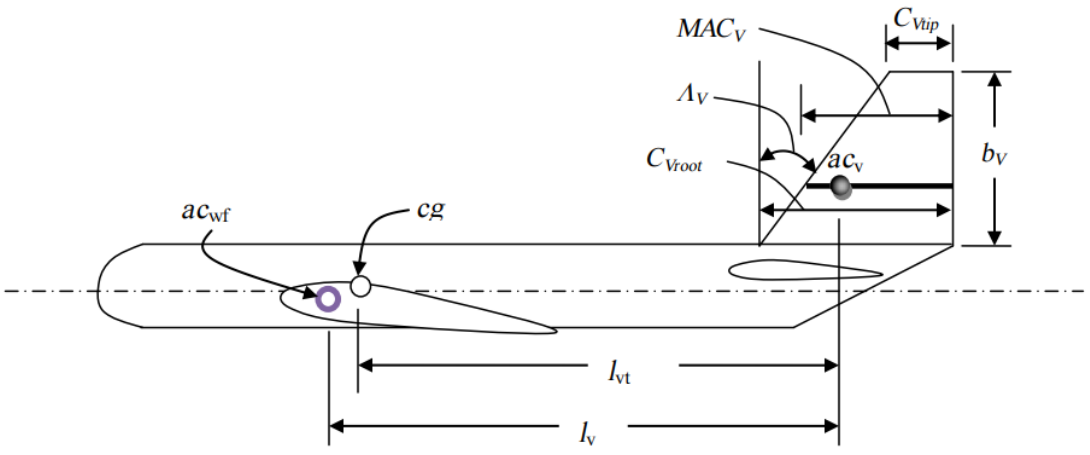

Figure 4.20. The vertical tail parameters

3. Planform area (*Sv*)

The parameter *Sv* is in the numerator which implies the larger vertical tail area is desirable. The vertical tail area must be large enough to satisfy lateral-directional stability, control, and trim requirements. Increasing the vertical tail area increases the values of the derivatives Cn_{β} and Cn_{r} and thus makes the aircraft lateral-directionally more stable. In addition, an increase in the vertical tail area improves the directional and lateral control ($Cn_{\delta R}$, $Cl_{\delta R}$). If the vertical tail area is too small, the lateral-directional stability requirements will not be satisfied.

On the other hand, when the vertical tail area is too large, the aircraft will be lateral-directionally too stable, but the directional control requirements are not satisfied. Thus, the middle value is very hard to determine. For this reason, the vertical tail design is utilizing a backward design technique. It means that we select a combination of vertical tail area and vertical tail moment arm in a ballpark area through a parameter called vertical tail volume coefficient. Another criterion for the vertical tail area is that it must be small such that to minimize the manufacturing cost and the aircraft weight.

It is interesting to note that a typical value for the ratio between vertical tail area and the wing area for a conventional GA aircraft is about 0.1 to 0.15. The vertical tail planform area is preliminary determined based on the selection of the vertical tail volume coefficient ($\bar{V}_V$). The typical value for the vertical tail volume coefficient for several aircraft type is introduced in Table 4.3. Hence the vertical tail area is determined as:

$$S_V = \frac{b.S.\bar{V}_V}{l_V} \qquad 4.33$$

4. Airfoil section

The vertical tail airfoil section is responsible for the generation of the vertical tail lift coefficient (CL_V). The airfoil must generate the required lift coefficient with a minimum drag coefficient.

Recall that a nonsymmetrical airfoil section creates an aerodynamic pitching moment. One of the basic aircraft design requirement is the symmetricity about the x-z plane. Therefore, to insure the symmetricity of the aircraft about x-z plane, the vertical airfoil section must be symmetric. Moreover, if the engines, wing, horizontal tail and fuselage are designed to be symmetric about x-z plane, the vertical tail is not required to produce any lift to maintain directional trim in a normal flight condition. Recall

from Chapter 2 that the indication of a symmetric airfoil is that the second digit in a 4-digit and the third digit in a 5-digit and 6-series NACA airfoil sections is zero. This denotes that the airfoil design lift coefficient and zero-lift angle of attack are both zero. NACA airfoil sections such as 0009, 0010, 0012, 63-006, 63-009, 63-012, 63-015, 63-018, 64-006, 64-012, 64A010, 65-009, 65-015, 66-012, 66-018, and 66-021 are all symmetric airfoils. In several GA aircraft, NACA airfoil sections 0009 or 0012 (with 9% or 12% maximum thickness-to-chord ratio) are employed for vertical tail. Both of this NACA airfoil sections are symmetric.

In addition, another tail requirement is that the vertical tail must be clean of compressibility effect. To satisfy this requirement, the flow Mach number at the vertical tail must be less than the flow Mach number at the wing. This objective will be realized by selecting a vertical tail airfoil section to be thinner (say about 2 percent of MAC) than the wing airfoil section. For instance, if the wing airfoil section is NACA 23015 (i.e. $(t/C)_{max}$ = 0.15 or 15%), the vertical tail airfoil section can be selected to be NACA 0009 (i.e. $(t/C)_{max}$ = 0.9 or 9%). Figure 4.14 shows the characteristics graphs of the NACA 0009 airfoil section. Table 4.2 illustrates the airfoil section for vertical tail of several aircraft.

The third desired feature for the vertical tail airfoil section is the high value for the lift curve slope ($C_{L_{\alpha V}}$), since the static directional stability derivative (Cnβ) is directly a function of $C_{L_{\alpha V}}$.

Thus, generally, a symmetric airfoil section with a high lift curve slope is desirable for the vertical tail. Recall that the theoretical value for an airfoil section is about 2π 1/rad. Table 4.3 shows airfoil section of the vertical tail for several aircraft.

5. Incidence (i_v)

The vertical tail incidence is defined as the angle between the vertical tail chord line and the aircraft x-z plane (when look at the aircraft from top view). The vertical tail is responsible for the generation of the vertical tail lift coefficient (C_{LV}). One of the basic aircraft design objective is the symmetricity about the x-z plane. Hence, if the engines, wing, horizontal tail and fuselage are designed to be symmetric about x-z plane, the vertical tail is not required to produce any lift to maintain directional trim in a normal flight condition. For this reason, the vertical tail incidence must be initially zero.

Table 4.3. Vertical tail characteristics for several aircraft

No	Aircraft	Type	m_{TO} (kg)	Airfoil	$(t/C)_{max}$ (%)	$\bar{V}_V$	S_V/S	AR_V	Λ_V (deg)
1	Wright Flyer	First aircraft in history	420	Flat plate	low	0.013	0.045	6.3	0
2	Cessna 177	GA single prop engine	1,100	NACA 0009/0006	7.5	0.14	0.107	1.41	35
3	C-130 Hercules	Large turboprop cargo	70,305	NACA 64A-015	15	0.06	0.18	1.84	18.8
4	DC-9/10	Large jet transport	41,100	DSMA	11	0.08	0.19	0.95	43.5
5	Cessna Citation I	Business jet	5,375	NACA 0012/0008	10	0.0806	0.191	1.58	33
6	Fokker F-27	Turboprop transport	19,773	modified NACA	15	0.07	0.203	1.55	33
7	Boeing 737-100	Large jet transport	50,300	-	12	0.11	0.27	1.88	35
8	Beechjet 400A	Business jet transport	7,303	-	12	0.123	0.263	1	55
9	DC-8-10	Large jet transport	141,000	DSMA-111/-112	9.85	0.05	0.122	1.91	35
10	Airbus 300B	Large jet transport	165,000	-	12.5	0.102	0.204	1.623	40
11	C-17A	Heavy jet cargo	265,352	-	9	0.08	0.195	1.36	36
12	Eurofighter 2000	Fighter	21,000	-	7	0.035	0.096	1.3	45
13	F-15 Eagle	Fighter	36,741	-	7	0.06	0.346[6]	1.3	35

1. Beech 200 Super King Air (dorsal and ventral fin) (Courtesy of Jenny Coffey) *2. Gates Learjet 35A (ventral fin) (Courtesy of Antony Osborne)* *3. General Atomics Predator (ventral fin)*

Figure 4.21. Dorsal fin and ventral fin in three aircraft

However, in a prop-driven aircraft with one single engine (or with odd number of prop-driven engines), the lateral trim is disturbed by the revolution of the propeller and engine shaft about x-axis. The aircraft body is going to roll as a reaction to the rotation of the propeller and its shaft (recall the third law of Newton). Although this rolling moment is not large, but the safety requirements requires the trim to be maintained and aircraft roll be avoided. To nullify this yawing moment, the vertical tail is required to generate a lift and cancels this rolling moment.

One solution for this problem is to consider a few degrees of incidence for the vertical tail. The vertical tail in most single engine prop-driven aircraft have about 1-2 degrees of incidence to insure the prevention of aircraft roll in a reaction to propeller revolution. Another solution is to select a non-symmetric airfoil for the vertical tail, but this technique has several disadvantages. The exact value for the vertical tail incidence is determined by calculating the propeller rotation's rolling moment. An experimental approach would be more accurate.

6. Aspect ratio (*ARv*)

The vertical tail aspect ratio is defined as the ratio between vertical tail span; by (see figure 4.20) and the vertical tail mean aerodynamic chord ($\bar{C}_V$).

$$AR_V = \frac{b_V}{\bar{C}_V} \qquad 4.34$$

The general characteristics of the aspect ratio are introduced in Chapter 2 (see Section 2.6), so they are not repeated here. The vertical tail aspect ratio has several other features than impact various aircraft characteristics. These must be noticed in determining the vertical tail aspect ratio.

1. First, a high aspect ratio results in a tall vertical tail that causes the aircraft overall height to be increased. Many aircraft especially large transport aircraft and fighter aircraft have parking limitations in the hangar space. Thus, an aircraft is not allowed to have an overall height beyond a pre-specified value.
2. A high tail aspect ratio weakens the aircraft lateral control, since the vertical tail mass moment of inertia about x-axis is increased.
3. A vertical tail with a high aspect ratio has a longer yawing moment arm compared with a low aspect ratio vertical tail. Hence, an aircraft with high aspect ratio has a higher directional control.
4. As the vertical aspect ratio is increased, the bending moment and bending stress at the vertical tail root are increase which causes the aft portion of the aircraft to be heavier.
5. A high aspect ratio vertical tail is prone to fatigue and flutter.
6. A high aspect ratio vertical tail is longitudinally destabilizing, since the vertical tail drag generates a nose-up pitching moment.
7. As the aspect ratio of the vertical tail is increased, the aircraft directional stability is improved, due to an increase in the yawing moment arm.
8. As the aspect ratio of the vertical tail is increased, the vertical tail induced drag is increased.
9. If the aircraft has a T-tail configuration, the horizontal tail location and efficiency are functions of vertical tail aspect ratio. Thus, if the deep stall is a major concern, the vertical aspect ratio must be large enough to keep the horizontal tail out of the wing wake when the wing stalls.
10. A high aspect ratio vertical tail is aerodynamically more efficient (i.e. has a higher $(L/D)_{max}$) than a vertical tail with a low aspect ratio. The reason is the vertical tail tip effect.

The above-mentioned advantages and disadvantages for a high and low aspect ratio are general guidelines for the vertical tail designer. As a

starting point, a value between 1 and 2 is recommended for the vertical tail aspect ratio. The final value will be determined in the overall aircraft directional stability analysis. Table 4.3 shows the value for aspect ratio of vertical tail for several aircraft.

7. Taper ratio (λ_w)

As with other lifting surfaces (e.g wing and horizontal tail), the vertical tail taper ratio is defined as the ratio between the vertical tail tip chord; C_{Vtip} (see figure 4.20) to the vertical tail root chord; C_{Vroot} .

$$\lambda_V = \frac{C_{Vtip}}{C_{Vroot}} \qquad 4.35$$

General features of the taper ratio are introduced in Chapter 2 (see Section 2.7), so they are not repeated here. The main purposes of the taper ratio are
1: to reduce the bending stress on the vertical tail root.
2: to allow the vertical tail to have a sweep angle.
The application of taper ratio adds a complexity to the tail manufacturing process and increases the empennage weight. As the taper ratio of the vertical tail in increased, the yawing moment arm is reduced which reduces the directional control of the aircraft. Moreover, an increase in the taper ratio of the vertical tail would reduce the lateral stability of the aircraft. A compromise between these positive and negative features determine the value for the vertical tail taper ratio.

8. Sweep angle (Λv)

The general features of the sweep angle are introduced in Chapter 2 (see Section 2.9), so they are not repeated here. As the sweep angle of the vertical tail in increased, the yawing moment arm is increased which improves the directional control of the aircraft. Subsequently, an increase in the vertical tail sweep angle weakens the aircraft directional stability, since the mass moment inertia about z-axis in increased. If the aircraft has a T-tail configuration, an increase in the vertical tail sweep angle increases the horizontal tail moment arm which improves the aircraft longitudinal stability and control.
Another reason for the application of the vertical tail sweep angle is to decrease the wave drag in high subsonic and supersonic flight regime. For this reason, it is suggested to initially adopt a sweep angle like the sweep angle of the wing. The final value for the vertical tail sweep angle will be the results of a compromise between these positive and negative features.

Table 4.3 shows the value for the sweep angle of vertical tail for several aircraft.

9. Dihedral angle (Γv)

Due to the aircraft symmetricity requirement about x-z plane, an aircraft with one vertical tail is not allowed to have any dihedral angle. However, if the aircraft has a twin vertical tail, (such as few fighters), the dihedral angle has positive contributing to the aircraft lateral control. But it reduces the aerodynamic efficiency of the vertical tails, since two vertical tails will cancel part of their lift forces. In addition, the vertical tail dihedral angle will contribute to detectability features of the aircraft. For instance, McDonnell Douglas F-15 Eagle twin vertical tails canted 15 deg to reduce radar cross section. The exact value for the dihedral angles of a twin vertical tail is determined in the overall aircraft lateral- directional stability analysis process.

10. Tip chord (C_{Vtip}), Root chord (C_{Vroot}), Mean Aerodynamic Chord (MAC_v or $\bar{C}v$), and Span (bv)

The other vertical tail geometries include vertical tail span (b_V), vertical tail tip chord (C_{Vtip}), vertical tail root chord (C_{Vroot}), and vertical tail mean aerodynamic chord (C_V or MAC_V). These unknown parameters (see figure 4.20) are determined by solving the following four equations simultaneously:

$$AR_V = \frac{b_V}{\bar{C}_V} = \frac{b_V^2}{S_V}$$

$$\lambda_V = \frac{C_{V_{tip}}}{C_{V_{root}}}$$

$$\bar{C}_V = \frac{2}{3} C_{V_{root}} \left(\frac{1 + \lambda_V + \lambda_V^{\,2}}{1 + \lambda_V} \right)$$

$$S_V = b_V \cdot \bar{C}_V$$

The first two equations have been introduced previously in this section, but the last two equations are reproduced from wing geometry governing equations (see Chapter 2). The required data to solve these equations are the vertical tail planform area, vertical tail aspect ratio, and vertical tail taper ratio.

4.9. Practical Design Steps:

The tail design flowchart was presented in section 4.1. Fundamentals of the tail primary functions and design requirements were reviewed in Sections 4.2 and 4.3. Sections 4.4 through 4.8 introduced the various tail configurations, horizontal tail parameters, vertical tail parameters and the technique to determine each parameter. The purpose of this section is to outline the practical design steps of the tail. The tail design procedure is as follows:

1. Select tail configuration (Sections 4.4 and 4.7) Horizontal tail
2. Select horizontal tail location (aft, or forward (canard)); Section 4.5
3. Select the horizontal tail volume coefficient; $\bar{V}_H$ (Table 4.1)
4. Calculate optimum tail moment arm (*lopt*) to minimize the aircraft drag and weight (Section 4.6) (equation 4.11).
5. Calculate horizontal tail planform area; S_{ht} (equation 4.12).
6. Calculate wing-fuselage aerodynamic pitching moment coefficient (not mentioned).
7. Calculate cruise lift coefficient (C_{Lc}); equation 4.13
8. Calculate horizontal tail desired lift coefficient at cruise from trim equation (4.14)
9. Select horizontal tail airfoil section (Section 4.7)
10. Select horizontal tail sweep angle and dihedral (Section 4.7)
11. Select horizontal tail aspect ratio and taper ratio (Section 4.7)
12. Determine horizontal tail lift curve slope; $CL_{\alpha h}$ (Equation 4.22)
13. Calculate horizontal tail angle of attack at cruise; (equation 4.22)
14. Determine downwash angle at the tail (equation 4.19)
15. Calculate horizontal tail incidence angle; i_t (equation4.18
16. Calculate tail span, tail root chord, tail tip chord and tail mean aerodynamic chord.
17. Calculate horizontal tail generated lift coefficient at cruise (e.g. lifting line theory; Chapter 2). Treat the horizontal tail as a small wing.
18. If the horizontal tail generated lift coefficient (step 17) is not equal to the horizontal tail required lift coefficient (step 8), adjust tail incidence
19. Check horizontal tail stall
20. Calculate the horizontal tail contribution to the static longitudinal stability derivative (Cmα). The value for Cmα derivative must be negative to insure a stabilizing contribution. If the design requirements are not satisfied, redesign the tail.

21. Analyze dynamic longitudinal stability. If the design requirements are not satisfied, redesign the tail.
22. Optimize horizontal tail.

Vertical Tail

23. Select vertical tail configuration (e.g. conventional, twin vertical tail, vertical tail at swept wing tip, V-tail) (Section 4.8.2-1).
24. Select the vertical tail volume coefficient; $\bar{V}_V$ (Table 4.3).
25. Assume the vertical tail moment arm (*lv*) as equal to the horizontal tail moment arm (*l*).
26. Calculate vertical tail planform area; *Sv* (equation 4.33).
27. Select vertical tail airfoil section (Section 4.8.2-4).
28. Select vertical tail aspect ratio; ARv (Section 4.8.2-6).
29. Select vertical tail taper ratio; λ_V (Section 4.8.2-7).
30. Determine the vertical tail incidence angle (Section 4.8.2-5).
31. Determine the vertical tail sweep angle (Section 4.8.2-8).
32. Determine the vertical tail dihedral angle (Section 4.8.2-9).
33. Calculate vertical tail span (*bv*), root chord (*Cvroot*), and tip chord (*Cvtip*), and mean aerodynamic chord (MACv).
34. Check the spin recovery.
35. Adjust the location of the vertical tail relative to the horizontal tail by changing lv, to satisfy the spin recovery requirements (Section 4.8.2-2).
36. Analyze directional trim (Section 4.8.1).
37. Analyze directional stability (Section 4.8.1).
38. Modify to meet the design requirements.
39. Optimize the tail.

Example 4.2

Problem statement: Design a horizontal tail for a two-seat motor glider aircraft with the following characteristics:

m_{TO} = 850 kg, D_{fmax} = 1.1 m, Vc = 95 knot (at 10,000 ft), α_f = 1 deg (at cruise) The wing has a reference area 18 m^2 of and the following features: C = 0.8 m, AR = 28, λ = 0.8, i_w = 3 deg, α_{twist} = -1.1 deg, Λ_{LE} = 8 deg, Γ = 5 deg, airfoil: NACA 23012, CLα = 5.8 1/rad

The aircraft has a high wing and an aft conventional tail configuration, and the aerodynamic center of the wing-fuselage combination is located at 23% of MAC. In cruising flight condition, the aircraft center of gravity is located at 32 percent of the fuselage length. Assume that the aircraft cg is 7 cm ahead of the wing-fuselage aerodynamic center.

Then following tail parameters must be determined: airfoil section, S_h, C_{htip}, C_{hroot}, b_h, i_h, AR_h, λ_h, Λ_h, Γ_h. At the end, draw a top-view of the aircraft that shows fuselage, wing and horizontal tail (with dimensions).

Solution:

The tail configuration has been already selected and stated, so there is no need to investigate this item. The only parameter that needs to be decided is the type of setting angle. Since the aircraft is not maneuverable and the cost must be low, a fixed tail is selected. Thus, the design begins with the selection of the horizontal tail volume coefficient.

Problems

1. Identify C_{li}, C_{dmin}, C_m, $(C_l/C_d)_{max}$, α_o (deg), α_s (deg), C_{lmax}, a_o (1/rad), $(t/c)_{max}$ of the NACA 2415 airfoil section (flap-up). You need to indicate the locations of all parameters on the airfoil graphs as shown in figure 1.

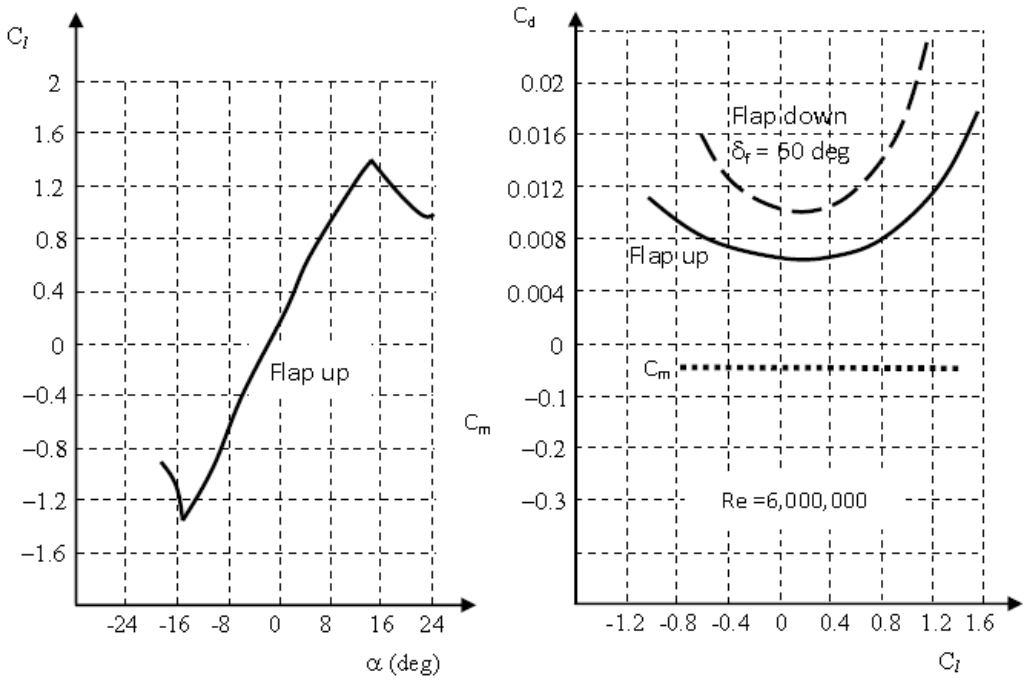

Figure 1. Airfoil section NACA 2415

Solution:

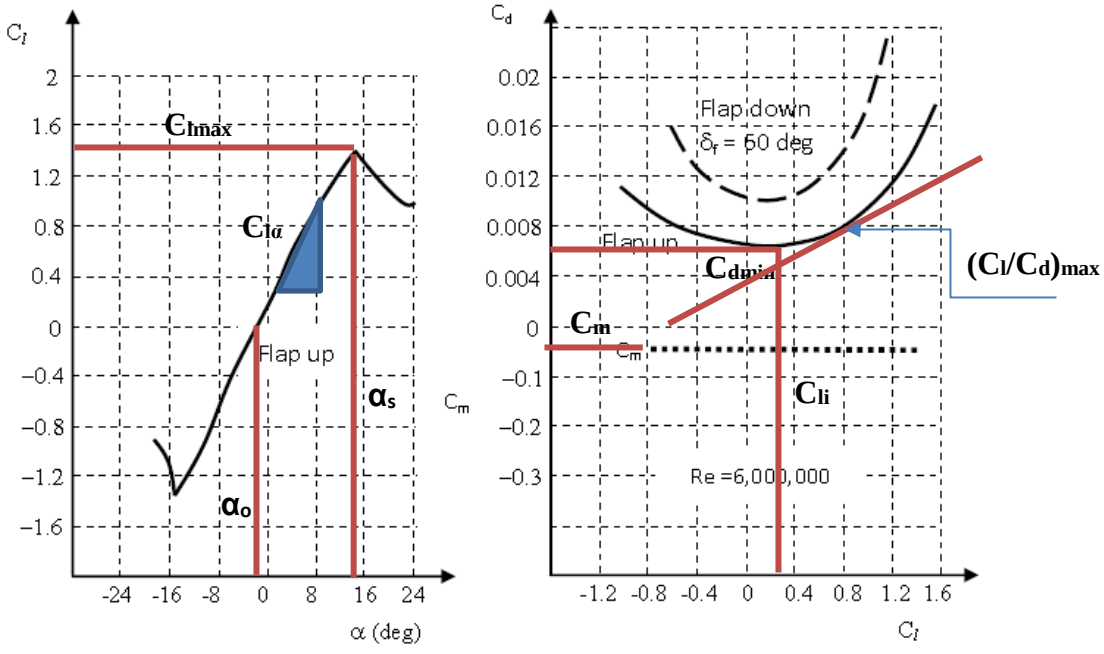

2. Identify C_{li}, C_{dmin}, C_m, $(C_l/C_d)_{max}$, α_o (deg), α_s (deg), C_{lmax}, a_o (1/rad), $(t/c)_{max}$ of the NACA 63_2-615 airfoil section (flap-up). You need to indicate the locations of all parameters on the airfoil graphs as shown in figure 2.

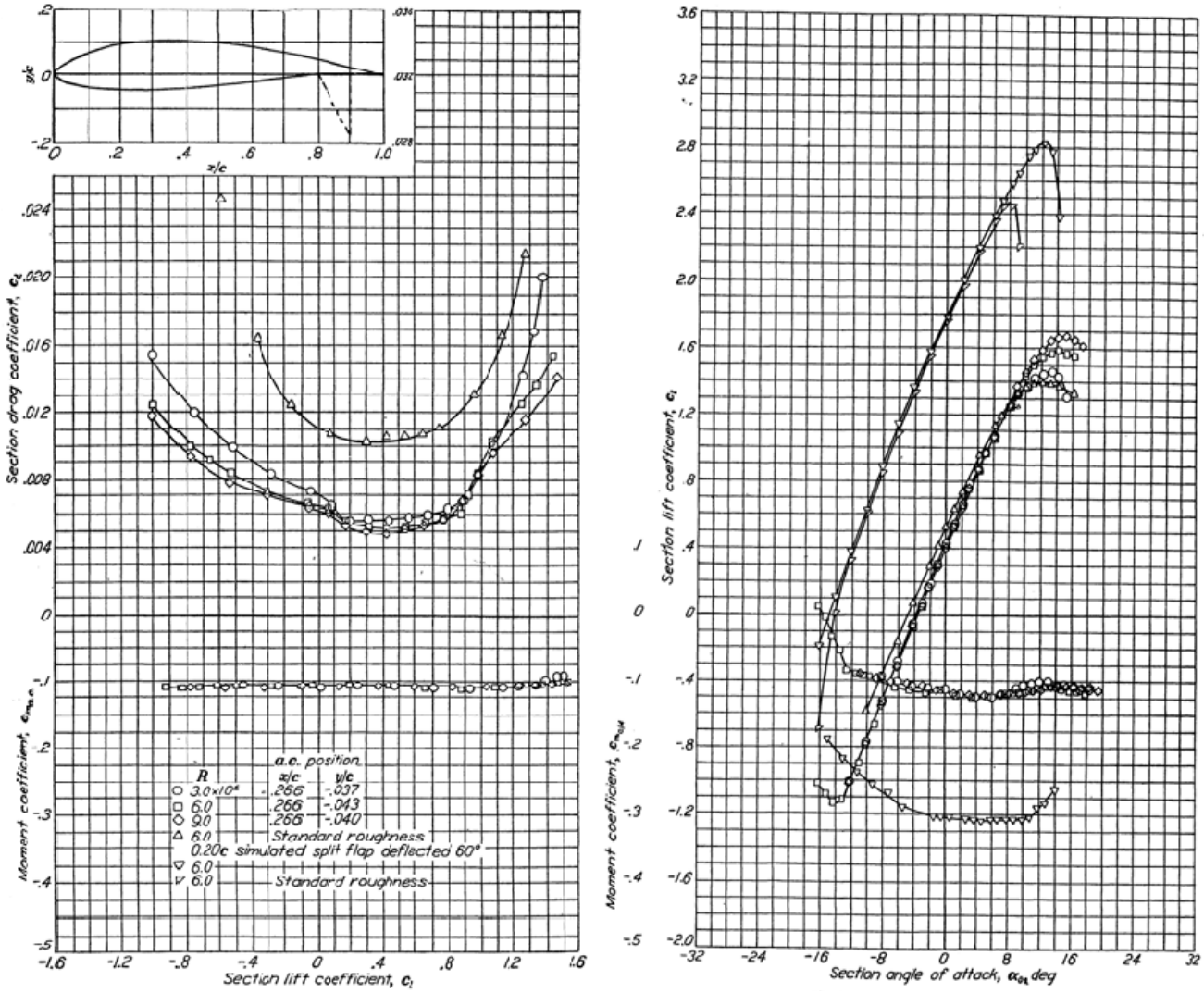

Figure 2. C_l-α, C_m- α, and C_d-C_l graphs of NACA 632-615 airfoil section

Solution:

Like in question 1 to have

C_{li}	C_{dmin}	C_m	$(C_l/C_d)_{max}$	α_o (deg)	α_s (deg)	C_{lmax}	$C_{l\alpha}$ (1/rad)	$(t/c)_{max}$
0.42	0.0045	-0.125	123	-4.5	12^o	1.65	5.95	15%

And, from NACA 632-615 max. pressure location is at 30% of the chord

It demonstrates that the bucket in Cd-Cl diagram (see figure 2) begins from lift coefficient of 0 (since 0.2 - 0.2 = 0) and ends at 0.4 (since 0.2 + 0.2 = 0.4).

3. A NACA airfoil has thickness-to-chord ratio of 18 percent. Estimate the lift curve slope for this airfoil in 1/rad.

Solution:

By using the empirical equation $C_{l_\alpha} = dC_l/d\alpha = 1.8\pi\left(1 + 0.8(t_{max}/c)\right)$ we estimate the lift curve slope for this NACA airfoil in 1/rad.

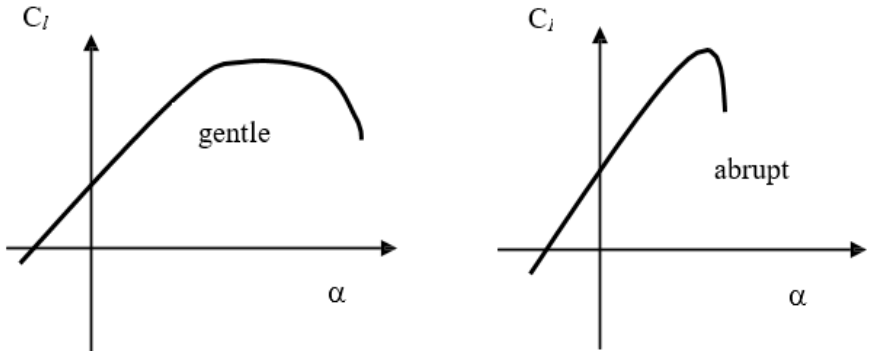

the shape of the lift curve at and beyond the stall angle of attack (stall behavior). An airfoil with a gentle drop in lift after the stall, rather than an abrupt or sharp rapid lift loss, leads to a safer stall from which the pilot can more easily recover.

4. Select a NACA airfoil section for the wing for a prop-driven normal category GA aircraft with the following characteristics:

m_{TO} = 3,500 kg, S = 26 m^2, V_c = 220 knot (at 4,000 m), V_s = 68 knot (at sea level)

The high lift device (plain flap) will provide $\Delta C_L = 0.4$ when deflected.

Solution:

Assume the velocity correction is 0.514 and density $\rho = 0.819$ kg/m^3 , $\rho_o = 1.225$ kg/m^3

$$C_{Lc} = \frac{2W_{avg}}{\rho V_c^2 S} = \frac{2 \times 3500 \times 9.81}{0.819(120 \times 0.514)^2 \times 26} = 0.252$$

$$C_{Lcw} = \frac{C_{Lc}}{0.95} = \frac{0.252}{0.95} = 0.265$$

$$C_{Li} = \frac{C_{Lcw}}{0.9} = \frac{0.265}{0.9} = 0.294 \cong 0.3$$

Maximum lift coefficient:

$$C_{Lmax} = \frac{2W_{To}}{\rho_o V_S^2 S} = \frac{2\times3500\times9.81}{1.225(68\times0.514)^2\times26} = 1.764$$

$$(C_{L_{max}})_w = \frac{C_{Lmax}}{0.95} = \frac{1.764}{0.95} = 1.857$$

$$(C_{L_{max}})_{gross} = \frac{(C_{L_{max}})_w}{0.90} = \frac{1.857}{0.90} = 2.064$$

$$\therefore C_{L_{max}} = (C_{L_{max}})_{gross} - \Delta C_{L_{HID}} = 2.064 - 0.4 = 1.664 \cong 1.7$$

Thus, we need to look for NACA airfoil sections that yield an ideal lift coefficient of 0.3 and a net maximum lift coefficient of 1.7 . Referring to figure 1.16, we find the airfoils whose characteristics match with our design requirements (C_{li} = 0.3, C_{lmax} =1.7) is NACA 23015

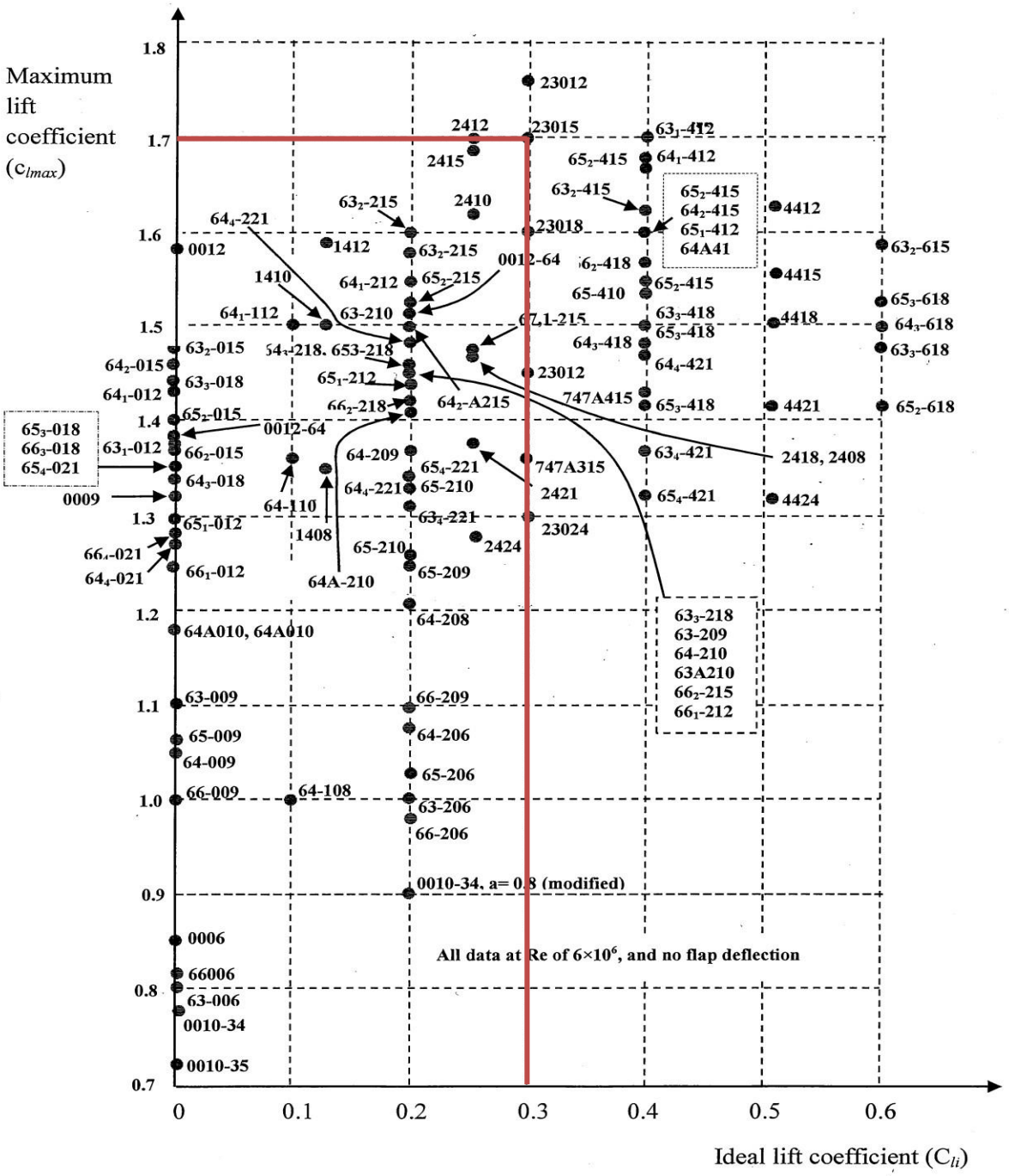

5. Select a NACA airfoil section for the wing for a prop-driven transport aircraft with the following characteristics:

m_{TO} = 23,000 kg, S = 56 m^2, V_c = 370 knot (at 25,000 ft), V_s = 85 knot (at sea level)

The high lift device (single slotted flap) will provide $\Delta C_L = 0.9$ when deflected.

Solution:

Assume the velocity correction is 0.514 and density ρ = 0.554 kg/m^3 at 7620 m, ρ_o = 1.225 kg/m^3

$$C_{Lc} = \frac{2W_{avg}}{\rho V_c^2 S} = \frac{2 \times 23000 \times 9.81}{0.554(370 \times 0.514)^2 \times 56} = 0.402$$

$$C_{Lcw} = \frac{C_{Lc}}{0.95} = \frac{0.402}{0.95} = 0.423$$

$$C_{Li} = \frac{C_{Lcw}}{0.9} = \frac{0.423}{0.9} = 0.47$$

Maximum lift coefficient:

$$C_{Lmax} = \frac{2W_{To}}{\rho_o V_s^2 S} = \frac{2 \times 23000 \times 9.81}{1.225(85 \times 0.514)^2 \times 56} = 3.446$$

$$(C_{L_{max}})_w = \frac{C_{Lmax}}{0.95} = \frac{3.446}{0.95} = 3.627$$

$$(C_{L_{max}})_{gross} = \frac{(C_{L_{max}})_w}{0.90} = \frac{3.627}{0.90} = 4.03$$

$$\therefore C_{L_{max}} = (C_{L_{max}})_{gross} - \Delta C_{L_{HID}} = 4.03 - 0.9 = 3.13$$

Thus, we need to look for NACA airfoil sections that yield an ideal lift coefficient of 6.5 and a net maximum lift coefficient of 3.1 . Referring to figure 1.16, we find the airfoils whose characteristics match with our design requirements (all have C_{li} = 6.5, C_{lmax} =3.1) is NACA 632-609

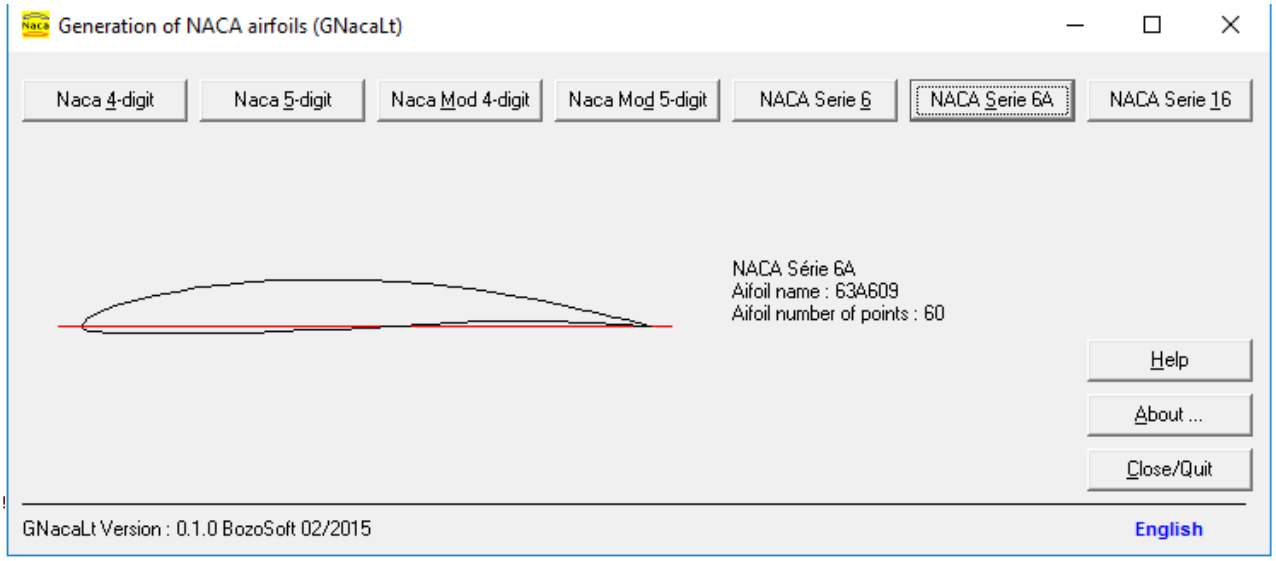

6. Select a NACA airfoil section for the wing for a business jet aircraft with the following characteristics:

m_{TO} = 4,800 kg, S = 22.3 m^2, V_c = 380 knot (at 33,000 ft), V_s = 81 knot (@sea level)

The high lift device (double slotted flap) will provide $\Delta C_L = 1.1$ when deflected.

Solution:

Assume the velocity correction is 0.514 and density $\rho = 0.413$ kg/m^3 at 10058.5 m, $\rho_o = 1.225$ kg/m^3

$$C_{Lc} = \frac{2W_{avg}}{\rho V_c^2 S} = \frac{2 \times 4800 \times 9.81}{0.413(380 \times 0.514)^2 \times 22.3} = 0.268$$

$$C_{Lcw} = \frac{C_{Lc}}{0.95} = \frac{0.268}{0.95} = 0.282$$

$$C_{Li} = \frac{C_{Lcw}}{0.9} = \frac{0.282}{0.9} = 0.313$$

Maximum lift coefficient:

$$C_{Lmax} = \frac{2W_{To}}{\rho_o V_s^2 S} = \frac{2\times4800\times9.81}{1.225(81\times0.514)^2\times22.3} = 1.988$$

$$(C_{L_{max}})_w = \frac{C_{Lmax}}{0.95} = \frac{1.988}{0.95} = 2.093$$

$$(C_{L_{max}})_{gross} = \frac{(C_{L_{max}})_w}{0.90} = \frac{2.093}{0.90} = 2.326$$

$$\therefore C_{L_{max}} = (C_{L_{max}})_{gross} - \Delta C_{L_{HID}} = 2.326 - 1.1 = 1.226$$

Thus, we need to look for NACA airfoil sections that yield an ideal lift coefficient of 0.313 and a net maximum lift coefficient of 1.226 . Referring to figure 1.16, we find the airfoils whose characteristics match with our design requirements (all have C_{li} = 0.313, C_{lmax} =1.226) is NACA 23024

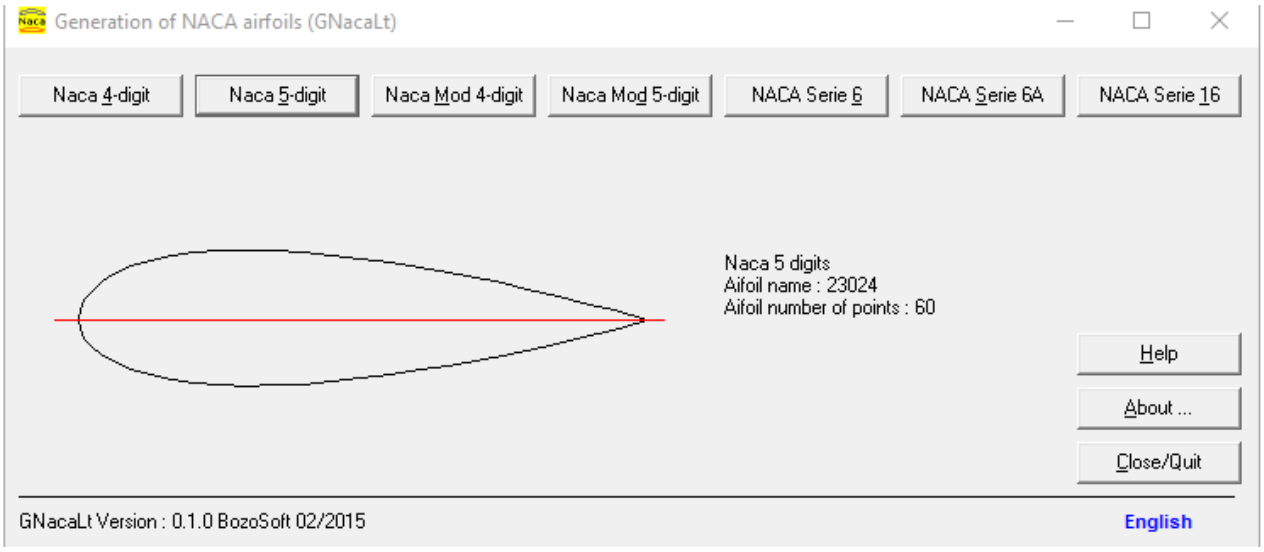

7. Select a NACA airfoil section for the wing for a jet transport aircraft with the following characteristics:

m_{TO} = 136,000 kg, S = 428 m^2, V_c = 295 m/sec (at 42,000 ft), V_s = 88 knot (at sea level)

The high lift device (triple slotted flap) will provide $\Delta C_L = 1.3$ when deflected.

Solution:

Assume the velocity correction is 0.514 and density $\rho = 0.203$ kg/m^3 at 12801.5 m, $\rho_o = 1.225$ kg/m^3

$$C_{Lc} = \frac{2W_{avg}}{\rho V_c^2 S} = \frac{2 \times 136000 \times 9.81}{0.203(295)^2 \times 428} = 0.352$$

$$C_{Lcw} = \frac{C_{Lc}}{0.95} = \frac{0.352}{0.95} = 0.371$$

$$C_{Li} = \frac{C_{Lcw}}{0.9} = \frac{0.371}{0.9} = 0.412$$

Maximum lift coefficient:

$$C_{Lmax} = \frac{2W_{To}}{\rho_o V_S^2 S} = \frac{2\times136000\times9.81}{1.225(88\times0.514)^2\times428} = 2.487$$

$$(C_{L_{max}})_w = \frac{C_{Lmax}}{0.95} = \frac{2.487}{0.95} = 2.618$$

$$(C_{L_{max}})_{gross} = \frac{(C_{L_{max}})_w}{0.90} = \frac{2.618}{0.90} = 2.909$$

$$\therefore C_{L_{max}} = (C_{L_{max}})_{gross} - \Delta C_{L_{HID}} = 2.909 - 1.3 = 1.609$$

Thus, we need to look for NACA airfoil sections that yield an ideal lift coefficient of 0.412 and a net maximum lift coefficient of 1.609 . Referring to figure 1.16, we find the airfoils whose characteristics match with our design requirements (all have C_{li} = 0.412, C_{lmax} =1.609) is

1. NACA 652-415
2. NACA 642-415
3. NACA 651-415
4. NACA 64A41

8. Select a NACA airfoil section for the wing for a fighter jet aircraft with the following characteristics:

m_{TO} = 30,000 kg, S = 47 m^2, V_c = 1,200 knot (at 40,000 ft), V_s = 95 knot (at sea level)
The high lift device (plain flap) will provide $\Delta C_L = 0.8$ when deflected.

Solution:

Assume the velocity correction is 0.514 and density $\rho = 0.205$ kg/m^3 at 12192 m, ρ_o = 1.225 kg/m^3

$$C_{Lc} = \frac{2W_{avg}}{\rho V_c^2 S} = \frac{2 \times 30000 \times 9.81}{0.205(1200 \times 0.514)^2 \times 47} = 0.160$$

$$C_{Lcw} = \frac{C_{Lc}}{0.95} = \frac{0.160}{0.95} = 0.169$$

$$C_{Li} = \frac{C_{Lcw}}{0.9} = \frac{0.169}{0.9} = 0.187$$

Maximum lift coefficient:

$$C_{Lmax} = \frac{2W_{To}}{\rho_o V_S^2 S} = \frac{2 \times 30000 \times 9.81}{1.225(95 \times 0.514)^2 \times 47} = 4.287$$

$$(C_{L_{max}})_w = \frac{C_{Lmax}}{0.95} = \frac{4.287}{0.95} = 4.513$$

$$(C_{L_{max}})_{gross} = \frac{(C_{L_{max}})_w}{0.90} = \frac{4.513}{0.90} = 5.014$$

$$\therefore C_{L_{max}} = (C_{L_{max}})_{gross} - \Delta C_{L_{HID}} = 5.014 - 0.8 = 4.214$$

Thus, we need to look for NACA airfoil sections that yield an ideal lift coefficient of 0.187 and a net maximum lift coefficient of 1.226 . Referring to figure 1.16, we find the airfoils whose characteristics match with our design requirements (all have C_{li} = 0.187, C_{lmax} =4.214) is NACA 64A110

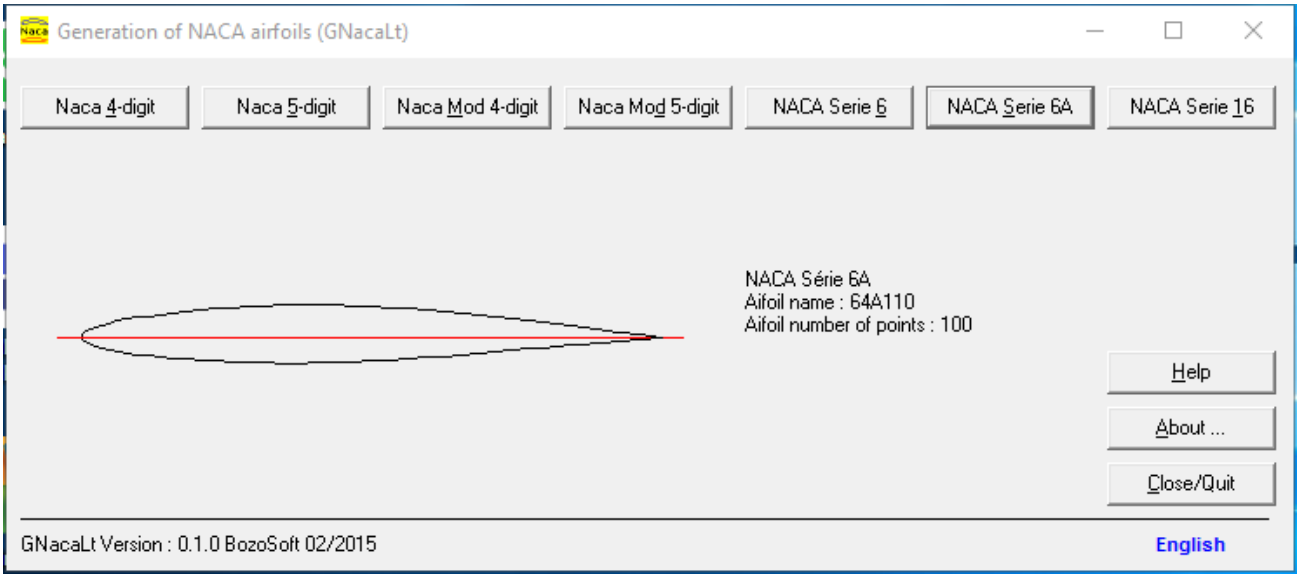

9. A designer has selected a NACA 2415 (figure 3) for an aircraft wing during a design process. Determine the wing setting angle.

Solution:

Wing setting angle is initially determined to be the corresponding angle to the airfoil ideal lift coefficient. Since the airfoil ideal lift coefficient is 0.416, figure 5.62 (left figure) reads the corresponding angle to be 2 degrees. The value (iw = 2 deg) may need to be revised based on the calculation to satisfy the design requirements later.

10. The airfoil section of a wing with aspect ratio of 9 is NACA 2415 (figure 2). Determine the wing lift curve slope in terms of 1/rad.

Solution:

By using the empirical equation $C_{l_\alpha} = dC_l/d\alpha = 1.8\pi\left(1 + 0.8(t_{max}/c)\right)$ we estimate the lift curve slope for this NACA airfoil in 1/rad with $(t_{max}/c) = 0.15$

11. Determine the Oswald span efficiency for a wing with aspect ratio of 12 and sweep angle of 15 degrees.

Solution:

The Oswald span efficiency for swept wing is given by the equation below:

$$e = 1.78(1 - 0.045AR^{0.68})[cos(\Lambda_{LE})]^{0.15} - 3.1$$

12. Determine the Oswald span efficiency for a wing with aspect ratio of 4.6 and sweep angle of 40 degrees.

Solution:

The Oswald span efficiency for swept wing is given by the equation below:

$$e = 1.78(1 - 0.045AR^{0.68})[cos(\Lambda_{LE})]^{0.15} - 3.1$$

13. A straight rectangular wing has a span of 25 m and MAC of 2.5 m. If the wing swept back by 30^o degrees, determine the effective span of the wing.

Solution:

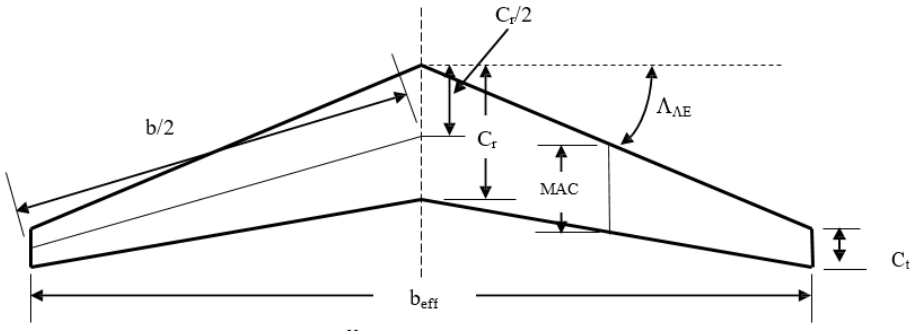

Since it's a straight rectangular wing then (λ =1)

$\bar{C} = \frac{2}{3} C_r \left(\frac{1+\lambda+\lambda^2}{1+\lambda}\right) \rightarrow \bar{C} = \frac{2}{3} C_r$ to find the value of Cr

$\left(\frac{b_{eff}}{2}\right) = \sqrt{\left(\frac{b}{2}\right)^2 - C_r^2}$ Pythagoras

Or, b_{eff} = b cos Λ

14. A trainer aircraft has a wing area of S = 32 m^2, aspect ratio AR = 9.3, and taper ratio of λ = 0.48. It is required that the 50 percent chord line sweep angle be zero. Determine tip chord, root chord, mean aerodynamic chord, and span, as well as leading edge sweep, trailing edge sweep and quarter chord sweep angles.

Solution:

$$AR = \frac{b^2}{S} \rightarrow b = \sqrt{S.AR} =$$

$$AR = \frac{b}{\bar{C}} \rightarrow \bar{C} = \frac{b}{AR} =$$

$$\bar{C} = \frac{2}{3} C_r \left(\frac{1+\lambda+\lambda^2}{1+\lambda}\right) \rightarrow \boldsymbol{C_r} =$$

$$\lambda = \frac{C_t}{C_r} \rightarrow \boldsymbol{C_t} =$$

Now sketch the wing to find $\Lambda_{L.E}$, $\Lambda_{T.E}$ and $\Lambda_{C/4}$

15. A cargo aircraft has a wing area of S = 256 m^2, aspect ratio AR = 12.4, and taper ratio of λ = 0.63. It is required that the 50 percent chord line sweep angle be zero. Determine tip chord, root chord, mean aerodynamic chord, and span, as well as leading edge sweep, trailing edge sweep and quarter chord sweep angles.

Solution:

$$AR = \frac{b^2}{S} \rightarrow b = \sqrt{S.AR} =$$

$$AR = \frac{b}{\bar{C}} \rightarrow \bar{C} = \frac{b}{AR} =$$

$$\bar{C} = \frac{2}{3} C_r \left(\frac{1 + \lambda + \lambda^2}{1 + \lambda} \right) \rightarrow \boldsymbol{C_r} =$$

$$\lambda = \frac{C_t}{C_r} \rightarrow \boldsymbol{C_t} =$$

Now sketch the wing to find $\Lambda_{L.E}$, $\Lambda_{T.E}$ and $\Lambda_{C/4}$

16. A jet fighter aircraft has a wing area of S = 47 m^2, aspect ratio AR = 7, and taper ratio of λ = 0.8. It is required that the 50 percent chord line sweep angle be 42 degrees. Determine tip chord, root chord, mean aerodynamic chord, span, and effective span, as well as leading edge sweep, trailing edge sweep and quarter chord sweep angles.

Solution:

$$AR = \frac{b^2}{S} \rightarrow b = \sqrt{S.AR} =$$

$$AR = \frac{b}{\bar{C}} \rightarrow \bar{C} = \frac{b}{AR} =$$

$$\bar{C} = \frac{2}{3} C_r \left(\frac{1 + \lambda + \lambda^2}{1 + \lambda} \right) \rightarrow \boldsymbol{C_r} =$$

$$\lambda = \frac{C_t}{C_r} \rightarrow \boldsymbol{C_t} =$$

$$\frac{\boldsymbol{b_{eff}}}{\boldsymbol{2}} = \frac{b}{2} \cos(42) \rightarrow b_{eff} =$$

$$AR_{eff} = \frac{b_{eff}^2}{S} \rightarrow AR_{eff} =$$

Now sketch the wing to find $\Lambda_{L.E}$, $\Lambda_{T.E}$ and $\Lambda_{C/4}$

17. A business jet aircraft has a wing area of S = 120 m^2, aspect ratio AR = 11.5, and taper ratio of λ = 0.55. It is required that the 50 percent chord line sweep angle be 37 degrees. Determine the tip chord, root chord, mean aerodynamic chord, span, and effective span, as well as leading edge sweep, trailing edge sweep and quarter chord sweep angles.

Solution:

$$AR = \frac{b^2}{S} \rightarrow b = \sqrt{S.AR} =$$

$$AR = \frac{b}{\bar{C}} \rightarrow \bar{C} = \frac{b}{AR} =$$

$$\bar{C} = \frac{2}{3} C_r \left(\frac{1 + \lambda + \lambda^2}{1 + \lambda} \right) \rightarrow \boldsymbol{C_r} =$$

$$\lambda = \frac{C_t}{C_r} \rightarrow \boldsymbol{C_t} =$$

$$\frac{\boldsymbol{b_{eff}}}{\mathbf{2}} = \frac{b}{2} \cos(42) \rightarrow b_{eff} =$$

$$AR_{eff} = \frac{b_{eff}^2}{S} \rightarrow AR_{eff} =$$

Now sketch the wing to find $\Lambda_{L.E}$, $\Lambda_{T.E}$ and $\Lambda_{C/4}$

18. A fighter aircraft has a straight wing with a planform area of 50 m^2, aspect ratio of 4.2 and taper ratio of 0.6. Determine wing span, root chord, tip chord, and Mean Aerodynamic Chord. Then sketch the wing.

Solution:

$$AR = \frac{b^2}{S} \rightarrow b = \sqrt{S.AR} =$$

$$AR = \frac{b}{\bar{C}} \rightarrow \bar{C} = \frac{b}{AR} =$$

$$\bar{C} = \frac{2}{3} C_r \left(\frac{1 + \lambda + \lambda^2}{1 + \lambda} \right) \rightarrow \boldsymbol{C_r} =$$

$$\lambda = \frac{C_t}{C_r} \rightarrow \boldsymbol{C_t} =$$

Now we could sketch the wing

19. A hang glider has a swept wing with a planform area of 12 m^2, aspect ratio of 7 and taper ratio of 0.3. Determine wing span, root chord, tip chord, and Mean Aerodynamic Chord. Then sketch the wing, if the sweep angle is 35 degrees.

Solution:

$$AR = \frac{b^2}{S} \rightarrow b = \sqrt{S.AR} =$$

$$AR = \frac{b}{\bar{C}} \rightarrow \bar{C} = \frac{b}{AR} =$$

$$\bar{C} = \frac{2}{3} C_r \left(\frac{1 + \lambda + \lambda^2}{1 + \lambda} \right) \rightarrow \boldsymbol{C_r} =$$

$$\lambda = \frac{C_t}{C_r} \rightarrow \boldsymbol{C_t} =$$

Now we could sketch the wing

20. The planform area for a cargo aircraft is 182 m2. The wing has an Anhedral of -8 degrees; determine the effective wing planform area of the aircraft.

Solution:

$$S_{eff} = S \cos(\Gamma)$$

21. Design a wing for a utility category General Aviation aircraft with the following features:

S = 22 m^2, m = 2,100 kg, V_C = 152 knot (@ 20,000 ft), V_S = 67 knot (@ sea level)

The aircraft has a monoplane low wing and employs the plain flap. Determine airfoil section, aspect ratio, taper ratio, tip chord, root, chord, MAC, span, twist angle, sweep angle, dihedral angle, incidence, high lifting device type, flap span, flap chord, flap deflection and wing angle of attack at take-off.

Solution:

The same steps of Q-4 to Q-8

As for the flap

$\frac{b_r}{2} = (0.45 \sim 0.65) \frac{b}{2}$ and C_r = (0.35~0.45) C then find b_r/b and C_r/C to find δ_r from table 2.9 or assume it for take-off and double it for landing

22. Design a wing for a jet cargo aircraft with the following features:

S = 415 m^2, m = 150,000 kg, V_C = 520 knot (@ 30,000 ft), V_S = 125 knot (@ sea level)

The aircraft has a monoplane high wing and employs a triple slotted flap. Determine airfoil section, aspect ratio, taper ratio, tip chord, root, chord, MAC, span, twist angle, sweep angle, dihedral angle, incidence, high lifting device type, flap span, flap chord, flap deflection and wing angle of attack at take-off. Plot lift distribution at cruise and sketch the wing including dimensions.

Solution:

The same steps of Q-4 to Q-8

As for the flap

$\frac{b_r}{2} = (0.45\sim0.65)\frac{b}{2}$ and C_r = (0.35~0.45) C then find b_r/b and C_r/C to find δ_r from table 2.9 or assume it for take-off and double it for landing

23. Design a wing for a supersonic fighter aircraft with the following features:

S = 62 m^2, m = 33,000 kg, V_C = 1,350 knot (@ 45,000 ft), V_S = 105 knot (@ sea level)

The controllability and high performance are two high priorities in this aircraft. Determine wing vertical position, airfoil section, aspect ratio, taper ratio, tip chord, root, chord, MAC, span, twist angle, sweep angle, dihedral angle, incidence, high lifting device type, HLD span, HLD chord, HLD deflection and wing angle of attack at take-off. Plot lift distribution at cruise and sketch the wing including dimensions.

Solution:

The same steps of Q-4 to Q-8

As for the flap

$\frac{b_r}{2} = (0.45\sim0.65)\frac{b}{2}$ and C_r = (0.35~0.45) C then find b_r/b and C_r/C to find δ_r from table 2.9 or assume it for take-off and double it for landing

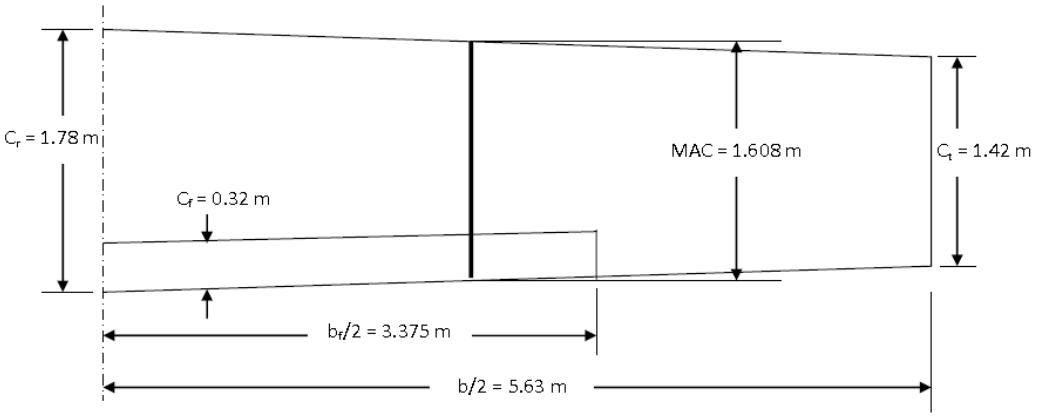

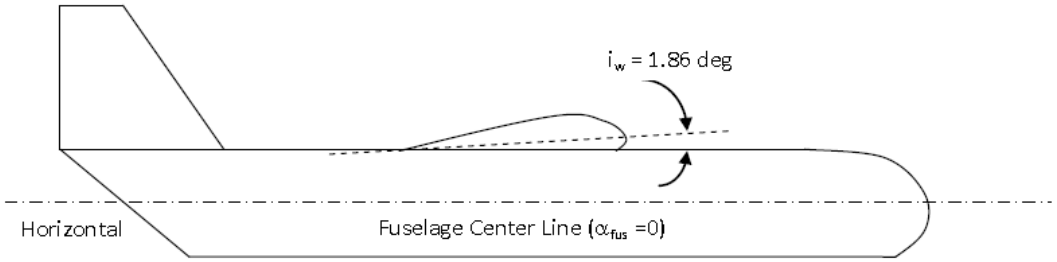

b. Side view of the aircraft in cruising flight

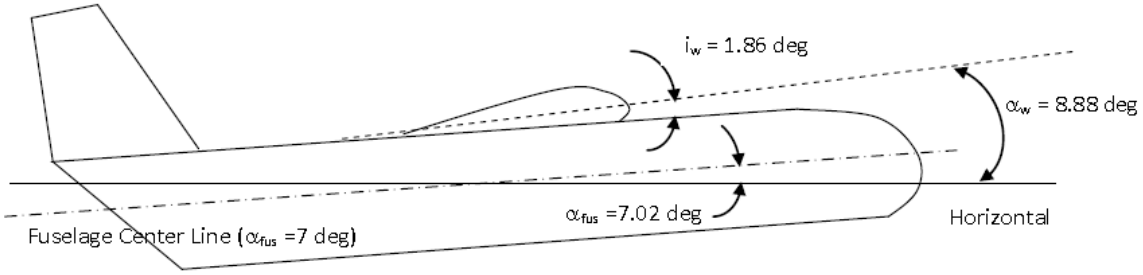

c. Side view of the aircraft in take-off

Figure-3. Wing parameters

Problems

1. An unmanned aircraft has the following features:

$$S = 55\ m^2,\ AR = 25,\ Sh = 9.6\ m^2,\ l = 6.8\ m$$

Determine the horizontal tail volume coefficient.

Solution:

$$AR = \frac{b^2}{S} \rightarrow b = \sqrt{S.AR} =$$

$$AR = \frac{b}{\bar{C}} \rightarrow \bar{C} = \frac{b}{AR} =$$

$$\bar{V}_h = \frac{l.S_h}{\bar{C}S}$$

2. The wing reference area of an agricultural aircraft is 14.5 m^2 and wing mean aerodynamic chord is 1.8 m. The longitudinal stability requirements dictate the tail volume coefficient to be 0.9. If the maximum fuselage diameter is 1.6 m, determine the optimum tail arm and then calculate the horizontal tail area. Assume that the aft portion of the fuselage is conical.

Solution:

$$l_{opt} = K_c \sqrt{\frac{4.\bar{C}.S.\bar{V}_h}{\pi.D_f}} = 1 \times \sqrt{\frac{4 \times 1.8 \times 14.5 \times 0.9}{3.14 \times 1.6}} \rightarrow l_{opt} = \quad m$$

$$\bar{V}_h = \frac{l.S_h}{\bar{C}S} \rightarrow S_h = \frac{\bar{C}.S.\bar{V}_h}{l_{opt}} = \frac{1.8 \times 14.5 \times 0.9}{l_{opt}} = \quad m^2$$

3. Consider a single-seat GA aircraft whose wing reference area is 12 m^2 and wing mean aerodynamic chord is 1.3 m. The longitudinal stability requirements dictate the tail volume coefficient to be 0.8. If the maximum fuselage diameter is 1.3 m, determine the optimum tail arm and then calculate the horizontal tail area. Assume that the aft portion of the fuselage is not conical.

Solution:

Since the aft portion of the fuselage is not conical, so the factor Kc is assumed to be 1.4

$$l_{opt} = K_c \sqrt{\frac{4.\bar{C}.S.\bar{V}_h}{\pi.D_f}} = 1.4 \times \sqrt{\frac{4 \times 1.3 \times 12 \times 0.8}{3.14 \times 1.3}} \rightarrow l_{opt} = \quad m$$

$$\bar{V}_h = \frac{l.S_h}{\bar{C}S} \rightarrow S_h = \frac{\bar{C}.S.\bar{V}_h}{l_{opt}} = \frac{1.3 \times 12 \times 0.8}{l_{opt}} = \quad m^2$$

4. Suppose that the angle of attack of the wing for GA aircraft is 2.3 deg ,S = 32 m^2, AR = 8.7, Wing lift coafficiant is 2.5, Wing airfoil: NACA 651-412 and the horizontal tail has an incidence of -1.5 deg. How much is the horizontal tail angle of attack at this flight condition?

Solution:

$$C_{l_{\alpha w}} = dC_l/d\alpha = 1.8\pi\left(1 + 0.8(t_{max}/c)\right)$$

$$\varepsilon = \varepsilon_o + \frac{\partial \varepsilon}{\partial \alpha}\alpha_w$$

$$\varepsilon_o = \frac{2C_{L_w}}{\pi . AR}$$

$$\frac{\partial \varepsilon}{\partial \alpha} = \frac{2C_{L_{\alpha_w}}}{\pi . AR}$$

$$\alpha_h = \alpha_f + i_h - \varepsilon$$

5. The horizontal tail of a transport aircraft has the following features:

$$AR_h = 5.4,\ \lambda_h = 0.7,\ S_h = 14\ m^2,\ \Lambda_{h\_LE} = 30 \text{ degrees}$$

Determine span, root chord, tip chord and the mean aerodynamic of the horizontal tail. Then sketch the top-view of the tail with dimensions.

Solution:

$$AR_h = \frac{b_h}{\overline{C}_h}$$

$$\lambda_h = \frac{C_{h_{tip}}}{C_{h_{root}}}$$

$$\overline{C}_h = \frac{2}{3} C_{h_{root}} \left(\frac{1 + \lambda_h + \lambda_h^{\,2}}{1 + \lambda_h} \right)$$

$$S_h = b_h \cdot \overline{C}_h$$

6. The horizontal tail of a fighter aircraft has the following features:

$$AR_h = 3.1,\ \lambda_h = 0.6,\ S_h = 6.4\ m^2,\ \Lambda_{h\_LE} = 40 \text{ degrees}$$

Determine span, root chord, tip chord and the mean aerodynamic of the horizontal tail. Then sketch the top-view of the tail with dimensions.

Solution:

$$AR_h = \frac{b_h}{\overline{C}_h}$$

$$\lambda_h = \frac{C_{h_{tip}}}{C_{h_{root}}}$$

$$\overline{C}_h = \frac{2}{3} C_{h_{root}} \left(\frac{1 + \lambda_h + \lambda_h^{\,2}}{1 + \lambda_h} \right)$$

$$S_h = b_h \cdot \overline{C}_h$$

7. The vertical tail of a transport aircraft has the following features:

$$AR_V = 1.6,\ \lambda_V = 0.4,\ S_V = 35\ m^2,\ \Lambda_{V\_LE} = 45 \text{ degrees}$$

Determine span, root chord, tip chord and the mean aerodynamic of the vertical tail. Then sketch the side-view of the tail with dimensions.

Solution:

$$AR_V = \frac{b_V}{\overline{C}_V} = \frac{b_V^2}{S_V}$$

$$\lambda_V = \frac{C_{V_{tip}}}{C_{V_{root}}}$$

$$\overline{C}_V = \frac{2}{3} C_{V_{root}} \left(\frac{1 + \lambda_V + \lambda_V^{\,2}}{1 + \lambda_V} \right)$$

$$S_V = b_V \cdot \overline{C}_V$$

8. The aircraft in problem 4 has other features as follows:

$$h = 0.18,\ h_o = 0.23,\ \eta_h = 0.97,\ l = 12\ \text{m},\ S_h = 8.7\ \text{m}^2$$

Determine the aircraft static longitudinal stability derivative (Cm_{owf}) and discuss whether the horizontal tail is longitudinally stabilizing or destabilizing.

Solution:

$$C_{m_{owf}} + C_L(h - h_o) - \eta_h . \bar{V}_h . C_{L_h} = 0$$

$$\bar{V}_h = \frac{l . S_h}{\bar{C} S}$$

$$AR = \frac{b^2}{S} = \frac{b}{\bar{c}}$$

9. Design a horizontal tail for a twin jet business aircraft with the following characteristics:

m_{TO} = 16,000 kg, D_{fmax} = 1.8 m, Vc = 270 knot (at 30,000 ft), α_f = 1.5 deg (at cruise)

The wing has a reference area of 49 m^2 and the following features:

AR = 8, λ = 0.6, i_w = 2.4 deg, α_{twist} = -1.3 deg, Λ_{LE} = 37 deg, Γ = 3 deg, NACA 652-415

The aircraft has a low wing and an aft conventional tail configuration, and the aerodynamic center of the wing-fuselage combination is located at 22% of MAC. In cruising flight condition, the aircraft center of gravity is located at 42% of the fuselage length. Assume that the aircraft cg is 15 cm ahead of the wing-fuselage aerodynamic center.

The following tail parameters must be determined: airfoil section, S_h, C_{h_tip}, C_{h_root}, b_h, i_h, AR_h, λ_h, Λ_h, Γ_h. At the end, draw a top-view of the aircraft that shows fuselage, wing and horizontal tail (with dimensions).

10. A large transport aircraft with a mass of 63,000 kg is supposed to cruise with a speed of 510 knots at 42,000 ft. The maximum fuselage diameter is 3.6 m and fuselage angle of attack at cruise is 3.2 degrees. The wing has a reference area 116 m^2 of and the following features:

AR = 11.5, λ = 0.5, iw = 2.7 deg, α_{twist} = -1.6 deg, Λ_{LE} = 30 deg, Γ = 6 deg, NACA 641-412

The aircraft has a low wing and a T-tail configuration, and the aerodynamic center of the wing-fuselage combination is located at 20% of MAC. In cruising flight condition, the aircraft center of gravity is located at 49% of the fuselage length. Assume that the aircraft cg is 18 cm ahead of the wing-fuselage aerodynamic center. Design a horizontal tail to satisfy longitudinal trail and static longitudinal stability requirements. Then determine airfoil section, S_h, C_{h_tip}, C_{h_root}, b_h, i_h, AR_h, λ_h, Λ_h, Γ_h. At the end, draw a top-view of the aircraft that shows fuselage, wing and horizontal tail (with dimensions).

11. A fighter aircraft has the following features:

$S = 57\ m^2$, $AR = 3$, $S_h = 10.3\ m^2$, $S_v = 8.4\ m^2$, $l = 6.8\ m$, $l_v = 6.2\ m$

Determine the horizontal and vertical tails volume coefficients.

Solution:

$$AR = \frac{b^2}{S} = \frac{b}{\bar{C}}$$

$$\bar{V}_h = \frac{l.S_h}{\bar{C}S}$$

$$\bar{V}_v = \frac{l.S_v}{\bar{C}S}$$

Fuselage Problem

1. A cylindrical mid-section fuselage with fuselage length of 18 m and fitness ratio $\lambda_f = 6$, calculate, fuselage volume V_f, fuselage wet area S_{fw}, fuselage diameter D_f, fuselage cross section area Ac.

   Solution: since the fuselage is cylindrical

$$\lambda_f = \frac{l_f}{D_f} \rightarrow D_f =$$

$$D_f = \sqrt{\frac{4}{\pi}} A_c \rightarrow A_c =$$

$$V_f = \frac{\pi}{4} D_f^2 . l_f . \left(1 - \frac{2}{\lambda_f}\right)$$

$$S_{fw} = \pi . D_f . l_f . \left(1 - \frac{2}{\lambda_f}\right)^{2/3} . \left(1 + \frac{1}{\lambda_f^2}\right)$$

2. For fully stream lined shapes without cylindrical mid-section fuselage with l_f =15 m, l_n = 2 m, D_f = 3 m and fitness ratio λ_f = 5, calculate, fuselage volume V_f, fuselage wet area S_{fw}.

   Solution:

$$V_f = \frac{\pi}{4} D_f^2 . l_f . \left(0.5 + 0.135 \frac{l_n}{l_f}\right)$$

$$S_{fw} = \pi . D_f . l_f . \left(0.5 + 0.135 \frac{l_n}{l_f}\right)^{2/3} . \left(1.015 + \frac{0.3}{\lambda_f^{1.5}}\right)$$

3. Calculate the fuselage total weight in kg if the aircraft dive speed is 150 m/sec, gross shell area = 25 m2 and tell arm of 21 m, take fuselage maximum width and height as 3 m, 4 m respectively. What will be the total volume of passenger cargo (V_C) if the number of travelers (n_t =50) and the total baggage volume of each traveler (V_b = 30 kg).

Solution:

$$W_f = K_{wf} \times \sqrt{V_D \times \frac{l_t}{b_f \, . \, h_f}} \times S_G^{1.2}$$

K_{wf} is Constant = 0.23 since the weight is in (kg).

V_D is dive speed, S_G is Gross shell area, l_t is the tell arm

b_f, h_f: Fuselage maximum width and height

$$V_C = n_t \cdot V_b$$